

# THEORETICAL AND EXPERIMENTAL STUDIES OF ITH PERCUSSIVE DRILL VIBRATION

Ming Jian

Department of Mining and Metallurgical Engineering  
McGill University  
Montréal, Québec, Canada

A thesis submitted to the Faculty of Graduate Studies and Research  
in partial fulfillment of the requirements for the degree of  
Master of Engineering

March 1994

© Ming Jian

# Abstract

During underground, long-hole drilling operations, the bending of the drill string and vibrations in the system exert significant effects on hole deviation and penetration rates. Little prior research has been conducted in the area of the bending and vibrations associated with ITH (In - The - Hole) drills. This thesis deals mainly with the modelling of the static and dynamic properties of the ITH drill system while drilling under such conditions.

The bending of the drill string is the result of the string becoming unstable when its length or applied feed force exceeds a particular limitation. Under such conditions, lateral forces are created by the effect of the bending, thus generating the hole deviation. The critical length and feed force of the ITH drill string before being unstabilized and its characteristics after unstabilization are studied. The vibrations, primarily the vertical vibration of the ITH drill string, are discussed with reference to both theoretical and case studies. By analyzing the static and dynamic properties of the drill string, a continuous system mathematical model of the drill string has been developed. Two different boundary conditions have been discussed and applied through computer simulations.

Measurements of downhole parameters and vibrations while drilling were acquired by a high-rate telemetry and data acquisition system from field tests of a CMS CD-90B long-hole ITH drill and prototype shock absorber in an underground nickel mine. The vibration data was analyzed using spectral analysis methods and system identification techniques. Determining the inter-relationships between the drilling

parameters, for example, feed force, torque, air pressure and penetration rate, and the vibrations in an ITH drilling system is also a principal objective of the thesis. The performance of a prototype shock absorber developed by a third party company was also evaluated through an analysis of the vibration modes present during the ITH drilling process to examine the specifications of a suitable shock absorber design. The results of the simulations and analyses of the vibration data indicate that a prototype shock absorber effectively reduces the amplitude of the vibrations, especially the vertical vibrations of the drill string. A mathematical model using a complex boundary condition has been developed which will be of use in further research relating to the development of a vibration-based control system for ITH drills. These results will not only be of use for developing a shock absorber for the CD-90B drill, but more importantly be applicable to future research work on developing advanced control for these drills. By decreasing the vibration levels acting on the drill head and rod, the instrumentation for an automated drill can be protected to ensure maximum life and proper performance during hammer operation.

## Resumé

Dans les mines souterraines à base de métal, le forage des trous de production, en fonction des contraintes de l'emplacement et de la trajectoire, est essentiel pour réussir l'exploitation du minerai. Le résultat de cette phase d'extraction affectera de façon significative toutes les opérations en aval, du chargement au transport, jusqu'au broyage et au bocardage.

À cause de la nature même des foreuses utilisées, du type de minerai à extraire et de la configuration de la mine, la trajectoire des trous peut dévier de façon importante par rapport à celle projetée au départ. Ces déviations peuvent entraîner une dilution substantielle du minerai et une perte de productivité, d'où l'augmentation possible des coûts d'opération.

Les déviations ITH (dans-le-trou) des foreuses percussives, sont généralement causées par une courbure du foret qui plie sous l'effet des forces latérales présentes au niveau du foret ou le long de l'acier à foret. Dans cet exposé, on analyse les vibrations responsables de ces forces latérales. Cette analyse est fondée sur des études théoriques et pratiques réalisées sur le terrain. Pour ces dernières, le rendement des variables et des vibrations a été évalué à partir de l'observation d'une foreuse CMS CD-90B ITH dans une mine souterraine de nickel. Durant ces tests sur le terrain, on a également évalué le rendement d'un amortisseur de chocs commercial et son impact sur l'atténuation ou la transmission des vibrations générées par la foreuse.

En analysant les propriétés dynamiques et statiques du foret, on a élaboré un modèle mathématique de système continu capable de décrire son fonctionnement

dans un milieu bien déterminé. Grâce aux résultats de ces études, il sera possible de concevoir de meilleurs amortisseurs de chocs et de développer une logique avancée permettant aux foreuses ITH de minimiser les déviations de trous et de maximiser la productivité.

# Acknowledgements

I would like to express my sincere appreciation to professor Jonathan Peck, Dr. Deyi Jiao and professor Laeeque K. Daneshmend, my research supervisors, for their guidance, assistance and encouragement, without which this research work could not have been completed.

The contributions of Inco Mines Research, Ontario, Canada is also acknowledged for funding this research work and providing the necessary technical information. I wish to thank the Little Stobie Mine for their help and assistance and to Continuous Mining Systems Limited (CMS), Sudbury, Ontario for providing technical support during the field testing.

I wish to thank CCARM, the Canadian Center for Automation and Robotics in Mining, McRCIM, The McGill Research Center for Intelligent Machines, and the Department of Mining and Metallurgical Engineering, McGill University, for providing excellent experiment and computer facilities.

I am indebted to my mother, my sister Wen Jian, Ching Jian, my wife Suiping Wang, and my son Jian Jian for their love, encouragement and support, with which my dream has come true.

# Notation

- $A_1$ : cross section area of hammer casing
- $A_2$ : cross section area of drill string
- $c$ : speed of propagation of longitudinal waves in material
- $c_1$ : damping factor
- $c_2$ : damping factor
- $D_1$ : constant, complex number
- $D_2$ : constant, complex number
- $d_1$ : constant, complex number
- $d_2$ : constant, complex number
- $D_{in}$ : diameter of inside of drill string
- $D_{out}$ : diameter of outside of drill string
- $D_h$ : diameter of hole
- $D_p$ : diameter of piston
- $E$ : modulus of elasticity
- $h_1$ : constant, complex number

- $h_2$ : constant, complex number
- $i$ : imaginary number
- $k$ : spring constant
- $L$ : distance from bit to surface
- $L_1$ : length of hammer casing
- $L_2$ : distance from bit to the bottom end of drill string
- $L_p$ : length of piston
- $m$ : meter
- $n$ : integer number
- $q$ : function of spatial coordinate  $x$
- $t$ : time
- $x$ : distance from bit to any point of drill string
- $z$ : longitudinal displacement
- $z_0$ : amplitude of bit displacement
- $\omega$ : circular frequency
- $\rho$ : mass per unit length of drill string

*To My Mother, My Wife*

# Contents

<b>Abstract</b>	<b>ii</b>
<b>Resumé</b>	<b>iv</b>
<b>Acknowledgements</b>	<b>vi</b>
<b>Notation</b>	<b>vii</b>
<b>List of Figures</b>	<b>xii</b>
<b>1 Introduction</b>	<b>1</b>
1.1 Overview of Drilling Mechanics and Equipment . . . . .	1
1.2 Statement of the Problem . . . . .	5
1.3 Objective and Methodology . . . . .	7
1.4 Thesis Overview . . . . .	9
<b>2 Review of Past Research into Drill String Vibration</b>	<b>11</b>
2.1 Rotary Tricone Drilling . . . . .	11
2.2 Percussive Drills . . . . .	15
<b>3 Field Monitoring of An ITH Drill</b>	<b>17</b>
3.1 Introduction . . . . .	17
3.2 Objectives . . . . .	18
3.3 Experimental Methodology . . . . .	20
3.3.1 The CD 90B ITH Test Drill . . . . .	20
3.3.2 Data Acquisition . . . . .	21
3.3.3 Data Conversion and Digitization . . . . .	23
3.4 Monitored Parameters . . . . .	24

3.4.1	Feed Force . . . . .	24
3.4.2	Torque . . . . .	25
3.4.3	Rotary Speed . . . . .	26
3.4.4	Air Pressure, Air Flow Rate and Penetration Rate . . . . .	26
3.4.5	Vibration . . . . .	27
<b>4</b>	<b>Analysis of the Percussive Drill String</b>	<b>30</b>
4.1	Static Analysis . . . . .	30
4.2	Analysis of the Buckling and Bending of the Drill String . . . . .	32
4.2.1	Critical Load and Critical Length . . . . .	34
4.2.2	The Bending of the String Before Unstabilizing . . . . .	35
4.2.3	The Deflection of the String After Unstabilizing . . . . .	38
4.2.4	Calculations of Critical Length and Generated Forces . . . . .	39
<b>5</b>	<b>Continuous System and Boundary Conditions</b>	<b>46</b>
5.1	Assumptions . . . . .	46
5.2	Boundary Conditions . . . . .	48
5.3	Natural Frequency . . . . .	50
5.4	Solution of Drill System Functions . . . . .	50
5.5	The Complex Boundary Condition . . . . .	52
5.6	Solution to the Boundary Condition . . . . .	54
<b>6</b>	<b>Model Simulation and Analysis</b>	<b>55</b>
6.1	Objectives . . . . .	55
6.2	Statement of Simulations . . . . .	56
6.2.1	The excitation forces . . . . .	56
6.2.2	The responses of the simulation . . . . .	56
6.2.3	The boundary condition . . . . .	57
6.2.4	The damping . . . . .	57
6.2.5	The system characteristics and the data . . . . .	57
6.3	Simulation of Multiple-Degree-of-Freedom Model . . . . .	58
6.3.1	Identification of the damping of the shock absorber . . . . .	58
6.3.2	Simulation with Harmonic Excitation Force for Modal Analysis	60
6.4	Simulation of Continuous System with Impulse Excitation Force . . .	62
6.5	Discussion of Results of the Simulations . . . . .	63
6.5.1	Multiple-Degree-of-Freedom Model . . . . .	63

6.5.2	Continuous System . . . . .	66
<b>7</b>	<b>System Identification and Spectral Analysis</b>	<b>72</b>
7.1	The Drilling System . . . . .	72
7.2	Identification of the System . . . . .	74
7.2.1	The ARX, ARMAX and BJ Models . . . . .	75
7.2.2	The Impulse Responses Models . . . . .	76
7.2.3	Comparison of the Simulated and Original Outputs . . . . .	77
7.3	Vibration Analysis Using System Identification Methods . . . . .	83
7.3.1	Spectral Analysis . . . . .	83
7.3.2	Data Analysis . . . . .	84
7.3.3	Harmonic Responses . . . . .	90
<b>8</b>	<b>Conclusion and Further Work</b>	<b>100</b>
8.1	Introduction . . . . .	100
8.2	Conclusion . . . . .	101
8.2.1	Theoretical Studies . . . . .	101
8.2.2	Experimental Studies . . . . .	102
8.3	Primary Contribution . . . . .	104
8.4	Recommendation for Further Work . . . . .	106
	<b>References</b>	<b>107</b>

# List of Figures

1.1	Basic Drilling Concepts for (a) Percussive Drill (b) Rotary Drill . . .	2
1.2	Types of drills (a) Rotary Drill (b) ITH Drill . . . . .	2
1.3	Typical Drill Bits (a) ITH (DTH) Drill Bit (b) Rotation Drill Bit (Tricone Bit) . . . . .	3
1.4	Diagram of CD90 ITH drill . . . . .	4
1.5	Diagram of Test Rig . . . . .	8
2.1	A Simplified Percussive ITH Drilling System . . . . .	15
3.1	Plan and Section Views of the Monitored Production Holes and Cored Holes, Little Stobie Mine . . . . .	19
3.2	CD 90B ITH Drill Used for the Field Tests . . . . .	20
3.3	Field Test data Acquisition Setup . . . . .	21
3.4	Experimental Testing Instrumentation Layout . . . . .	22
3.5	General Scheme for the Data Converting and Digitizing . . . . .	23
4.1	Free-Body Diagram of a Percussive Drilling System . . . . .	31
4.2	Critical Load <i>versus</i> Length of the Drill String . . . . .	33
4.3	Diagram of Buckling of Drill String . . . . .	35
4.4	3-D Plot for Maximum Deflection . . . . .	37
4.5	3-D Plot for Maximum Angle . . . . .	38
4.6	Vertical Load <i>versus</i> Deflection . . . . .	39
4.7	Boundary Condition and Initial Deflection of the Drill String and Cal- culation of Horizontal Forces of the Drill String . . . . .	40
4.8	Feed Force <i>versus</i> Critical Length without Initial Deflection . . . . .	41
4.9	Feed Force <i>versus</i> Critical Length with Different Initial Deflection . .	42
4.10	Feed Force <i>versus</i> Horizontal Force . . . . .	45
4.11	Length of String <i>versus</i> Horizontal Force . . . . .	45

5.1	Analysis Diagram of the ITH Drill String . . . . .	47
5.2	Complex Diagram of the ITH Drill with the Surface Equipment Included . . . . .	53
6.1	Result of the Simulation of the Multiple-Degree-of-Freedom Model . . . . .	59
6.2	Normalized Model of Drill String; Top Left: Second Model, Top Right: Third Model, Bottom Left: Fourth Model, Bottom Right: Fifth Model . . . . .	61
6.3	Phase Angle . . . . .	64
6.4	Maximum Vibration Amplitude Ratio with Different Damping Ratio . . . . .	67
6.5	Maximum Vibration Amplitude Ratio with Different Spring Rates . . . . .	68
6.6	Stress Along the Drill String . . . . .	68
6.7	Axial Acceleration of a point of the String at a Certain Frequency (27 Hz) . . . . .	70
6.8	Axial Velocity of a point of the String at a Certain Frequency (27 Hz) . . . . .	70
6.9	3-D Plot for the Simulation Results . . . . .	71
6.10	3-D Plot for the Simulation Results for the Complex Boundary Condition . . . . .	71
7.1	Input and Output Diagram of the Drilling System . . . . .	73
7.2	System Original Output and Spectrum: a) Original Output at the Drill Head; b) Original Output at the Drill Rod; c) Spectrum of Output at the Drill Head; d) Spectrum of Output at the Drill Rod . . . . .	78
7.3	Comparison of Original the Output and Simulation Signal . . . . .	79
7.4	Comparison of the Filtered Output and Simulation Signal . . . . .	79
7.5	Comparison of the Output and Simulation Signal . . . . .	80
7.6	Comparison of the Output and Simulation Signal . . . . .	80
7.7	Bode Plot for the Identified System I . . . . .	81
7.8	Comparison of the Original and Simulated Output of System I . . . . .	81
7.9	Comparison of the Output of Model and System . . . . .	82
7.10	Comparison of the Output of Model and System . . . . .	82
7.11	Equivalent Damping Ratio and Harmonic Responses of the Drilling System for Vertical Vibration . . . . .	87
7.12	Spectrum of the Output of System II . . . . .	88
7.13	Spectrum of the Output of System II . . . . .	88
7.14	Spectrum of the Output of System II . . . . .	89
7.15	Spectrum of the Output of System II . . . . .	89

7.16	Spectrum of the Output of System I . . . . .	90
7.17	Harmonic Responses of Lateral Vibration (L-R) . . . . .	92
7.18	Harmonic Responses of Lateral Vibration (F-B) . . . . .	93
7.19	Variables and Damping for Hole Under02 . . . . .	94
7.20	Harmonic Responses of Vertical Vibration for Hole Under02 . . . . .	95
7.21	Harmonic Responses of Vertical Vibration and Equivalent Damping Ratio for Hole Under04 . . . . .	96
7.22	Harmonic Responses of Vertical Vibration and Variables for Hole Un- der04 . . . . .	97
7.23	Harmonic Responses of Lateral Vibration (F-B) for Hole Under04 . . . . .	98
7.24	Harmonic Responses of Lateral Vibration (L-R) for Hole Under04 . . . . .	99

# Chapter 1

## Introduction

### 1.1 Overview of Drilling Mechanics and Equipment

Production drills are used to create holes in rock materials in open-pit or underground mines in order to facilitate the removal and exploitation of ore minerals. The drilled holes are then loaded with explosives and detonated according to a particular design, which depends upon the predefined method and sequence of ore extraction, the intact strength of the rock and the desired size of the broken material. For different types of rock, hole diameter and length and mining method, a particular drilling method will be used to maximize production and minimize costs.

Traditionally, drilling has been performed by two different methods: 1) percussive and 2) rotary drilling where the former can be subdivided into top-hammer and ITH (in-the-hole) methods. There are four main components involved in these drilling methods: feed, rotation, percussion and flushing. The percussive drilling methods - top hammer and ITH drilling - utilize all these components, whereas rotary drilling lacks the percussion, but depends primarily on high feed force and rotation torque for breaking rock. The basic drilling concept for percussive drilling and rotary drilling has been illustrated in Fig. 1.1 (a) and (b).

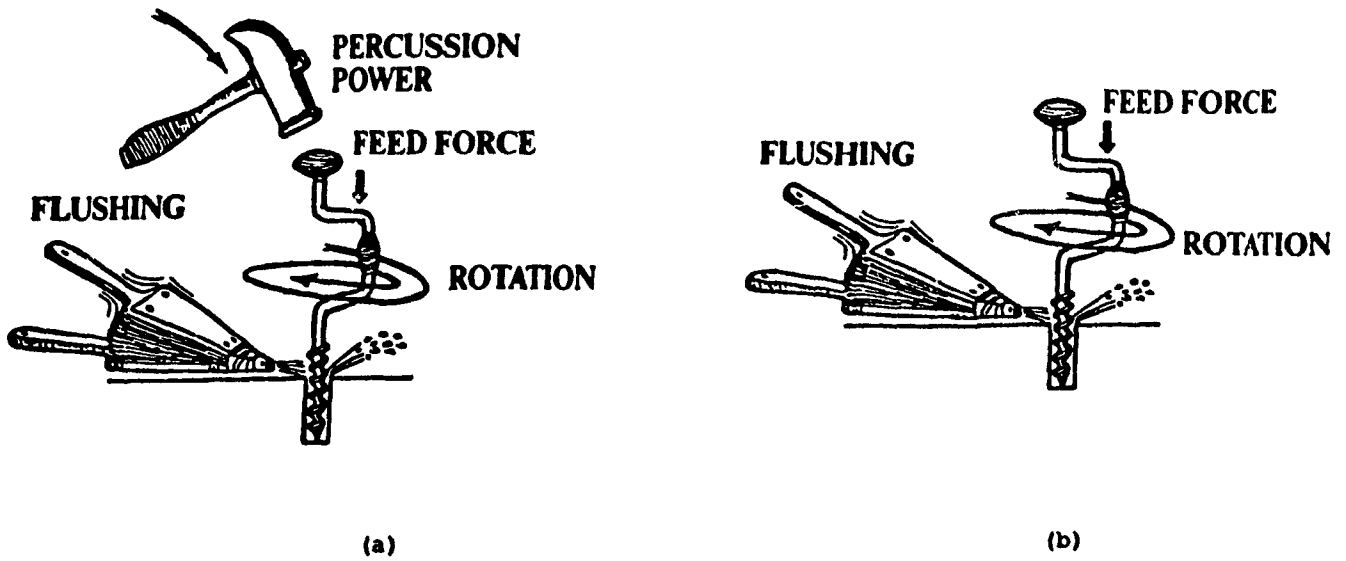
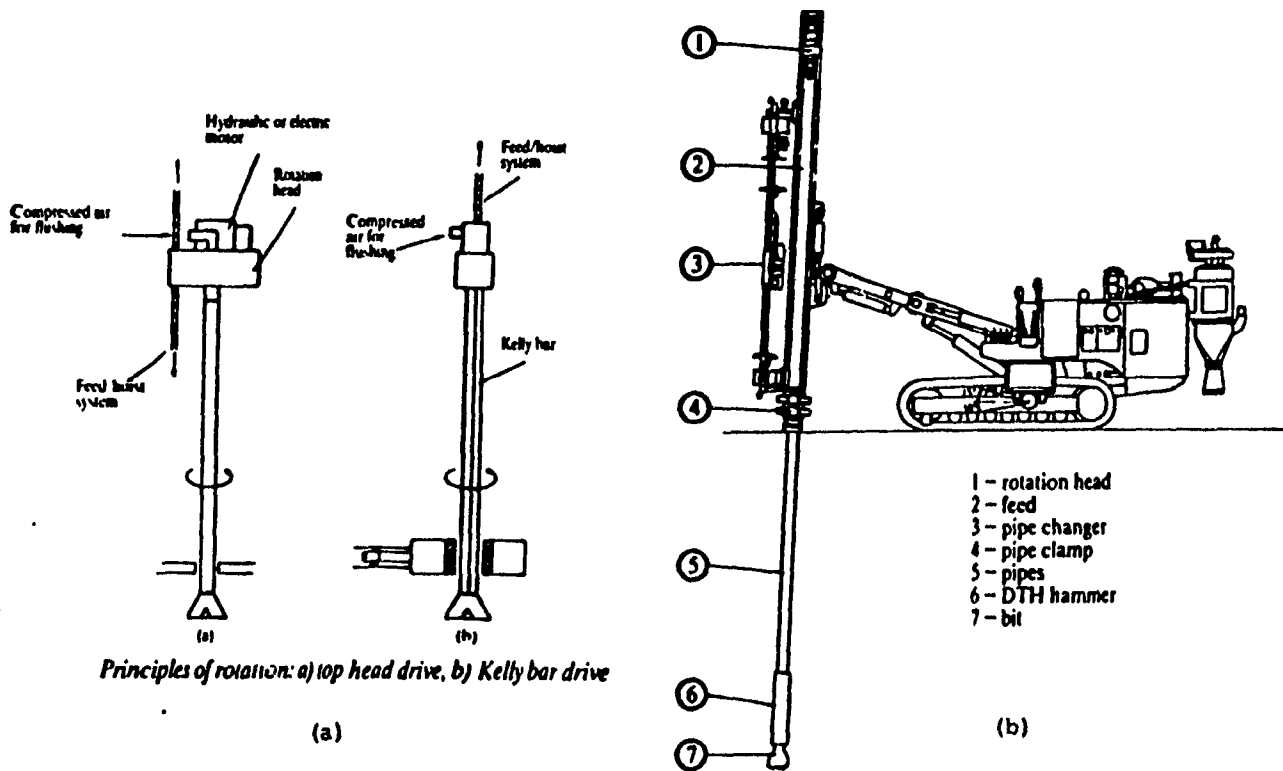


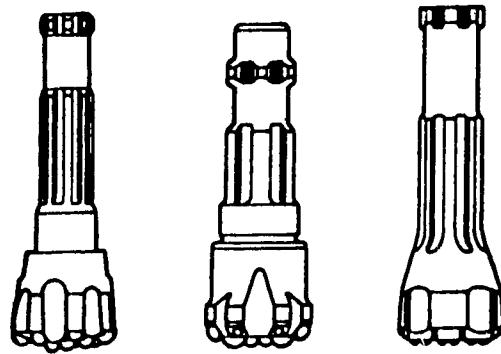
Figure 1.1: Basic Drilling Concepts for (a) Percussive Drill (b) Rotary Drill



Principles of rotation: a) top head drive, b) Kelly bar drive

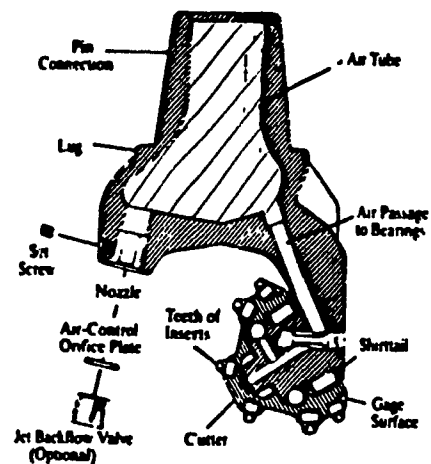
Figure 1.2: Types of drills (a) Rotary Drill (b) ITH Drill

In most major open pit mining operations, blasthole diameters larger than 251 mm and up to 50 m in depth are generally drilled with rotary drills and tricone rock bits [45]. This type of drilling is usually the most practical and economical for hole sizes, hole depths, rock properties and mining methods used in such operations. The drills used are primarily diesel or electrically powered to drive electric rotary and/or hydraulic feed motors as shown in Fig. 1.2 (a). In underground mines, greater than 95 percent of all production drilling is accomplished using percussive type drills, i.e. either top hammer or ITH drills. Figure 1.2 (b) shows a typical crawler mounted ITH drill. Typical drill bits, an ITH drill button bit and a tricone rock bit, used on percussive and rotary drills, are shown respectively in Figure 1.3 (a) and (b). Drill bits are designed according to the different requirements for rock breaking according to rock strength and variability and type of drill.



*Typical DTH bit designs.*

(a)



*Bit Components*

*Rotary drill bit components.*

(b)

Figure 1.3: Typical Drill Bits (a) ITH (DTH) Drill Bit (b) Rotation Drill Bit (Tricone Bit)

In ITH drilling, the hammer, which provides the percussive energy to break rock follows directly behind the bit rather than remaining mounted on a feed arm out of the hole as for top hammer drills. The length of the drill string and thus the hole, are increased through the addition of sections of drill rod which are connected via threaded ends. This feature results in ITH drills being able to drill longer and straighter holes than top hammer drills due to a more efficient, consistent energy transmission to the bit and lighter drill rod. A Continuous Mining System CD90B drill, shown in figure 1.4, was similar to the one used in the underground field tests, and is a typical ITH percussive drill.

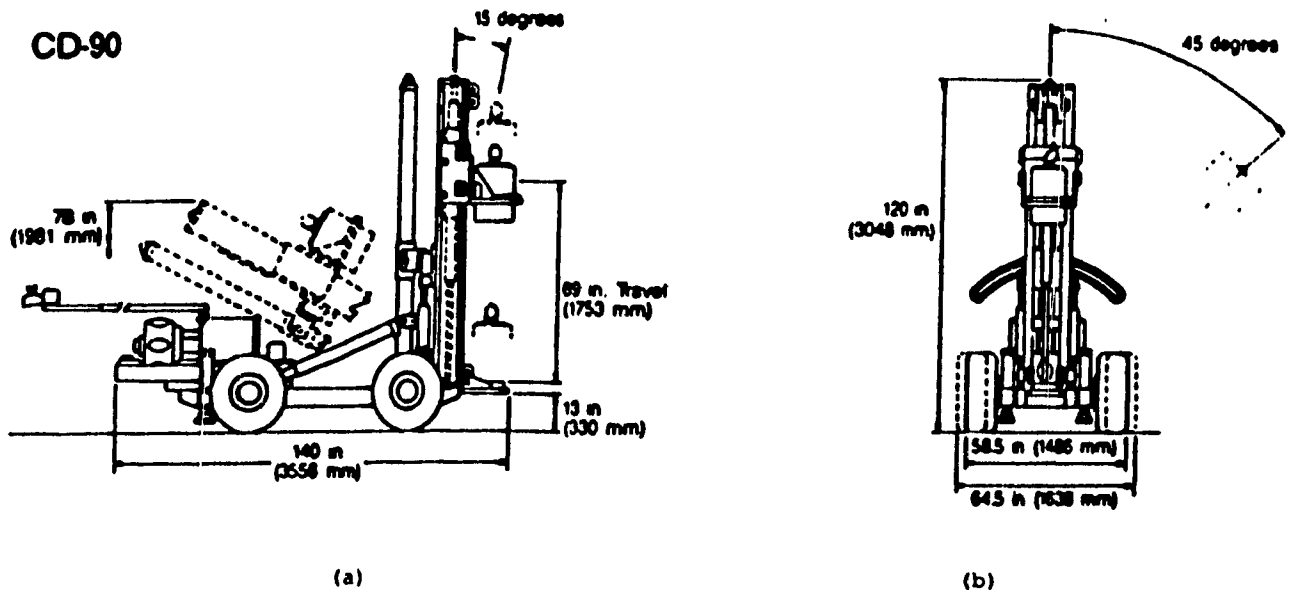


Figure 1.4: Diagram of CD90 ITH drill

As shown in figure 1.4, the CD90B ITH blasthole drill is composed of a mast, an independent mast support column, a motor head assembly, a rubber tire carrier and a remote control panel. The hydraulic head motor, which travels along the mast in the direction of drilling, develops the rotation of the drill rod. The drill feed is achieved with a patented, double acting hydraulic cylinder mounted in a trunion block. Compressed air is used to generate the percussive mechanism in the ITH hammer and the exhaust air is ported through the bit to provide flushing air to

clean the bottom of the hole and convey the cuttings to the collar. The piston in the ITH drill hammer strikes directly on the shank end of the bit to break the rock. All of the working parameters, such as feed force, air pressure and rotation speed are monitored from the control panel by the operator and can be adjusted by him to achieve higher penetration rates while attempting to reduce the vibrations on the drilling system and thus minimize hole deviation.

Like most mechanical systems, the drill string of an ITH percussive drill, which acts as a long shaft to transmit energy from the surface to the drill bit, exhibits longitudinal, torsional and lateral vibrations while drilling is underway. The amplitude of the vibration depends not only on the rock type, hammer characteristics and feed force levels but also on such parameters as bit design, hole length and composition of the drill string.

## 1.2 Statement of the Problem

In bulk underground mining, as is the case at most Inco mines, hole accuracy is of utmost importance when drilling production holes of up to 140 m lengths. The phenomenon of hole deviation dramatically influences the results of the blast and determines the proper use of the explosive, redrilling requirements, size of the broken rock material, ore dilution and stability of the surrounding work areas.

There are many factors surrounding the drilling process which cause or influence hole deviation. These include initial set-up errors, variation in the geology and excessive feed force thus contributing to the bending of the drill steel and development of vibration in the drill string. Over-thrusting of the bit contributes to drill string bending and since the drill string acts as a column to support the applied load, bending is a response of the system when the design load for this component is surpassed. As the hole gets deeper, the drill string will eventually become unstabilized and begin to bend under the effect of the applied feed force, thus causing hole deviation to occur. The vibrations generated by the ITH percussive hammer also contribute

to the hole deviation. These forces are very complicated as a result of the nature of the rock breaking mechanisms of percussive hammers. These become even more complex according to such factors as drill machine design, including uphole (carrier) and downhole (hammer, bit, steel and shock absorber designs) assemblies, hole geometries (diameter, length and inclination) and geological properties (structure and rock types).

Under certain conditions, drill string vibrations have a detrimental effect on the equipment (accelerated steel and bit wear), the penetration rate and even the hole stability [1]. All of these factors will increase the total time and cost spent on the drilling operation. The mechanical energy lost to drill string vibrations thereby reduces the amount of energy available at the bit to break rock. The generated vibrations can also lead to premature failure of some shock sensitive sensors and electronic components in advanced drilling systems with monitoring and/or control capabilities. Furthermore, when the drill string is excited at one of its natural frequencies (assuming it has several frequencies), resonance could be expected to occur.

A way to reduce vibration in the drill string is to place a shock absorber directly behind the hammer piston. The purpose of using a shock absorber is to both reduce the vibration generated by the piston and the amplitudes of vibrations transmitted to the drill string. Currently, commercially available shock absorbers do not efficiently reduce drill string vibration. This is a result of both poor shock absorber designs and a lack of understanding as to their true influence in damping drilling vibrations [1]. In this regard, effective shock absorbers for use in ITH percussive drilling applications have yet to be developed.

### 1.3 Objective and Methodology

Theoretically, when the feed force acts on the top end of the drill string and the length of the string exceeds its critical force and/or critical length, bending of the string will occur. The lateral force on the drill bit due to the bending is thought to be one of the most important factors affecting hole deviation. Therefore, it was considered necessary in this research to undertake a static analysis of the drill string in order to better understand its behaviour. This approach is a fundamental component in understanding both the vibration characteristics of the ITH drill string and the phenomenon of hole deviation due to the unstabilizing of the drill string.

Both theoretical and empirical approaches have been combined for the drill string vibration research. Lumped mass and continuous system mathematical models of the drill string, based on the data acquired from monitoring a CD90B ITH drill in field tests, have been established. A shock absorber was placed at the top of the hammer casing during these same tests to decrease the stress in the drill string due to the percussive action. The shock absorber was composed of mechanical springs and damping material where the former was designed as axial-force-acted elements only making them unsuitable to transmit the torsional torque. As a result of this, chapter 7 of the thesis examines the damping of the shock absorber with reference to the vertical and lateral vibration signals obtained during the field tests.

Underground field trials at the Little Stobie Mine, Sudbury, Ontario, were conducted as part of the thesis work using a fully instrumented CD90B ITH drill during the period January 20, 1992 to March 26, 1992. A comprehensive data set was obtained from the monitoring of eight (8) production blastholes of lengths up to 70 m while drilling within the nickel orebody. To examine the vibration properties of the drill string and the hammer, a metal collar (test rig) with vibration sensors attached was temporarily installed on the drill pipe, see figure 1.5. Using a wireless FM communication system connected to these sensors and transmitted via a telemetry system, vibrations on a rod out of the hole were measured while drilling. Another

two sets of sensors measuring the lateral and longitudinal vibrations were fixed on the drill head. The signals from the FM receiver and the fixed-on-drill-head sensors were then demodulated into a voltage, passed through the signal conditioning module and recorded by a 16 channel DAT (Digital Audio Tape) recorder. Using this set-up, tests were conducted with and without a shock absorber to examine the effects on the transmitted vibrations through the drill string. In order that the vibration data could be properly analyzed, the influence of such factors as feed force, air and oil temperature, and air pressure were also monitored by using appropriate sensors mounted on the drill. In addition, the feed force, torque and penetration rate were also monitored in parallel to the vibration data to ensure that any unexplained responses could be justified as a change by the operator in either feed force or air pressure levels. After the holes were completed, geophysical surveys in the same holes were conducted to isolate any variations in rock type and geological structure which could also generate anomalous vibration responses.

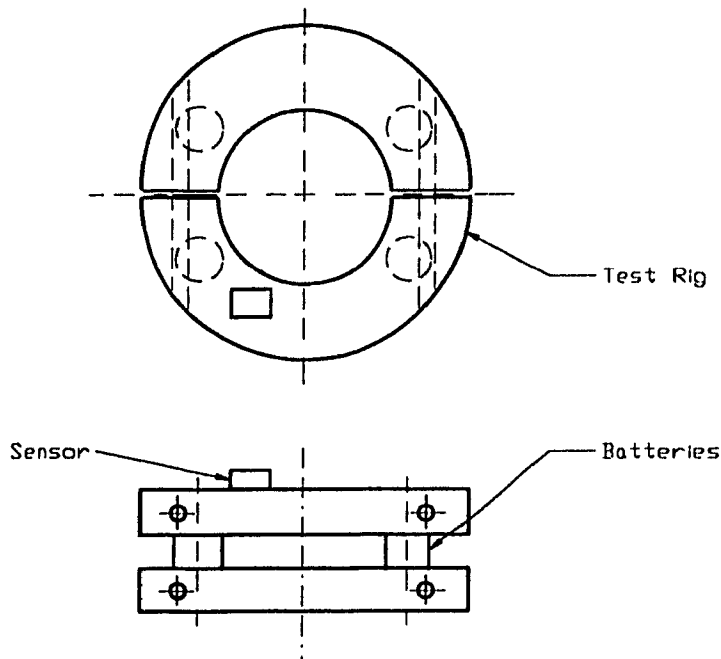


Figure 1.5: Diagram of Test Rig

The data measured from field monitoring of a CMS CD-90B long-hole ITH drill and shock absorber were subsequently analyzed by signal processing and system identification methods to understand the nature and origins of the drill vibrations.

Although the drill string vibrates in three directions, only the excited-damped longitudinal vibration were studied in this thesis. Since the longitudinal and torsional vibrations in the drill string are analogous, the same frequency functions will be obtained when the symbols are changed. Both vertical and lateral drill string vibrations have been analyzed during the signal processing and spectral analysis. In the model used, the boundary conditions are also the same, hence, the equations and results of the torsional vibrations can be obtained at the same time if needed. However, these two kinds of vibrations are considered to be independent of one another.

The results of the analysis should assist in the design of a shock absorber with more efficient vibration damping characteristics while also resulting in a more comprehensive understanding of ITH drill string vibrations.

## 1.4 Thesis Overview

The thesis is divided into seven chapters following the present section. In Chapter 2, a literature review is presented in relation to past research into drill generated vibration and deals mainly with studies using rotary drills. Rotary drills were extensively researched due to the fact that the majority of these efforts were undertaken and financed by the oil and gas industry in which rotary drilling and tricone bits are predominant. Chapter 2 also discusses the differences between percussive and rotary drills in terms of rock breakage mechanisms, the generation of vibration and the definition of boundary conditions. The field experiment using a CD-90B ITH drill forms the basis of chapter 3 including a statement of experimental objectives and methodology. Chapter 4 analyzes the static characteristics of the drill string, examines the critical length and feed force of the drill string and provides results for the lateral forces acting on the bit due to the bending of the drill string. Chapter 5 concentrates

on the mathematical models of the drill system, where some boundary conditions of the continuous system are discussed. The simulation of the drill system and discussion of the results are provided in Chapter 6. In this chapter, theoretical studies relating to ITH drill vibration are discussed. Chapter 7 outlines an analysis of the field experimental data in relation to drilling variables and generated vibrations by using system identification and spectral analysis techniques. The conclusions of the thesis and recommendations for further research work are outlined in chapter 8.

## **Chapter 2**

# **Review of Past Research into Drill String Vibration**

The following chapter discusses drill system vibrations with reference to research conducted from 1960 to the present time. Very few references were found in relation to the analysis of percussive drill vibrations; most of the research conducted was for rotary tricone drilling for oil and gas applications. However, these studies were undertaken primarily to examine the influence of vibration on hole deviation and so are of some use for the current work. Due to the lack of information on percussive drill string vibration, only those studies on tricone drilling which exhibited a close similarity to the current study in terms of the system components and objectives i.e. hole deviation, are thus discussed.

### **2.1 Rotary Tricone Drilling**

In petroleum and surface mining applications, drill strings of varying diameters and lengths, with or without shock absorbers, but having a tricone rotary bit at its bottom end are used. The drill string generally consists of sections of drill pipe having a uniform diameter and collars of one or more different sizes. In oil drilling, the length of the collar is relatively short compared to the total length of the drill string under

normal conditions. Both the drill pipe and collar in such applications have been observed to vibrate in three modes: 1) axially or longitudinally, 2) torsionally, and 3) transversely or laterally. The lateral vibration, due to bending, bucking, whirling or whipping, especially near the drill bit, affects the hole direction and probably contributes to the development of bottom-hole formation patterns which produce periodic axial and torsional bit loads [2]. Generally, lateral vibration levels are considerably larger than longitudinal vibration levels [3]. Longitudinal and torsional vibrations result in dynamic stresses which are amplified as the stress wave travels up the drill string. It was clear from past research that these dynamic stresses directly affected string and bit life through premature wear and reduced the overall drilling rate by damping the energy required to break rock at the bit [5].

As a long shaft with a small cross sectional area, this type of drill string is more sensitive to the vibrations generated by drilling and thus has an infinite number of natural frequencies. If the drill string is acted upon by fluctuating forces whose frequency is close to the natural frequency of the string, vibrations of very large amplitude may result. When the exciting frequency is equal to the natural frequency, the amplitude of vibration will be limited only by damping (i.e., energy dissipation) in a system [3]. If the damping is insufficient, failure of system components can occur. The damping of the drill string is a result of the combined effects of the surrounding fluid in the case of mud drilling, and friction due to contact between it and the hole wall. The collar, which is part of the drill string, plays a very important role in drill string vibration. Past research has indicated that the natural frequency of the drill collar section or bottom-hole assembly is a major factor in establishing and controlling vibrations throughout the drill string [7]. In other words, the bottom-hole assembly alone dictates whether or not the entire drill string vibrates excessively regardless of hole depth. This can be explained by the fact that the drill collar section is the primary recipient of vibration energy generated at the drill bit.

The tricone bits used to drill oil and gas wells contain three cutters on cones

which are attached to a rigid metal body (see figure 1.3(b)). Upon rotation of the drill steel, the cones of the bit also rotate and tungsten-carbide inserts impact against the rock, breaking it into rock fragments or chips through compressive and shear failure mechanisms. The broken materials are cleaned away by either a fluid (water and/or mud) or air which is fed down through the hollow steel into the bit and out through ports to the rock interface and then to surface.

Field and laboratory measurements of drill string vibrations by several researchers over the past 25 years indicate that tricone drill bit displacement frequencies are generally in the range of three cycles per bit revolution. Therefore, the frequency of bit displacement can be defined by;

$$f = \frac{N}{20} \quad \text{or} \quad \omega = 2\pi f = \pi \frac{N}{10} \quad (2.1)$$

where  $N$  is the rotary speed of the drill string (r.p.m.). The displacement of the bit can be simply expressed by;

$$x(t) = x_0 \sin \omega t \quad (2.2)$$

It is believed that the bit teeth and cone action at the bit-rock interface and the rotation and fluid pressure pulsations are the main sources of vibration in the drill string in oil and gas well drilling [8]. Particularly, the motion of the cone teeth is the main source of longitudinal and torsional vibration of drill string. As mentioned above, resonance or severe vibration could be expected to occur when the drill string is excited at one of its natural frequencies. Although resonance is possible, the large bit vibrations are believed to be due mainly to the relatively large amplitude of bit displacement rather than resonance [8]. Eccentric motion of the bit due to the formation of irregular surfaces at the bit-rock interface is a result of improper bit design for the type of rock or insufficient feed force causing bit bouncing. If there are many surface irregularities produced by the bit action, large amplitudes of bit displacement will result inducing large amplitude vibrations in the drill string. In order to reduce the drill string vibration amplitudes, it was seen necessary to control

the force on the bit and thus decrease the amplitude of bit displacement. This may be done by using a more suitable drill bit for the formation type which would give better performance through more efficient rock breakage to thus produce lower vibration levels. In addition, the use of a suitable drill operation strategy (manual or automatic) to modify both rotary speed and weight on bit according to changing downhole conditions, would also assist in reducing vibrations.

Another effective method to reduce drill string vibration in rotary drilling is to place a shock absorber, designed to provide localized axial flexibility in the drill string, as close to the bit as possible. The effectiveness of this approach is confirmed by both practical and theoretical studies based on linear drill string models [1]. According to vibration theory, whether or not a shock absorber decreases the dynamic forces in a drill string depends on the spring constant and damping ratio of the shock absorber as well as the bit displacement frequency (a function of the rotary speed) and force applied on the bit. Under certain drilling conditions, the ability of a shock absorber to reduce drill string vibrations increases as both spring rate and degree of damping are reduced [1]. On the other hand, at a vibration frequency in resonance with the drill string, damping should at least reduce the resonant amplitudes. A small but non-zero value of the damping has a favourable effect on drill string vibration. Some authors believe that a shock absorber used in a rotary drill system presents a case of non-linear behaviour due to the strong Coulomb friction between the drill system and hole wall and that in the shock absorber [9]. However, what should be noted is that if a shock absorber has too stiff a spring element (high spring rate), the dynamic forces on the bit and drill string stress may be higher at low rotary speeds than if no shock absorber were used. Also mechanical springs in shock absorbers are more effective at the higher operation frequencies (or rotary speeds) than they are at lower operation frequencies.

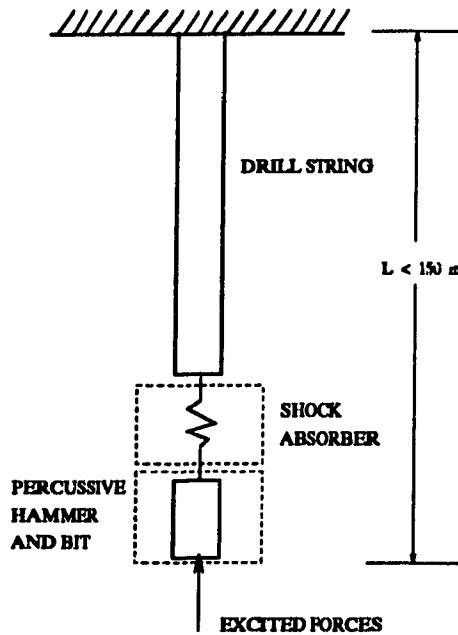


Figure 2.1: A Simplified Percussive ITH Drilling System

## 2.2 Percussive Drills

A comparison of rotary tricone bit and percussive ITH drills indicates that there are many differences between the two systems, for example the drilling method and drill string components. Figure 2.1 shows a diagram illustrating a simplified percussive ITH drilling system consisting of a drill string, possibly a shock absorber, a hammer and a bit. The length of these components do not generally exceed 150 m. The difference in the drilling methods, however, is considered to be more important for an analysis of the boundary conditions and nature of the excited forces. For example, in tricone rotary drilling, both ends of the drill string exhibit more complex boundary conditions than in the percussive system. Although a vast amount of data was measured from past field drilling experiments, it was considered unsatisfactory for the calculation of the boundary conditions for rotary tricone bit drills [10]. The boundary conditions for percussive drills will be compared with rotary drill systems in a later section.

The different drilling methods also generate different excited forces. In rotary

drilling, the main cutting action is due to the rotation of the bit. The drills attack the rock with energy supplied to the bit from the rotation of the steel under applied thrust. The bit cones with rows of tungsten-carbide inserts are pressed into the rock to first crush the rock through compressive failure and then shear the material along predeveloped fracture surfaces under rotation. The main similarity between rotary and percussive drilling is the crushing of rock under an axial load. In the former, the impact mechanism is due to continuous rotating of the cones bringing the inserts into contact with the rock, while in percussive drills, the impacting is generated by a hammer at a constant blow rate. In percussive drills, bit indexing i.e.. rotation clears the broken fragments away from the rock interface in preparation for the next impact. If the index rate is insufficient, the impact energy will be dampened due to the presence of crashed rock material under the bit. Drill cuttings are removed from the hole by flushing air in most percussive drills, which is provided by a compressor on board the drill. In rotary drilling, flushing is by air, water or mud or combination of these media.

The axial vibrations of rotary drill are mainly the result of the tricone bit rolling over high and low spots at the bit-rock interface and the axial impacting of inserts [8,2]. ITH percussive drills generate vibrations as a result of the hammer action which propagates a stress wave through the bit to fracture the rock beneath. The vibrations caused by the indexing is believed to be much less than that due to the percussive action of the hammer on the bit. The nature of the excited force in percussive systems also depends on the rock properties, bit shape/design, piston final velocity, air pressure, and the cross sectional area of the hammer casing and the piston.

## Chapter 3

# Field Monitoring of An ITH Drill

### 3.1 Introduction

In this thesis, the research work has combined both theoretical and empirical approaches in which data acquired from monitoring the performance of a CD-90B ITH drill in underground tests is analyzed. Underground field trials at INCO's Little Stobie Mine, Ontario, were conducted using a fully instrumented CD-90B ITH drill during the period January 20, 1992 to March 26, 1992. Data was acquired from the monitoring of eight (8) production blastholes of lengths up to 68.6 m (225 feet) and dips ranging from 56° to 88° from the horizontal while drilling within the nickel orebody. Three (3) cored holes were also drilled in close proximity to the production holes. Figure 3.1 shows the location of the production holes and the cored holes.

A total of 18 different signals were monitored during the underground field tests, including feed force, torque, rotary speed, air pressure, air and oil temperatures, air flow, displacement, and vibrations in different directions and locations. To better understand the vibration on the ITH drill, the three modes of vibration – longitudinal, torsional and lateral, were measured by installing a triaxial vibration transducer mounted on a metal block onto the drill rotation head. Since this thesis is mainly concerned with the transmission of vibration along the drill string, a metal test rig

(see Figure 1.5 on page 8) with vibration sensors and transducers attached was assembled which was then temporarily installed on the last drill pipe. Using a wireless FM communication system, the vibration transducers and the telemetry system were used to measure the vibration signals on the drill string while drilling. With use of this set-up, the longitudinal and lateral vibration responses of the drill string, with or without a shock absorber, can be compared to evaluate the capability of the shock absorber to absorb the vibration from being transmitted from the drill hammer, through the drill string to surface.

All the signals from the transducers and telemetry system were first passed through a signal conditioning/isolation block and recorded by a TEAC RD 200T Digital Audio Tape (DAT) recorder. The digital signals were obtained by playing back the DAT tapes, filtering the analog signals, and then digitizing by an analog to digital card. Geophysical logging of the production and core holes was undertaken by two companies, IFG Corp., Toronto, and GPR Geophysique, Montreal, to provide a comprehensive suite of data to correlate to the monitored drilling data.

## 3.2 Objectives

The objectives of the field tests are listed as follows:

1. Evaluate the capacity of the shock absorber to absorb or isolate the vibration transmission from drill hammer to the drill machine.
2. Find the relationship between the operation variables and the vibration, especially the longitudinal vibration on the drill string and drill head.
3. Attempt to validate the vibration equations to be defined in subsequent chapters using the field test data, or to identify new empirical equations.
4. Acquire knowledge about the drilling process dynamics.
5. Acquire knowledge regarding the design of the shock absorber used on an ITH drill.

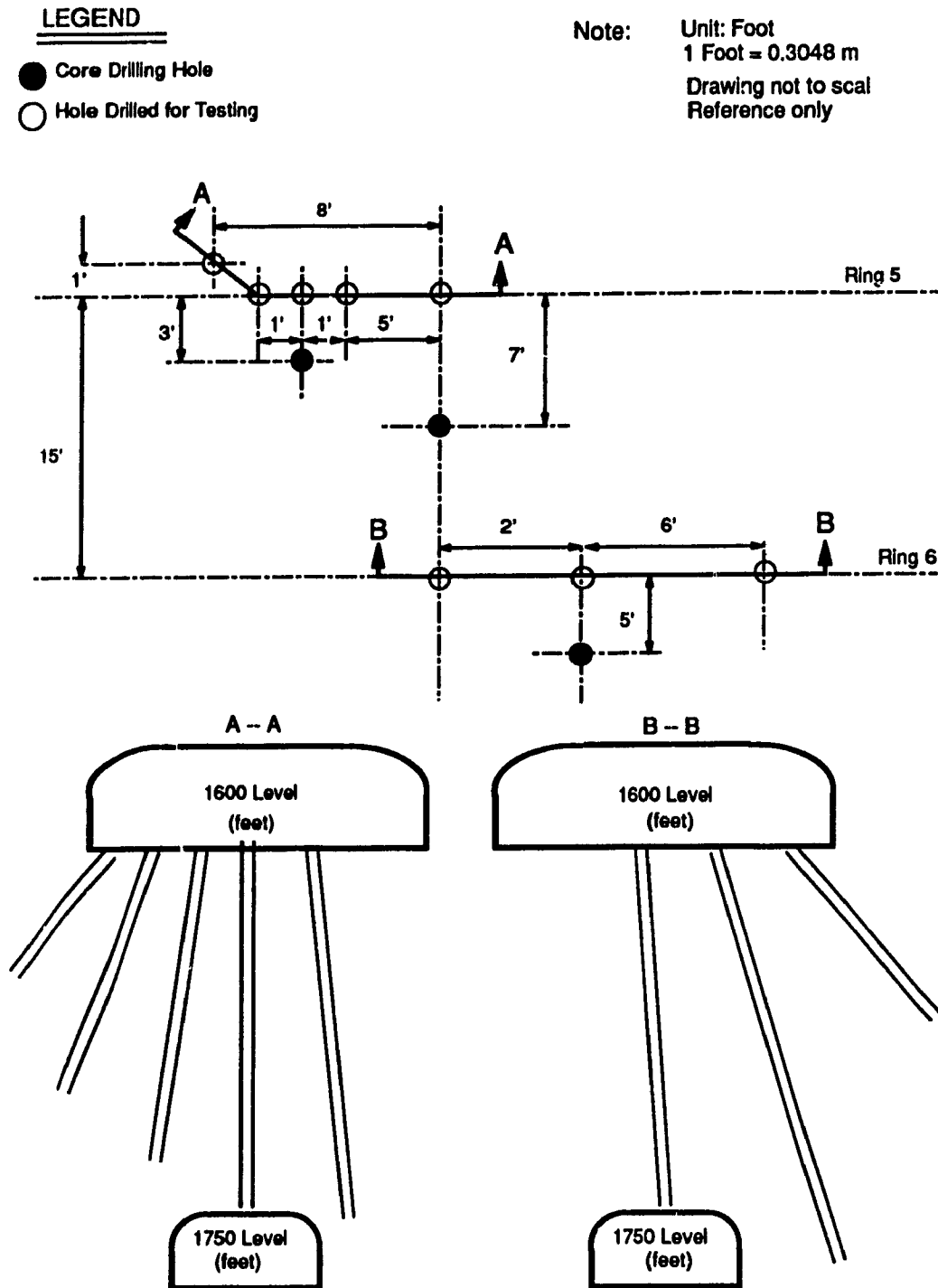


Figure 3.1: Plan and Section Views of the Monitored Production Holes and Cored Holes, Little Stobie Mine

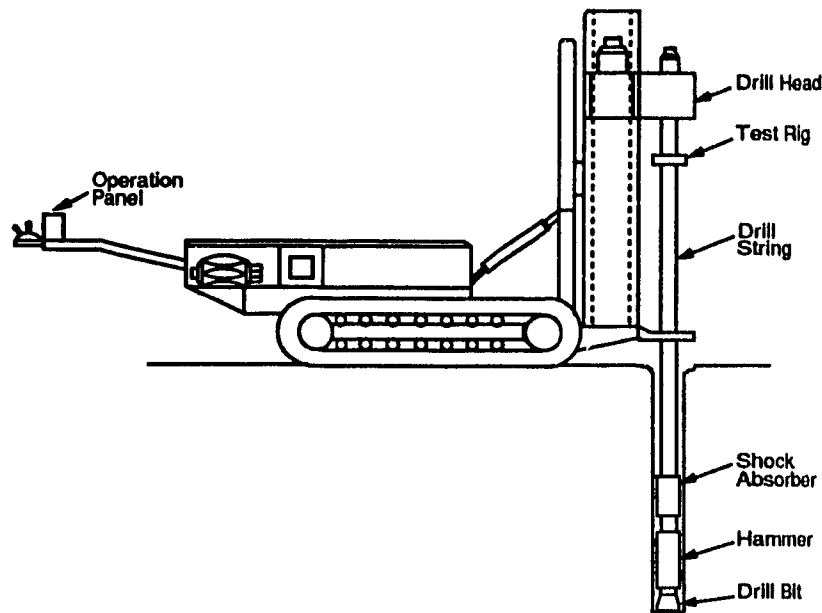


Figure 3.2: CD 90B ITH Drill Used for the Field Tests

### 3.3 Experimental Methodology

#### 3.3.1 The CD 90B ITH Test Drill

The CD 90B ITH drill is a product of CMS Ltd., Ontario, Canada. Before the experimentation, several changes of the drill have been done according to the requirements of the underground field tests. The drill rig was instrumented by installing sensors, transducers or power unit on it. A testing rig used for the measuring the vibration on the drill rod with the telemetry system was also built and assembled before the tests. As a part of the ITH drilling process monitoring and data measuring, the vibration testing has been made at different drilling conditions: with the shock absorber installed on the drill rod; drilling without the shock absorber; drilling at normal feed force; drilling beyond the normal feed force range. Figure 3.2 shows the CD 90B ITH drill used during the field tests which is with the shock absorber and the test rig installed.

### 3.3.2 Data Acquisition

Data acquisition during the field tests was composed of data measurement, transmission, and recording. The 18 transducers installed on the drill were connected directly to a signal conditioning interface. A telemetry system using a wireless FM communication system was used to monitor two identical vibration transducers on the drill head. This signal was demodulated into a voltage, and then to be sent to the signal conditioning interface. Figure 3.3 shows its overall strategy of this process.

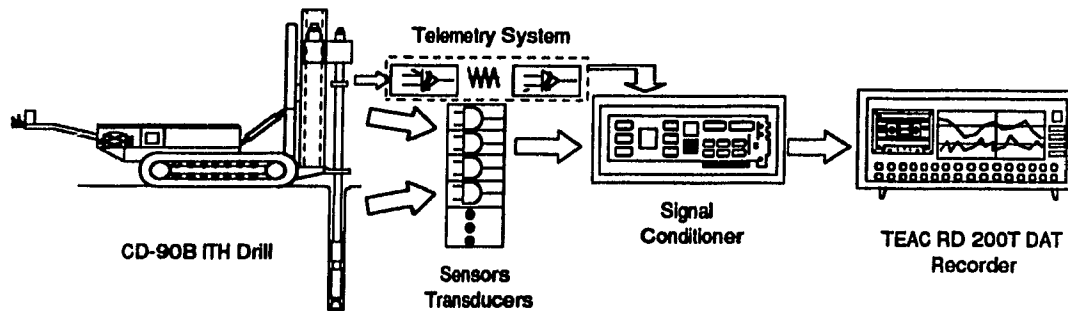


Figure 3.3: Field Test data Acquisition Setup

The signal conditioning interface shown in figure 3.3 is a subsystem to filter and amplify the signals which come from the transducers before being stored on the DAT (Digital Audio Tape) recorder. This subsystem also provides complete magnetic isolation, high common-mode noise rejection and easy field calibration. A TEAC RD 200T DAT recorder was used to record the data during the field tests and can simultaneously store 16 analog signals of 2.5 *KHz* bandwidth each at this sampling rate. Each tape for the DAT recorder can store two hours of data. Figure 3.4 shows the global layout of the field testing electronic instrumentation.

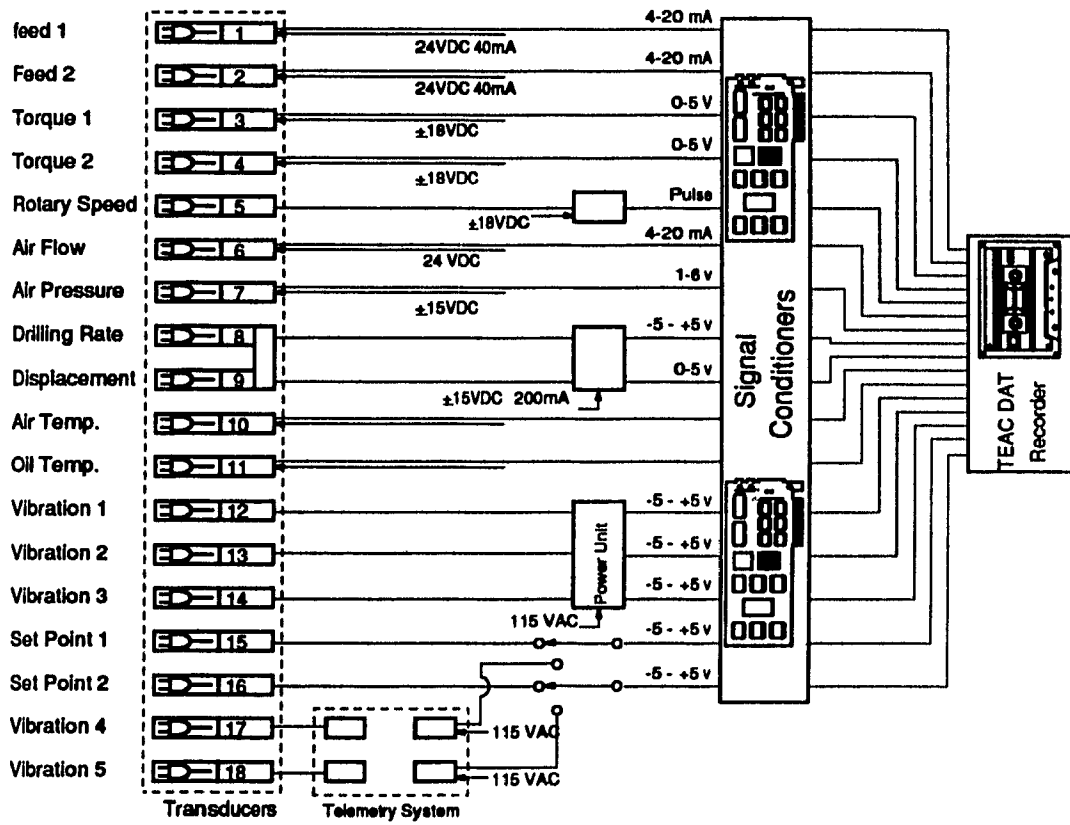


Figure 3.4: Experimental Testing Instrumentation Layout

### 3.3.3 Data Conversion and Digitization

The data conversion and digitization was at McGill University following the field tests. The data tapes were played back by the TEAC RD 200T recorder with analog signals passed through a series of filter. An Analog Device's RTI-815 analog-to-digital converter card, installed in a computer's expansion slots, was used to digitize the analog signals. The computer used for the data converting, digitizing, storing and processing was a PACKARD BELL Force 386/33 Personal Computer (with 80387 co-processor) equipped with 640 Kb of RAM memory, 4 Mb of extended memory, a 120 Mb hard disk, two floppy disk drives (double side/high density) and an EGA color monitor. The general scheme used for the data converting and digitizing is illustrated in figure 3.5.

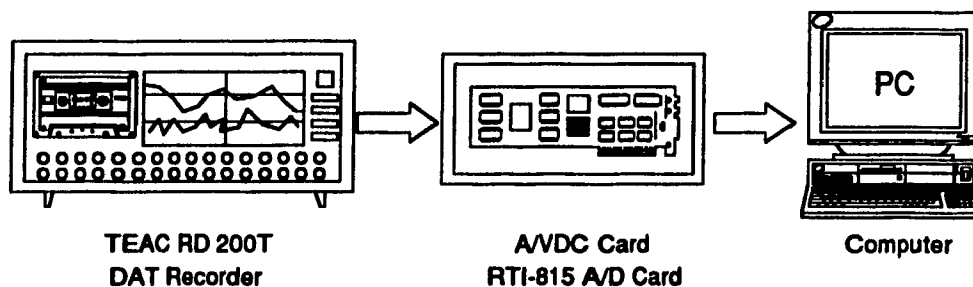


Figure 3.5: General Scheme for the Data Converting and Digitizing

## **3.4 Monitored Parameters**

There are 16 variables which were monitored on the CD-90B ITH drill which were monitored during the field test. However, only 12 variables were of interest for the vibration analysis in this thesis. These are:

- Feed force
- Torque
- Rotary speed
- Air pressure
- Air flow
- Penetration rate
- Torsional vibration on drill head
- Lateral vibration on drill head
- Longitudinal vibration on the drill head
- Lateral vibration on the drill string
- Longitudinal vibration on the drill string

A detailed explanation of the monitored variables listed above can be found in the following subsections.

### **3.4.1 Feed Force**

Feed force is required for a percussive drill in order to ensure that the bit is in good contact with the rock when the piston strikes the bit. The reflected stress wave will first cause the bit and hammer to rebound and the whole system to vibrate. The amount of reflected stress energy will depend on the rock properties and the amount of applied feed force. The feed force is also used to move the bit back in contact

with the rock prior to the next piston blow and used for balancing the reaction force produced by the compressed air which accelerates the piston.

During the drilling tests at the Little Stobie Mine, an optimum feed force was used in most of the production holes. The pressure in the feed cylinder was maintained at about  $6.8947 \times 10^6 \text{ N/m}^2$  (1000 psi) (gauge) to obtain the best drilling performance. Excessive feed force was applied in an attempt to obtain data from which the effect of this condition to influence deviation.

Feed force was monitored, during the field tests, by measuring the differential pressure acting on the piston inside the feed cylinder. The cylinder used for the CD90-B ITH drill was a compound 2-stage double acting cylinder. The feed force then can be calculated by;

$$F_{cyl} = (P_d - P_u)A \quad (3.1)$$

where

$F_{cyl}$  = Feed force produced by the feed cylinder

$P_d, P_u$  = Downward and upward pressures of the piston

$A$  = Cross-sectional area of the piston

### 3.4.2 Torque

The torque of an ITH drill is the response composed of bit chipping action, the friction between the rod and hole wall and the friction from all rotating drill components. Some drilling variables such as feed force, piston blow rate, hole depth and rock properties can also affect the torque. Bending of the rod and flushing conditions also exert some influence on the measured torque level.

Torque was determined by measuring the differential pressure between the inlet and outlet parts of the hydraulic rotation motor on the CD-90B ITH drill. For the Sauer Sundstrand Series 40 M46 Axial piston fixed displacement motor on this drill,

the torque can be defined as;

$$T = \frac{qR(P_{in} - P_{out})\eta_1\eta_2}{2\pi} - T_f \quad (3.2)$$

where

$T$  = Torque acting on the hammer

$P_{in}, P_{out}$  = Pressure at inlet and outlet parts of the motor

$q = 7.11 \text{ cm}^3/\text{rev.}$ , Geometrical displacement of the motor

$R = 27.75 \times 2.8 = 77.7$ , Gear Ratio

$\eta_1 = 0.85$ , Motor efficiency (varies between 0.8 and 0.89)

$\eta_2 = 0.9$ , Gear transmission efficiency

$T_f$  = Torque due to friction

Because the efficiency varies with different RPM's and pressures, an average value of efficiency  $\eta_1$  should be adopted when calculating the torque.

### 3.4.3 Rotary Speed

The CD-90B ITH drill is designed to have a maximum rotation speed of 20 RPM. During the field tests, the RPM was varied over its operational range while the feed force was held constant. The rotary speed was measured using a magnetic pick-up sensor which counted a magnetic strip affixed to the rotary head.

### 3.4.4 Air Pressure, Air Flow Rate and Penetration Rate

A vortex type flow transducer, model FV-520G-F, was used in the field tests to measure air flow rate. A 4-20 mA current output of this transducer was then proportional to the flow rate. The air pressure transducer used in the tests provides a maximum output of 6.347 V for  $3.44 \times 10^6 \text{ N/m}^2$  (500 psi) with a 1.347 V offset. In addition, drilling displacement and penetration rate were measured by a transducer which produced two separate outputs for displacement and velocity. Due to

a very low penetration rate measured by this transducer, the penetration rate was calculated by differentiating the measured drilling displacement. According to the method of measurement of the field tests, the air pressure, air flow rate and drilling displacement can be expressed by the following equation;

$$Q(\text{or } P, \text{ or } S) = \frac{x_f}{O_{max} - O_{min}} \frac{Q_{max} - Q_{min}}{V_f} \frac{V_i}{V_o} \frac{V_d}{A_f} \quad (3.3)$$

where

$Q, P, S$  = Measured air flow rate or air pressure ,or drilling displacement respectively

$x_f$  = Full range of the transducer

$V_f$  = Full output range of the signal conditioner

$O_{max}, O_{min}$  = Output range of the transducer

$Q_{max}, Q_{min}$  = Input range of the signal conditioner

$V_i$  = Input setting of the DAT recorder

$V_o$  = Output setting of the DAT recorder

$V_d$  = Data in voltage

$A_f$  = Gain of the filter

### 3.4.5 Vibration

There were two sets of vibration signals monitored during the field tests. The first set were the vibration responses on the drill head measured by a triaxial vibration transducer mounted on a metal block. Depending on the test, this set of vibration signals contained either the responses on the drill head when a shock absorber was or was not used. The vibration transducers were connected directly to the signal conditioners and the DAT recorder. Another set of sensor used to obtain the vibration signals on the drill rod while drilling. These sensors were monitored and measured by the transducers mounted on a test rig (see Figure 1.5 on page 8) and the telemetry system. Due to technical difficulties with the instrumentation, the vibration signals

on the drill head and the drill rod were not able to be measured simultaneously.

The triaxial vibration transducer used to measure the vibration signal on the drill head was composed of three identical accelerometers. The output range of the each transducer was  $\pm 5V$  for  $\pm 50 g$  of acceleration. The vibration level measured for each transducer can be calculated by;

$$A = \frac{x_f}{O_{max} - O_{min}} \frac{Q_{max} - Q_{min}}{V_f} \frac{V_i}{V_o} \frac{V_d}{A_f} \quad (3.4)$$

where

$A$  = Measured acceleration, 0 - 50 g

$x_f$  = Full range of the transducer

$V_f$  = Full output range of the signal conditioner

$O_{max}, O_{min}$  = Output range of the transducer

$Q_{max}, Q_{min}$  = Input range of the signal conditioner

$V_i$  = Input setting of the DAT recorder

$V_o$  = Output setting of the DAT recorder

$V_d$  = Data in voltage

$A_f$  = Gain of the filter

The equation to be used to calculate the vibration responses on the drill rod by using the vibration transducers on the test rig and the telemetry system, however, is slightly different from that used for the vibration on the drill head by adding the factors of the telemetry system. It is;

$$A = \frac{x_f}{O_t O_{max} - O_{min}} \frac{Q_c}{V_f} \frac{Q_{max} - Q_{min}}{V_f} \frac{V_i}{V_o} \frac{V_d}{A_f} \quad (3.5)$$

where

$A$  = Measured acceleration, 0 - 50 g

$x_f$  = Full range of the transducer

$O_t$  = Full output range of the transducer

$Q_c$  = Full input range of the telemetry transmitter

$V_f$  = Full output range of the signal conditioner

$O_{max}, O_{min}$  = Output range of the transducer

$Q_{max}, Q_{min}$  = Input range of the signal conditioner

$V_i$  = Input setting of the DAT recorder

$V_o$  = Output setting of the DAT recorder

$V_d$  = Data in voltage

$A_f$  = Gain of the filter

## Chapter 4

# Analysis of the Percussive Drill String

### 4.1 Static Analysis

As mentioned in earlier chapters, very few references related to the static and dynamic analysis of percussive drills have been found. Static analysis forms the basis for undertaking a comprehensive study of percussive drill dynamic characteristics. On the other hand, every effort has been made to determine the relationship between the buckling and bending of the drill string and hole deviation under assumed static feed forces through the static analysis. It is believed that the lateral forces created by both the bending or buckling and vibration of the drill string are the main causes of hole deviation and as such will be analyzed in detail in this research.

The drill string for a percussive drill can be considered as an elastic body of distributed mass and theoretically has an infinite number of degrees of freedom. To analyze the static-dynamic characteristics of the drilling system, it is necessary to model the system to a Single-Degree-of-Freedom-System as shown as figure 4.1. The model system consists of the masses (the drill string, hammer, and drill bit), the damping along the drill string and the elastic element (the drill string and shock

absorber) i.e. the spring-and-mass system. It is assumed that the system is linear and the damping is viscous.<sup>1</sup> From the free body diagram of the mass, the differential equations of motion of the system can be derived. Figure 4.1 shows the mass placed in its static-equilibrium position with the spring stretched a distance  $x_s$  from its free-length position. Summing the forces vertically, the equation,

$$W = k \cdot (x_s) \quad (4.1)$$

is derived, where  $x_s$  = static movement of mass from a static-equilibrium position.

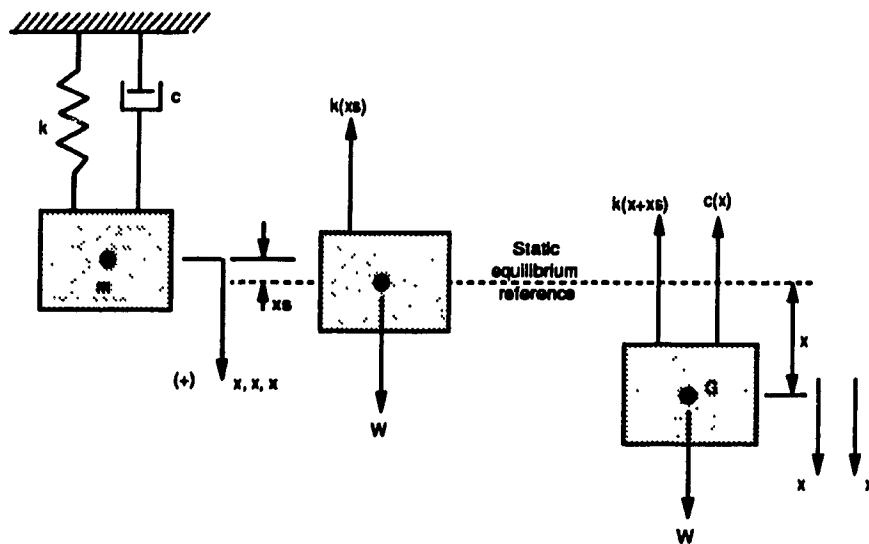


Figure 4.1: Free-Body Diagram of a Percussive Drilling System

When the mass ( $m$ ) has a positive displacement  $x$  from the static-equilibrium position, it undergoes both a positive downward velocity and acceleration as shown in figure 4.1. The forces acting on the mass are the spring force  $k(x + x_s)$  and the

<sup>1</sup>Although in reality, Coulomb friction deals mainly with the damping of vibration and axial forces [1], viscous damping is assumed in the current case for reasons of simplicity, in order to derive the differential equations which describe both the static and dynamic conditions of the drill string.

viscous-damping force  $c\dot{x}$ , where both the spring and damping force act upwards. Applying Newton's second law,

$$W - k(x + x_s) - c\dot{x} = m\ddot{x} \quad (4.2)$$

where

$W$  = weight of the mass

$\dot{x}$  = velocity of the mass

$\ddot{x}$  = acceleration of the mass

and substituting equation (4.1) into (4.2), then,

$$\ddot{x} + \frac{c}{m}\dot{x} + \frac{k}{m}x = 0 \quad (4.3)$$

From this differential equation, it is apparent that the gravity force and/or its moment acting on the system will be cancelled by the force and/or moment produced by the elastic elements in the static-equilibrium position. In other words, for the static situation, the total weight on bit will not change with an increase in length of the drill string while drilling.

## 4.2 Analysis of the Buckling and Bending of the Drill String

Since the drill string is considered as a long-uniform pipe which is slender compared to its length, it is necessary to investigate its failure by buckling under the longitudinal feed force and the critical load under certain boundary conditions. Generally speaking, the stability of the drill rod acted on by the feed forces at its top end, depends on its material, boundary conditions at both ends, length and axial forces. If either the length or the axial forces of the rod exceeds the critical limit, bending or buckling will produce lateral forces which act on the drill rod. Therefore the results of examining the stability of the drill string are useful for studying the deviation of

an ITH percussive drill. All the calculations for the buckling or bending of the drill string are based on the theory of strength of materials.

An ideal drill string is assumed to be initially straight and subjected to axial compressive loads to maintain good bit contact with the rock. However, in reality, the string always has unavoidable eccentricities due to excessive axial loads and/or wear which produce the moments along the string. If the eccentricity is small and the string is short, the lateral deflection is negligible and the flexural stress is insignificant compared with the direct compressive stress. A long string, however, is quite flexible because deflection is proportional to the cube of the length. A relative low value of axial load may thus cause a large flexural stress by the moments. Therefore, as the length of the string increases, the flexural stress increases. Figure 4.2 shows that when the axial loads (Y-axis) and/or length of the string (X-axis) exceed the critical load and/or critical length, buckling of the string will occur with subsequent failure.

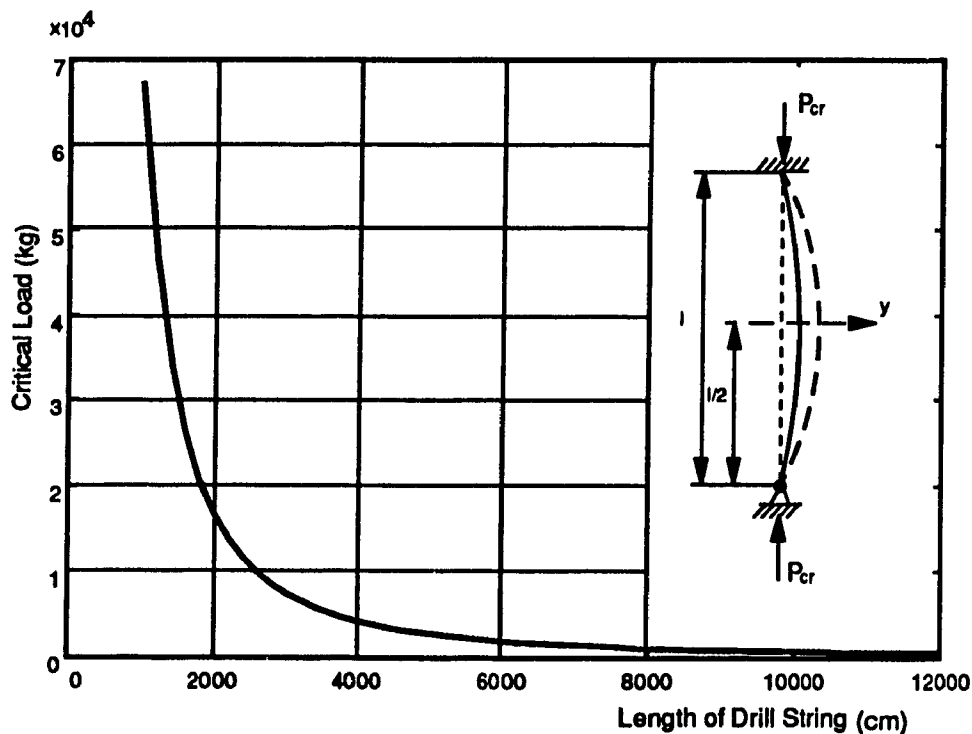


Figure 4.2: Critical Load *versus* Length of the Drill String

### 4.2.1 Critical Load and Critical Length

In this section, the simple but basic theory of critical load and/or length of rod which are subjected to the axial forces from drilling are reviewed to provide a better understanding of these concepts. A theoretical analysis of the critical load for a long drill string is based on Euler's Formula, defined as

$$P_{cr} = \frac{\pi^2 EI}{(k_l l)^2} \quad (4.4)$$

where

$l$  = length of the drill string

$I$  = moment of inertia of the drill string

$k_l$  = coefficient of length

$P_{cr}$  = critical load

$E$  = modulus of elasticity

The value of  $k_l$  depends on the boundary conditions of both ends of the string. There is some difference between the boundary conditions considered here and those discussed above. The boundary condition of the drill string can be considered as fixed-pinned, where according to Euler's Formula,  $k_l$  would be equal to 0.7. A sample calculation was made based on actual data obtained from field tests with a CD-90B ITH drill (refer to Section 4.2.4). These results are represented in figure 4.2, where, for example, when the length of the drill string exceeds 20 m, the axial compressive loads are seen to decrease quickly.

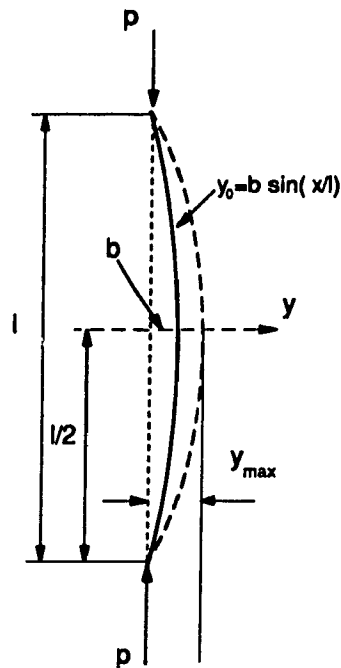


Figure 4.3: Diagram of Buckling of Drill String

### 4.2.2 The Bending of the String Before Unstabilizing

The condition investigated in this section is quite different from that discussed in section 4.2.1. Here it is assumed that the drill string has a small initial curvature<sup>2</sup> which produces a large change in the effect of the axial force on the deflection, see figure 4.3.

Let  $y_0$  (thick solid line) denote the initial deflection curve of the string and  $y_1$  the deflection curve produced by the axial force, so that the total deflection  $y$  (thick dashed line) after bending is

$$y = y_0 + y_1 \quad (4.5)$$

and let the initial deflection curve be

$$y_0 = b_1 \sin \frac{\pi x}{l} + b_2 \sin \frac{2\pi x}{l} + \dots \quad (4.6)$$

<sup>2</sup>Actually, most drill strings have initial curvatures due to hole deviation, drill string joints and bending due to wear and tear

and the deflection curve produced by the axial load is

$$y_1 = a_1 \sin \frac{\pi x}{l} + a_2 \sin \frac{2\pi x}{l} + \dots \quad (4.7)$$

then, the work done by the axial force ( $w_1 - w_0$ ) is

$$w_1 - w_0 = \frac{1}{2} \int_0^l \left[ \frac{d(y_1 + y_0)}{dx} \right]^2 dx - \frac{1}{2} \int_0^l \left[ \frac{dy_0}{dx} \right]^2 dx \quad (4.8)$$

If the string is given an infinitely small additional deflection,  $da_n \sin(n\pi x/l)$ , the work done by the axial load  $P$  during this deflection is

$$P \frac{\partial(w_1 - w_0)}{\partial a_n} da_n = P \frac{n^2 \pi^2}{2l} (a_n + b_n) da_n \quad (4.9)$$

The increase in strain energy in this case is

$$\frac{EI\pi^4}{2l^3} n^4 a_n da_n \quad (4.10)$$

and the increase in strain energy is equal to the work done by the axial force  $P$ , from equation (4.9) and (4.10), that is

$$\frac{EI\pi^4}{2l^3} n^4 a_n da_n = P \frac{n^2 \pi^2}{2l} (a_n + b_n) da_n \quad (4.11)$$

Let  $q = Pl^2/EI\pi^2$ , the relationship of  $a_n$  and  $b_n$  can be found as

$$a_n = b_n \frac{q}{n^2 - q} \quad (4.12)$$

Substituting  $a_n$  into equation (4.7), the deflection curve of the string produced by the axial load can be defined as

$$y_1 = q \left[ \frac{b_1 \sin \frac{\pi x}{l}}{1 - q} + \frac{b_2 \sin \frac{2\pi x}{l}}{2^2 - q} + \dots \right] \quad (4.13)$$

If it is also assumed that the initial deflection is  $y_0 = b \sin(\pi x/l)$ , then

$$y_1 = \frac{qb \sin \frac{\pi x}{l}}{1 - q} \quad (4.14)$$

Therefore, according to the equation (4.5), the total deflection  $y$  is equal to

$$y = y_0 + y_1 = \frac{b}{1 - q} \sin \frac{\pi x}{l} \quad (4.15)$$

and the angle or the slope at  $x$  is

$$\theta(x) = \frac{dy}{dx} = \frac{b\pi}{(1-q)l} \cos \frac{\pi x}{l} \quad (4.16)$$

When  $x = l$  and  $x = 0$ , in equation (4.15) and (4.16), there will be a maximum deflection  $y_{max}$  in the middle of the string and maximum angle  $\theta_{max}$  at both ends of the string. Generally speaking, when maximum deflection exceeds the tolerance between the drill rod and hole wall, it will touch the hole wall, which implies that the lateral forces needed to induce the hole deviation will be created at both the middle point and each end of the drill rod. The angle,  $\theta$ , especially at the bottom end of the drill rod, should be one of the characteristics to evaluate hole deviation. 3-D plots, in figure 4.4 and figure 4.5, are results based on calculations using equation 4.15 and 4.16. These plots indicate the relationship between the maximum deflection and/or the maximum angle of the string, axial load and change of length of the string. When the axial load and length increases, the maximum deflection increases, and the maximum angle decreases (figure 4.4 and 4.5). What should be noted is that all the calculations and derivations of the equations are based on the assumption of a small initial deflection and the axial load not exceeding the critical load.

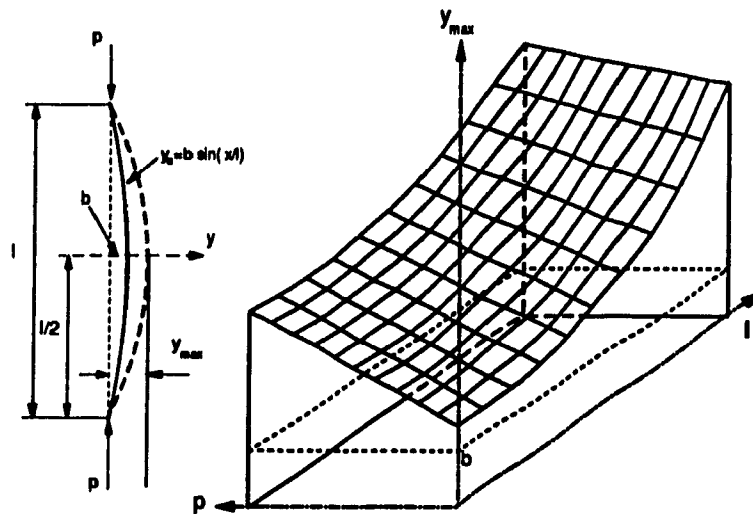


Figure 4.4: 3-D Plot for Maximum Deflection

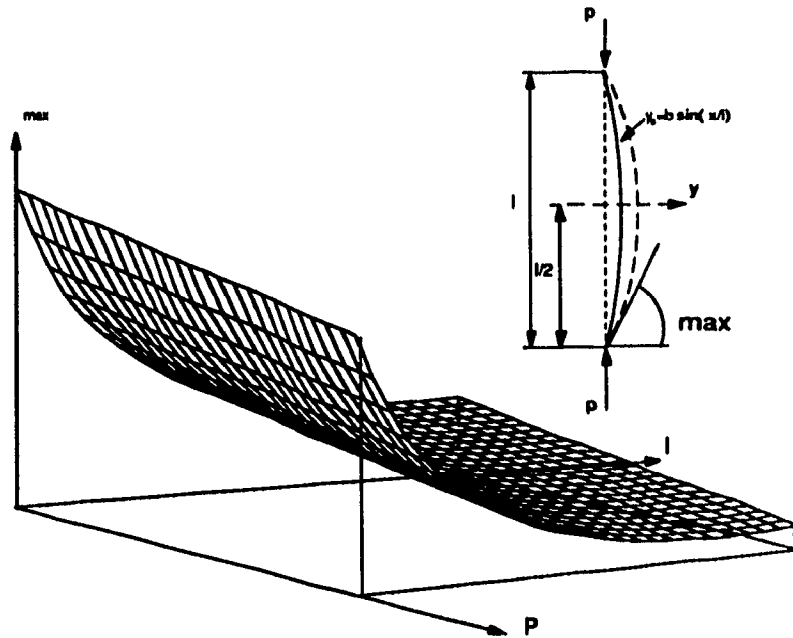


Figure 4.5: 3-D Plot for Maximum Angle

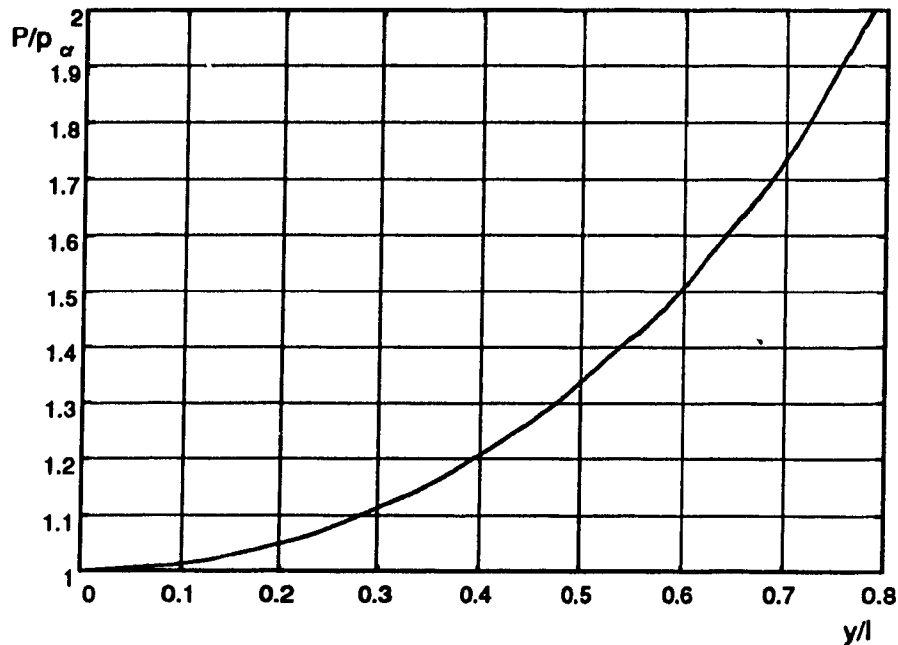
### 4.2.3 The Deflection of the String After Unstabilizing

If the axial load is larger than the critical load, then drill string buckling will occur. The deflection of the string can be expressed by the equation [14]:

$$Y = \frac{l\sqrt{8}}{\pi} \sqrt{\frac{p}{P_{cr}} - 1} \left[ 1 - \frac{1}{8} \left( \frac{p}{P_{cr}} - 1 \right) \right] \quad (4.17)$$

The relationship between the load and deflection can be represented as shown in figure 4.6. As long as the load is smaller than  $P_{cr}$  ( $p/P_{cr} < 1$ ), the deflection<sup>3</sup> is zero. Beyond this limit, the deflection will increase rapidly with the load. It is very important, therefore, to determine the critical load for a long drill string to avoid buckling. If the drill string has an initial deflection before unstabilizing, the deflection of the string increases rapidly due to the axial compressive load. After unstabilizing, the string fails very quickly.

<sup>3</sup> $Y/l$  is ratio of deflection to length of rod

Figure 4.6: Vertical Load *versus* Deflection

#### 4.2.4 Calculations of Critical Length and Generated Forces

For practical applications, the critical length at particular feed forces was calculated for both cases i.e. with and without a small initial deflection. The forces acting on the drill string (or on the borehole wall) due to the buckling and bending of the string were also analyzed.<sup>4</sup> It is believed that if the buckling or bending happens (the string touches the borehole wall), it will result in deviations of the desired hole trajectory. The following values were used in the calculations and analysis based on data monitored from a CD-90B ITH long-hole drill operating at the Little Stobie Mine:

$$E = 200 \times 10^9 \text{ Pa} = 200 \times 10^9 \text{ N/m}^2$$

$$P \text{ (feed force)} = 3000 \text{ lb} = 1.3345 \times 10^4 \text{ N}$$

$$D_{in} = 6.125 \text{ in} = 0.1556 \text{ m}$$

$$D_{out} = 6.5 \text{ in} = 0.1651 \text{ m}$$

$$D_h = 8.5 \text{ in} = 0.216 \text{ m}$$

<sup>4</sup>The effect of the distribution of the mass along the drill string is not taken into account.

$$b \text{ (initial deflection)} = 0.1 \text{ in} = 0.0025 \text{ m}$$

$$y_{1max} = (D_h/2 - D_{out}/2) - b = 0.9 \text{ in} = 0.02286 \text{ m}$$

$$b_1 \text{ (new initial deflection)} = (D_h/2 - D_{out}/2) = 1 \text{ in} = 0.0254 \text{ m}$$

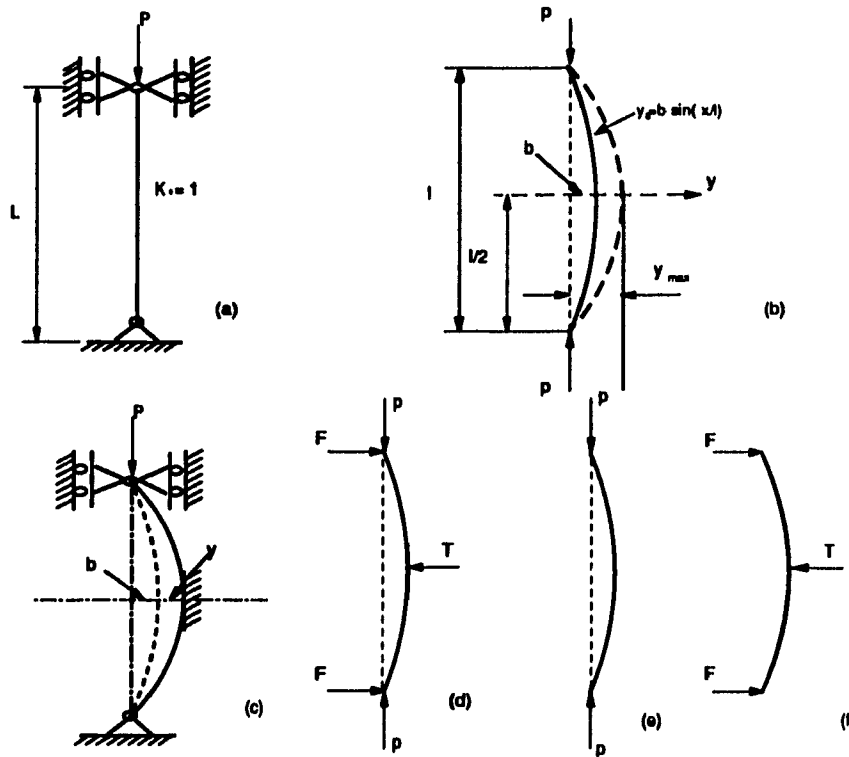


Figure 4.7: Boundary Condition and Initial Deflection of the Drill String and Calculation of Horizontal Forces of the Drill String

### Calculation of Critical Length Without Initial Deflection

According to equation (4.4), if the boundary condition is assumed as in figure 4.7 (a), and the critical force is assumed to be the feed force, the critical length of the drill string can be expressed as:

$$L = \sqrt{\frac{\pi^2 EI}{K_0^2 P}} \quad (4.18)$$

where

$I$  = moment of the drill string

$K_0$  = coefficient of the length (depends on the boundary condition)

Substituting the values listed above into equation (4.18), then

$$L = 34 \text{ m}$$

This is to say that when the feed force is kept constant ( $1.3345 \times 10^4 \text{ N}$ ), the maximum length of the drill string without unstabilizing will be equal to 34 m. Figure 4.8 shows the relationship between the critical length of the string and the feed force without the initial deflection. What should be noted is that the calculations were made based on assumptions of an uniform cross sectional area drill string, constant feed force and certain boundary conditions for the drill system.

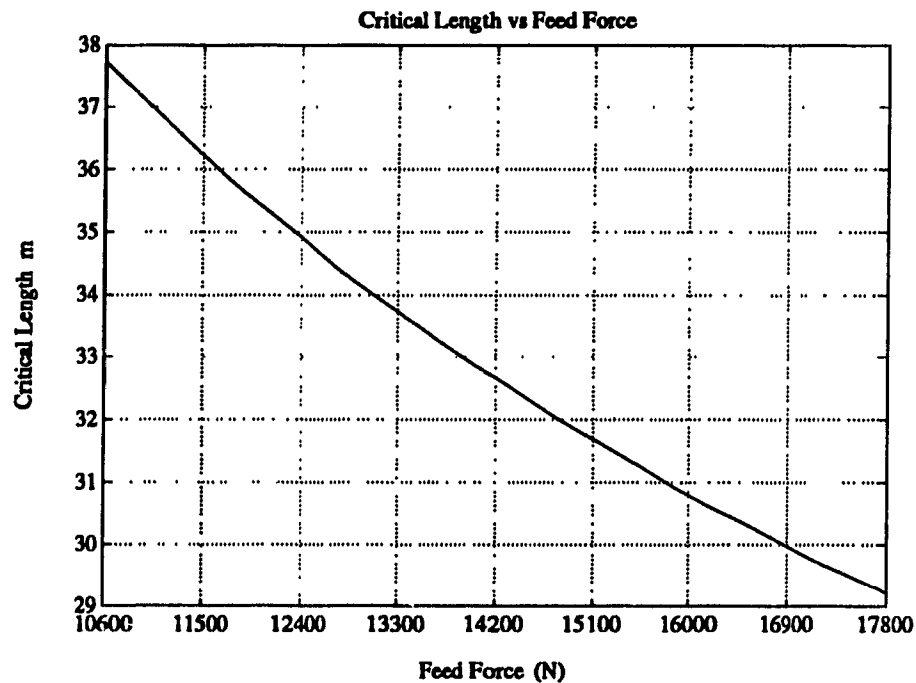


Figure 4.8: Feed Force *versus* Critical Length without Initial Deflection

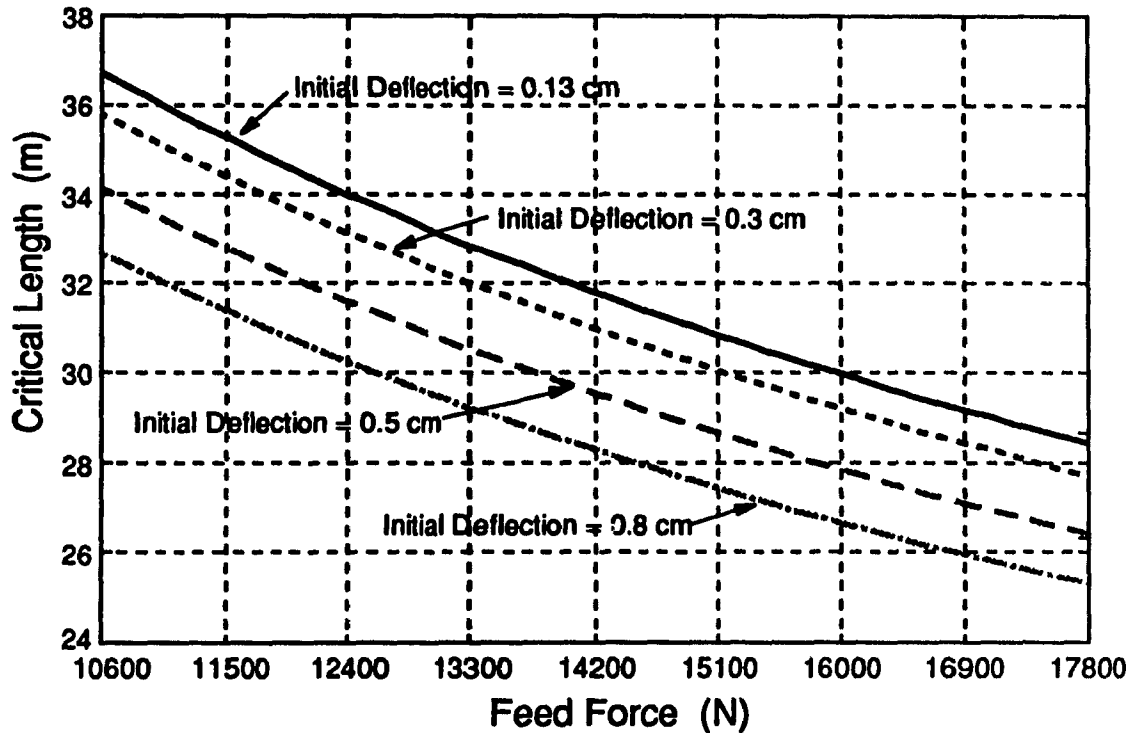


Figure 4.9: Feed Force *versus* Critical Length with Different Initial Deflection

#### Calculation of Critical Length with Initial Deflection

Figure 4.9 shows another case when the critical length of the string with initial deflection is calculated. In this calculation, the same boundary conditions and feed forces have been assumed as in the previous case. Based on the theory of section 4.2.2, the initial deflection curve of the string should be  $y_0 = b \sin(\pi x/l)$ . Equation (4.14) gives, (note that  $q = Pl^2/EI\pi^2$ )

$$L = \sqrt{\frac{y_{1max} EI \pi^2}{P(y_{1max} + b)}} \quad (4.19)$$

where

$b$  = maximum initial deflection of string

$y_{1max}$  = maximum deflection produced by axial load

Substituting the values given earlier into this equation gives,

$$L = 32 \text{ m}$$

This implies that the maximum length of the string, with an initial deflection insufficient to allow any drill string contact with the borehole wall due to bending, is less than that without the initial deflection. The results also indicate that the more the initial deflection, the shorter will be the maximum length of string without serious bending. This feature was clearly indicated by figure 4.8 which reveals the relationship between the feed force, critical length and initial deflection.

### Calculation of Lateral Forces Due to String Bending

When there is considerable steel bending, lateral forces  $T$  and  $F$  (see figure 4.7 (d), (e) and (f)) will be created to act on both sides and at the middle point of the string due to contact with the borehole wall. The feed force is still being applied to the upper end of the string at the same time, thus producing hole deviation. Figure 4.7 (e) is a diagram of the forces acting on the string for the case where there is no contact with the borehole walls. Figure 4.7 (f) shows the horizontal forces acting on the string when it touches the walls of the hole due to the bending. In this case, the deflection of the middle point of the string will be:

$$y = \frac{Tl^3}{48EI} \quad (4.20)$$

Examining equations (4.14) and (4.20) and the results of force balances, yields

$$\frac{Pl^2b_1}{EI\pi^2 - Pl^2} = \frac{Tl^3}{48EI} \quad (4.21)$$

or,

$$T = \frac{48EIPb_1}{l(EI\pi^2 - Pl^2)} \quad (4.22)$$

Substituting  $E, I, P, b_1$  and  $l = 32 \text{ m}$  into equation (4.22), then,

$$T = 514 \text{ N}$$

and

$$F = T/2 = 257 \text{ N}$$

where  $T$  and  $F$  are lateral forces acting on the middle and both sides of the string due to its bending (refer to figure 4.7 (d)(f)).

Figure 4.10 and 4.11 are results of the calculations based on some initial assumptions. Because equation (4.22) was derived from a classical beam deflection equation (equation (4.14)) and the bending equation (4.20), it is necessary to assume the string should be nearly straight when its middle point touches the wall of the hole because of bending. These same assumptions apply when calculating the lateral forces in the region where the string is unstabilized either for the critical length or critical feed force limit. When the length of string or feed force exceeds the critical limit, equation (4.22) can not be used any more. This is due to the fact that when the string oscillates due to unstabilizing, there will be a non-linear deflection acting on it and thus no certain deflection curve can be predicted. Some results from the monitoring of a CD-90B drill underground show that most hole deviations have only one deflection along a particular direction for the entire length of hole. Therefore, it is important to study the initial bending of the string when dealing with the problems of hole deviation.

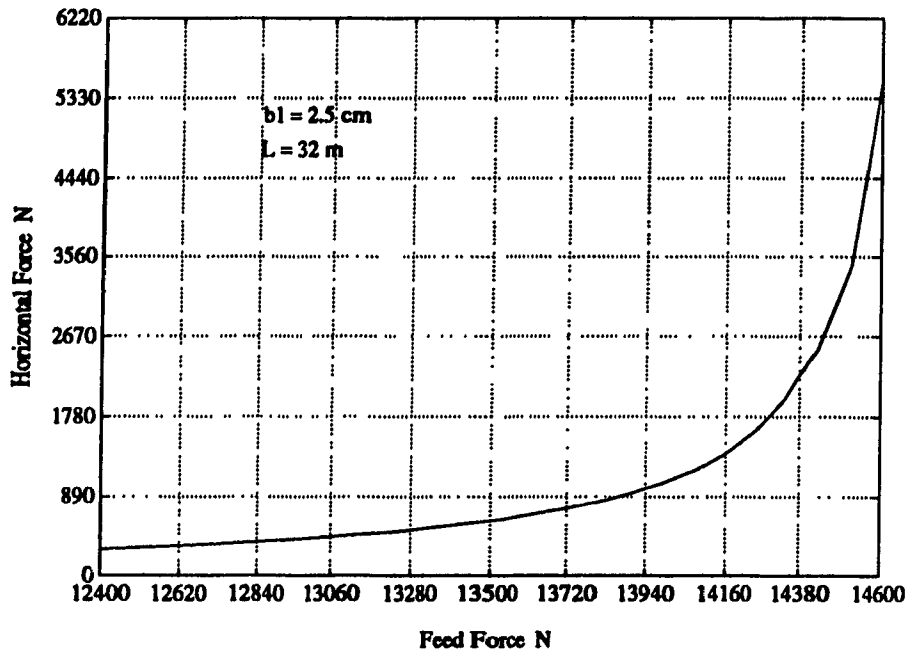


Figure 4.10: Feed Force *versus* Horizontal Force

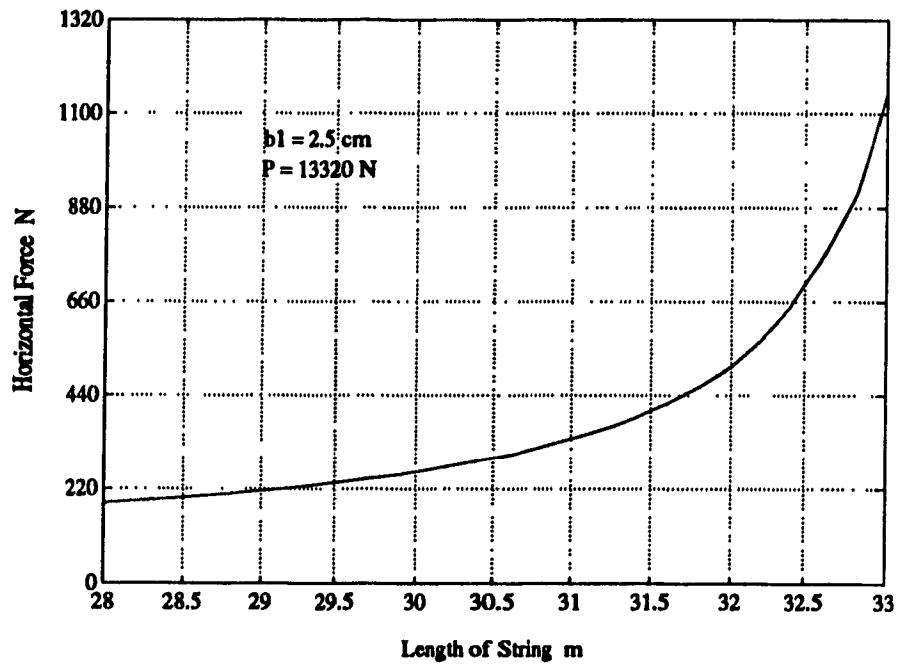


Figure 4.11: Length of String *versus* Horizontal Force

## Chapter 5

# Continuous System and Boundary Conditions

An analysis diagram of the CD-90B ITH percussive drill monitored in underground tests is shown in figure 5.1 (a)(b). All the basic elements of the drill system such as the string, the hammer case, and the shock absorber are included. Also shown is the coordinate system used in the analysis.

### 5.1 Assumptions

The CD-90B ITH percussive drilling system consists of the drill string, the hammer assembly and the equipment out of the hole (carrier). To reduce the complexity of the system and thus derive a mathematical model, it is necessary to make some initial assumptions and simplifications of the system when the boundary conditions are selected.

It is assumed that the drill string is a long pipe having a uniform cross-sectional area and without any joints with the latter assumed to have a negligible effect on the longitudinal and torsional vibrations. The forces that excite the drill string are assumed to act on the bit, that is they act on the bottom end of the hammer assembly. In reality, the excited force is related to the rock properties, bit shape, piston final

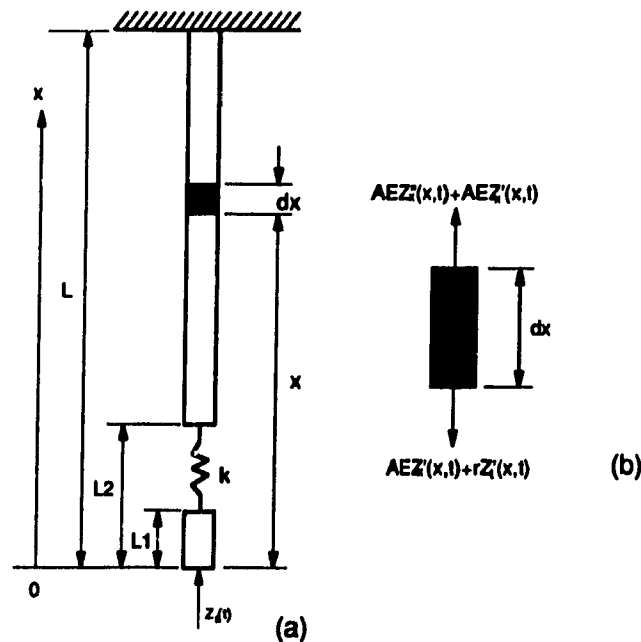


Figure 5.1: Analysis Diagram of the ITH Drill String

velocity, air pressure, cross sectional area of the hammer casing and the piston [12]. It is known from the current field studies, however, that the main source of the drill string vibration is the force generated by the action of the piston. It can be defined as an harmonic force for the purpose of the derivation of the mathematical equations. The bit displacement, which is the remaining boundary condition, is defined by (see Figure 5.1(a))

$$z_1(0, t) = z_0 \sin(\omega_0 t)$$

where

$z_1$  = longitudinal displacement of the bit

$z_0$  = amplitude of bit displacement

$\omega_0$  = frequency of bit displacement

Each type of drill system vibration (longitudinal, torsional and lateral) is assumed to be independent of the other two. The functions developed only in terms of longitudinal parameters, however, can be used for an analysis of the drill string torsional vibration problems simply by changing the symbols of the functions. The friction between the drill string, the case and the wall of the hole are approximated as viscous friction. The damping in the shock absorber is also considered to be viscous.

## 5.2 Boundary Conditions

In order to calculate the natural frequencies of the drill string, the boundary conditions at the ends of the string must be known when the frequency functions are derived. Due to the complex structure of the drill system, however, some boundary conditions can only be chosen through an analysis of the data measured from actual experiments conducted while drilling. Therefore, it is necessary to make some initial assumptions to choose these boundary conditions.

Because there are many differences between the tricone rotary and percussive drill systems, both are defined by a different set of boundary conditions. In many papers dealing with the vibrations of rotary drills, the bottom end of the boundary condition of the drill string was specified as a fixed end. This is the result of the rock breakage mechanism of a tricone rock bit, where the up-and-down motion of the bit due to the rolling of the teeth (generally speaking 1.5 cm or less ) was neglected.

For the percussive drill system, the main cutting action is the axial impact of the bit. The bit moves up-and-down and rebounds under the impact of the hammer where relatively speaking, this motion is quite large. This means that the bottom end of the drill string (and the bottom end of the hammer case) moves like a free end of a beam as shown in figure 5.1 (a). Therefore, the bottom end of the hammer case can be considered as a free end with an exciting force. In one set-up, the structure of the drill string and the hammer case are connected by a shock absorber. The exciting force acting on the bottom end of the case is also considered part of the

boundary conditions. The boundary conditions of the bottom end of the drill string, and hammer case and the top end of the hammer are, therefore, (refer to Figure 5.1

(a))

$$z_1(L_1, t) = z_2(L_2, t) \quad (5.1)$$

$$A_1 E_1 \frac{\partial z_1}{\partial x(L_1)} = A_2 E_2 \frac{\partial z_2}{\partial x(L_2)} \quad (5.2)$$

and

$$z_1(0, t) = z_0 \sin(\omega t) \quad (5.3)$$

where

$z_1(L_1, t)$  = longitudinal displacement of the top end of the case

$z_2(L_2, t)$  = longitudinal displacement of the bottom end of the string

$z_1(0, t)$  = longitudinal displacement of the bit

Assuming the feed cylinder exerts a load on the top of the drill string and the feed force is much larger than the force associated with string stress, the displacement of the top of string can be estimated to be equal to zero. This means that it is possible to assume the boundary condition at the top end of the string to be fixed-end. (Relatively speaking, from the data obtained from measurements of field tests of CD-90B ITH drill, the displacement of the drill head was much less than that of drill bit. Refer to chapter 7.) From this assumption, the boundary condition at the top end of the string can be expressed as (see figure 5.1(a))

$$z_2(L, t) = 0 \quad (5.4)$$

Where

$z_2(L, t)$  = longitudinal displacement of the top of the string

### 5.3 Natural Frequency

After the boundary conditions have been selected, the natural frequencies of the drill system can be defined from the frequency functions. As a continuous system, the drill string has infinite natural frequencies. Only a few of the lower frequencies, however, are of interest because the longitudinal resonance occurs in this region. The first to fifth natural frequencies will be selected for undertaking a mode analysis of the drill string.

### 5.4 Solution of Drill System Functions

Since continuous systems are different from a lumped system, the derivation of the frequency or wave functions is more difficult, especially in the case of a force-excitation system. For an uniform and fixed-free long string, applying the concept of equilibrium to a section of drill string (figure 5.1(b)), and summing the material stresses, viscous friction forces and inertial forces, the wave function can be derived as,

$$AE \frac{\partial^2 z}{\partial x^2} = c_1 \frac{\partial z}{\partial t} + \rho \frac{\partial^2 z}{\partial t^2} \quad (5.5)$$

The solution to equation (5.5) is

$$z(x, t) = q(x)e^{i\omega t} \quad (5.6)$$

Where substituting the complex equation (5.6) into (5.5) gives

$$AE \frac{\partial^2 q(x)}{\partial x^2} + (\rho\omega^2 - ic_1\omega)q(x) = 0 \quad (5.7)$$

That is

$$\frac{\partial^2 q(x)}{\partial x^2} + h^2 q(x) = 0 \quad (5.8)$$

Where

$$h^2 = \frac{\rho\omega^2 - i\omega c_1}{AE} = \frac{\omega^2}{c^2} - i \frac{c_1\omega}{AE} \quad (5.9)$$

The solution to equation (5.8) is

$$q(x) = D \sin(hx + d) \quad (5.10)$$

and, therefore, the solution to equation (5.5) is

$$z(x, t) = D \sin(hx + d)e^{i\omega t} \quad (5.11)$$

The solution (5.11) of equation (5.5) can be applied to both the string and hammer casing section. By finding  $D$  and  $d$ , the function  $z(x, t)$  can be determined to get an overall response of the drill string due to the source of excitation described by equation (5.3).

For an undamped, fixed-free uniform string, another form of equation (5.11) can be derived as,

$$z(x, t) = (A \cos \frac{\omega}{c}x + B \sin \frac{\omega}{c}x)e^{i\omega t} \quad (5.12)$$

with the boundary conditions

$$z(L, t) = 0, \quad \frac{\partial z}{\partial x}(0, t) = 0 \quad (5.13)$$

It is found that

$$A = 0$$

and

$$\cos\left(\frac{\omega l}{c}\right) = 0$$

which is satisfied when

$$\frac{\omega_n l}{c} = \frac{n\pi}{2} \quad n = 1, 3, 5, \dots$$

The undamped natural frequencies are then found to be

$$\omega_n = \frac{n\pi c}{2l} \quad n = 1, 3, 5, \dots$$

which is the so called frequency function. For the damped, excited, fixed-free system as shown in Figure 5.1 (a), the boundary conditions are

$$z(0, t) = iz_0 e^{i\omega t} \quad (5.14)$$

and

$$z(L, t) = D_2 \sin(h_2 L + d_2) e^{i\omega t} \quad (5.15)$$

and

$$[z(L_1, t) - z(L_2, t)] k = A_1 E \frac{\partial z_1}{\partial x} = A_2 E \frac{\partial z_2}{\partial x} \quad (5.16)$$

Substituting equations (5.14), (5.15), (5.16) into equation (5.11) respectively, then,

$$D_1 = -i \frac{z_0}{\sin d_1} \quad (5.17)$$

$$d_2 = -h_2 L \quad (5.18)$$

$$D_2 = \frac{\sin(h_1 L_1 + d_1) k D_1}{A_2 E h_2 \cos(h_2 L_2 + d_2) + \sin(h_2 L_2 + d_2) k} \quad (5.19)$$

$$d_1 = \tan^{-1} \left[ \frac{A_1 h_1}{A_2 h_2} \left( \frac{A_2 E h_2}{k} + \tan(h_2 L_2 + d_2) \right) - h_1 L_1 \right] \quad (5.20)$$

In order to calculate the relative magnitude of the displacements or stresses of each section of the string, it is necessary to solve equation (5.11) by choosing some natural frequencies, determining the boundary conditions and  $D_1, D_2, d_1, d_2$ , and starting at one end of the drill string. For each mode of interest, the procedure can be repeated to determine the solutions.

It is apparent that the numerical calculations are very tedious if data for many different sections of the drill string are needed. Several programs have been developed by the author to solve the functions with the use of a computer.

## 5.5 The Complex Boundary Condition

In the previous section, several different boundary conditions of the drill string have been discussed such as fixed-free (top end of string fixed and bottom end of string free) and free-fixed. The wave function and frequency function of the system were derived based on the typical fixed-free boundary condition of the drill string (Figure 5.2). As mentioned in the previous section, the actual drill system and subsequent simplification of the system are the primary reasons for choosing this boundary

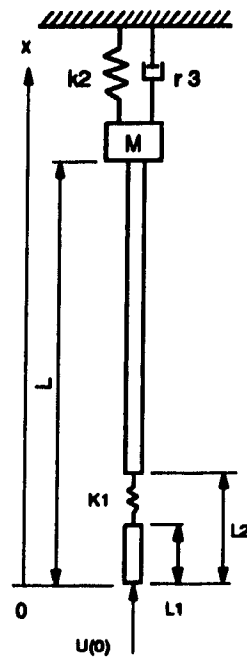


Figure 5.2: Complex Diagram of the ITH Drill with the Surface Equipment Included condition. Another more complex boundary condition of the drilling system will also be considered here in order to achieve more acceptable results from calculations using the analysis model for the actual working conditions of drilling.

When also considering the surface equipment of the ITH drilling system, this component can be described as being composed of a spring-damping element and a lumped mass connected directly to the top end of the drill string, see figure 5.2. Since in reality, there are displacements at the top end of the drill string and on the drill head, it is appropriate to choose this boundary condition to simulate the drilling system. The boundary condition of the bottom end of the drilling system is still considered, however, as a free end. As a result of this approach, only the boundary condition of the top end of the drill string will be investigated in the following analysis.

## 5.6 Solution to the Boundary Condition

The solution for the damped-forced continuous system is (refer to equation (5.11))

$$z(x, t) = D \sin(hx + d)e^{i\omega t} \quad (5.21)$$

At  $x = L$ , applying the concept of equilibrium to the mass  $M$ , we get

$$z(L, t)k_2 + \frac{M}{g} \frac{\partial^2 z(L, t)}{\partial t^2} + A_2 E \frac{\partial z(L, t)}{\partial x} + r_3 \frac{\partial z(L, t)}{\partial t} = 0 \quad (5.22)$$

where

$k_2 =$  spring rate of the surface equipment

$r_3 =$  damping ratio of the surface equipment

$z(L, t) =$  displacement of the top end of the string

Substituting equation (5.21) into equation (5.22) gives

$$k_2 \sin(h_2 L + d_2) - m\omega^2 \sin(h_2 L + d_2) + A_2 E h_2 \cos(h_2 L + d_2) + i\omega r_3 \sin(h_2 L + d_2) = 0 \quad (5.23)$$

That is

$$d_2 = \tan^{-1} \left[ \frac{A_2 E h_2}{m\omega^2 - i\omega r_3 - k_2} \right] - h_2 L \quad (5.24)$$

where  $D_1, D_2, d_1$  are described by equations (5.17) (5.19) (5.20) respectively.

## Chapter 6

# Model Simulation and Analysis

### 6.1 Objectives

In chapter 5, the mathematical models of the ITH percussive drill system for both lumped mass and continuous systems have been defined based on the theory of vibration. Several sets of boundary conditions have also been analyzed for different drill system models. Since the research described in this thesis form parts of a project on developing automatic control for an ITH percussive drill, the mathematical models will be a component of the control simulator while also providing the necessary tools to analyze the drill system vibration responses. Therefore, it becomes necessary to simulate mathematical models by using the actual characteristics of the CD-90B ITH drill. Comparison of the simulation responses with the real data measured from field testing of CD-90B ITH drill will be means by which the models are modified and to adjust some of the constants in the mathematical functions. Furthermore, an analysis of the simulation results reveal some of the vibration characteristics of the ITH percussive drill system, especially in light of its ability to dampen and thus determine an appropriate spring rate for a shock absorber to absorb or/and isolate the vibration from transferring to drill string. Another goal of the simulation was to study the vibration responses such as acceleration, velocity and displacement versus

time, along the drill string and the frequencies.

Considering the complexity of the vibrations for an ITH percussive drill, either the lumped model and continuous system model will be simulated to study both short and long rod vibration responses. Several sets of boundary conditions for the continuous system of the ITH drill also need to be validated. On the other hand, it becomes convenient for the mode analysis to use some results of the simulation of the continuous system.

## **6.2 Statement of Simulations**

### **6.2.1 The excitation forces**

The excitation forces were assumed as either the harmonic or impulse input. In order to undertake a mode analysis of the continuous system,<sup>1</sup> harmonic forces will be used as the input of the drill system in the simulation of the continuous system. However, the simulation of the lumped mass model and continuous system for different boundary conditions will be undertaken using the impulse input as the excitation forces of the drill system.

### **6.2.2 The responses of the simulation**

Since all of the vibration data measured from field testing of the CD-90B ITH percussive drill was acquired using accelerometers, the main output of the simulation will also be acceleration data for easy comparison to the real data. Velocity, displacement and stress along the drill string can also be easily obtained from the acceleration data by a mathematical calculation. For the lumped mass model, the damping ratio will be recovered as the results of the simulation through the use of one set of real vibration data.

---

<sup>1</sup>The forces acting on the drill bit will be confirmed as impulse input in chapter 7.

### 6.2.3 The boundary condition

Several sets of boundary conditions, such as Fixed-Fixed and Free-fixed, will be chosen to run the simulations.

### 6.2.4 The damping

The damping of the ITH percussive damping will still be assumed as viscous damping due to the lack of the data to evaluate the constant factor of the friction damping.<sup>2</sup>

### 6.2.5 The system characteristics and the data

The data chosen to run the lumped model simulation is STG06A (Shock absorber Test rod 6, rod length was equal to 4.6 meter or 15 feet).<sup>3</sup> for the reason that it was obtained using a short rod drilling case. The following data was derived from actual field tests at INCO's Little Stobie Mine of a CMS CD-90B ITH production drill with a shock absorber and input into the computer simulation program: (refer to figure 5.1)

$$\begin{array}{ll}
 A_1 = 160 \text{ cm}^2 & A_2 = 23.8 \text{ cm}^2 \\
 L_1 = 9.6 \text{ m} & L_2 = 10.67 \text{ m} \\
 D_h = 203.2 \text{ mm} & D_p = 144.78 \text{ mm} \\
 D_{in} = 155.58 \text{ mm} & D_{out} = 165.1 \text{ mm} \\
 c = 50038 \text{ m/s (for steel)} & k = 4.9 \times 10^7 \text{ N/m} \\
 E = 10^4 \text{ kg/cm}^2 \text{ or } 98 \text{ GPa} & \\
 \omega_n = n\pi c/2l \text{ rad/s} & n = 1, 3, 5 \dots
 \end{array}$$

<sup>2</sup>However, there is little difference with viscous and friction damping for the vibration responses when the length of the drill string is relatively short, i.e. as for the lumped mass model

<sup>3</sup>When the rod length is relatively short, the drill string can be defined as a lumped mass system

### 6.3 Simulation of Multiple-Degree-of-Freedom Model

As mentioned in chapter 5, for an single-degree-of-freedom-system, equation (5.3) represented the differential equation of the drill string. For a forced-multiple-degree-of-freedom (forced-discrete-lumped-mass <sup>4</sup>) vibration system, this equation should be:

$$[m][\ddot{x}] + [c][\dot{x}] + [k][x] = [F] \quad (6.1)$$

where the matrix  $m$ ,  $c$  and  $k$  are the mass matrix, damping matrix and stiffness matrix respectively and  $F$  is the excitation force acting at the bottom end of the drill string.

#### 6.3.1 Identification of the damping of the shock absorber

In general, discrete and lumped-mass systems have finite numbers of degrees of freedom. For this simulation, considering a relatively short drill string, four degrees of freedom were used. The general form of the matrix equation for such four-degree-of-freedom vibration systems when subjected to an excitation force  $F$  is

$$\begin{bmatrix} m_{11} & \cdots & m_{14} \\ m_{21} & \cdots & m_{24} \\ m_{31} & \cdots & m_{34} \\ m_{41} & \cdots & m_{44} \end{bmatrix} \begin{Bmatrix} \ddot{x}_1 \\ \ddot{x}_2 \\ \ddot{x}_3 \\ \ddot{x}_4 \end{Bmatrix} + \begin{bmatrix} c_{11} & \cdots & c_{14} \\ c_{21} & \cdots & c_{24} \\ c_{31} & \cdots & c_{34} \\ c_{41} & \cdots & c_{44} \end{bmatrix} \begin{Bmatrix} \dot{x}_1 \\ \dot{x}_2 \\ \dot{x}_3 \\ \dot{x}_4 \end{Bmatrix} + \begin{bmatrix} k_{11} & \cdots & k_{14} \\ k_{21} & \cdots & k_{24} \\ k_{31} & \cdots & k_{34} \\ k_{41} & \cdots & k_{44} \end{bmatrix} \begin{Bmatrix} x_1 \\ x_2 \\ x_3 \\ x_4 \end{Bmatrix} = \begin{Bmatrix} F \\ 0 \\ 0 \\ 0 \end{Bmatrix} \quad (6.2)$$

The main damping comes from the friction between the drill string and bore hole wall and that in the shock absorber. The stiffness of the system, except that of

<sup>4</sup>A discrete system is one in which the inertial, elastic, and damping properties are all clearly described by distinct mass, springs, and damping mechanisms, respectively. When the distributed properties of the drill rod are discretized by modeling them as systems composed of lumped mass, lumped elastic elements, and modal damping, such systems are generally referred to as lumped-mass systems or lumped-parameter systems. These discrete system should not be confused with discrete-time systems, for which the variables are determined at distinct instants of time, and which are described by difference equations rather than by differential equations.[14]

the shock absorber, depend on the length of drill string chosen for every degree of freedom, the cross-sectional area of the drill string and what the material composition of the drill string. The numerical impulse input was defined at the bottom end of the drill string as the excitation force. It is apparent that the major effort for this simulation is the definition of the mass, damping and stiffness matrices. There are different types for such matrixes with different boundary conditions of the drilling system. The boundary condition used in the simulation is Fixed-Free.

This simulation is aimed mainly at finding the damping of the shock absorber, in which the field test measurements (Data STG06A) have been used as the output of the system. Since the original signal was acceleration, the velocity and displacement are the results of the double integral or single integral of the acceleration data. Figure 6.1 is a plot of the simulation which shows the relationship between the vibration outputs and the damping of the drilling system.

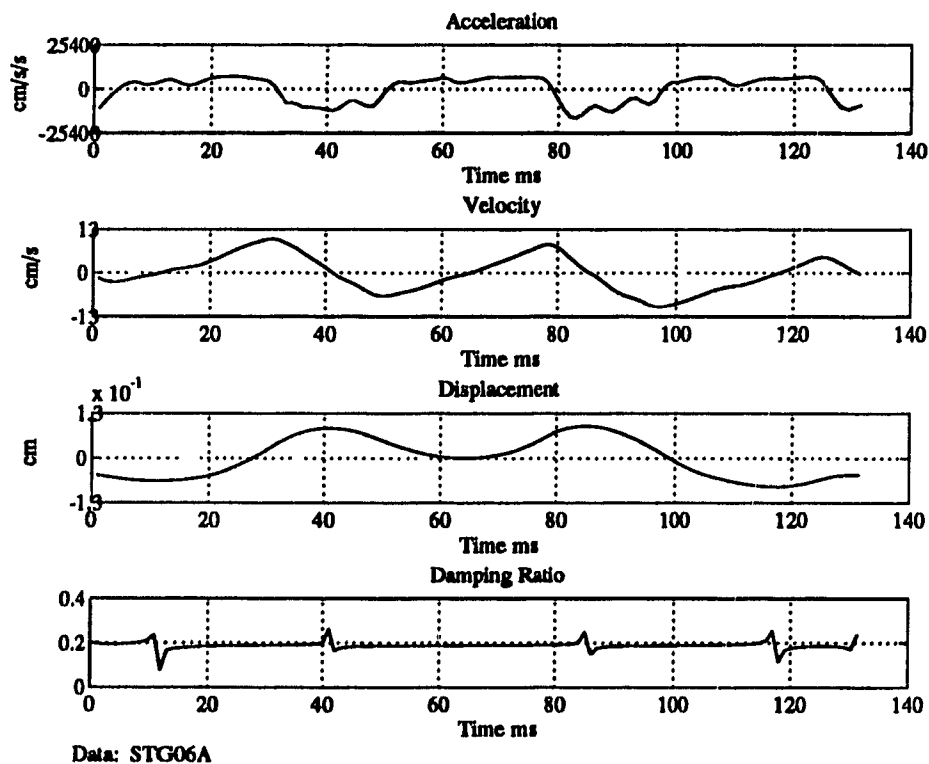


Figure 6.1: Result of the Simulation of the Multiple-Degree-of-Freedom Model

### 6.3.2 Simulation with Harmonic Excitation Force for Modal Analysis

Modal analysis basically involves the uncoupling of differential equations of motion as a means of obtaining independent equations to facilitate the response analysis of multiple-degree-of-freedom and continuous systems. The independent equations that result from the decoupling process are expressed in terms of coordinates that are referred to as *principal coordinates*, and in terms of normal-mode parameters that include the natural frequencies and modal-damping properties of the system. In this process there is one independent equation for each normal (natural) mode of vibration, and it can be solved as if it were the equation of a single-degree-of-freedom system. The system response is then obtained by superposition of the responses of the individual normal modes.<sup>5</sup>

In order to do modal analysis of the multiple-degree-of-freedom, the harmonic excitation forces acting on the bottom end of the hammer casing were assumed as the input of the drilling system. Since the lower frequency responses of the vibration are more important for the analysis of the system, the second to fifth normalized models of the drill string as shown in figure 6.3 to figure 6.7.

---

<sup>5</sup>For the continuous system, with the same principle, the modal analysis also plays an important role in studying vibration and the forced vibration of continuous systems characterized by a wave function (see chapter 5 for details) and can be analyzed by means of the superposition of the normal modes as well. The general procedure consists of assuming a solution of the form (see equation 5.6)

$$z = \sum_{i=1,2,\dots}^{\infty} q_i \phi_i$$

in which  $q_i$  is a normal-mode function that is a function of the spatial coordinate  $x$  and  $\phi_i$  is a generalized coordinate that is a function of time. The normal-mode function for a particular problem is determined from the pertinent boundary conditions, while the generalized coordinate is obtained from the solution of a second order differential equation.

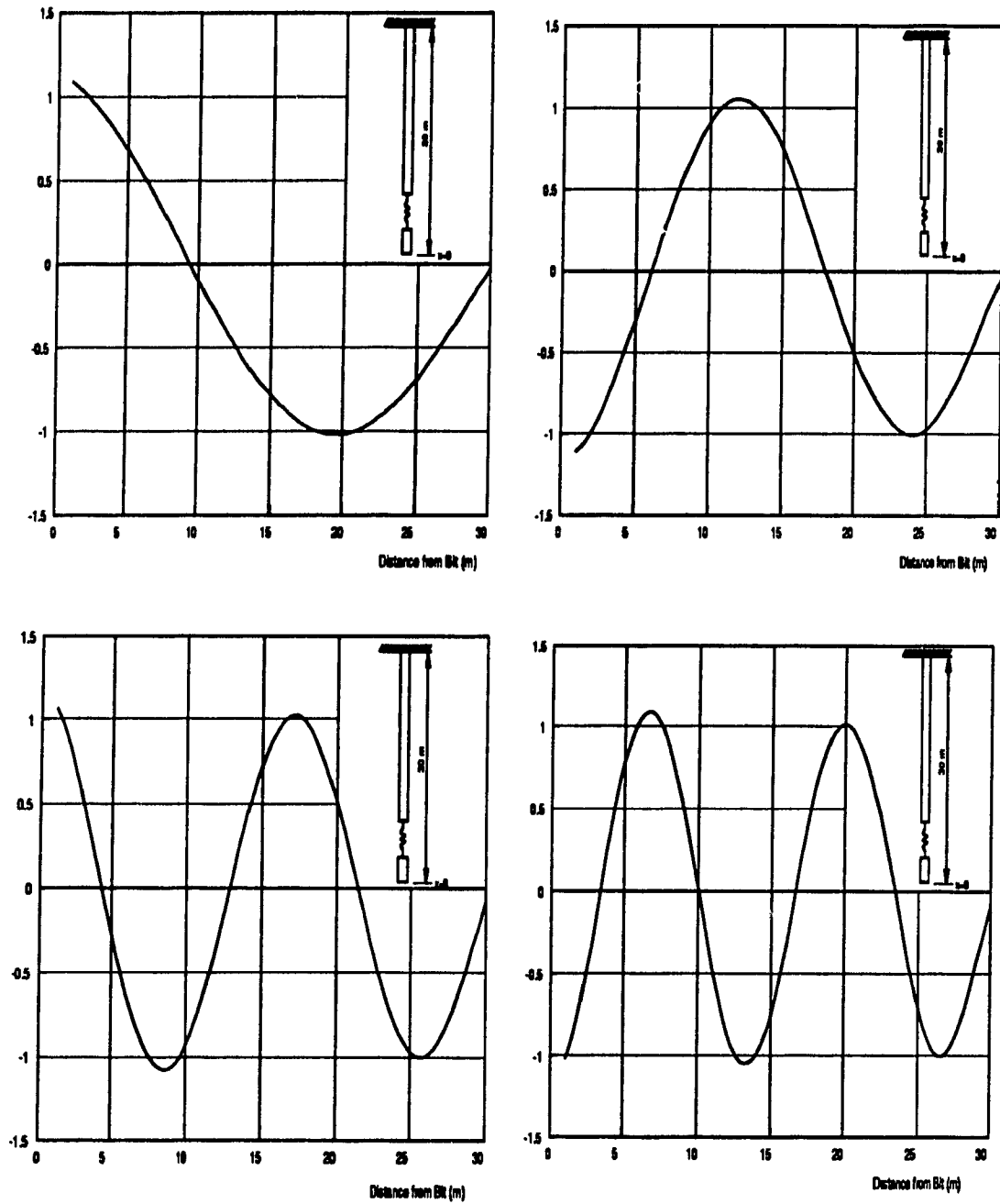


Figure 6.2: Normalized Model of Drill String; Top Left: Second Model, Top Right: Third Model, Bottom Left: Fourth Model, Bottom Right: Fifth Model

## 6.4 Simulation of Continuous System with Impulse Excitation Force

In the following simulation of the continuous system of the ITH drill, two sets of boundary conditions were used and the impulse force was defined as the input of the continuous system. The results were concentrated on determining the vibration responses for both sets versus the length of the drill rod and time at different boundary conditions based on the functions derived in chapter 5.

The actual forces causing the hammer casing and the drill string vibrations are periodic rather than harmonic, which will be verified later on in chapter 7. The resulting vibrations of the string are, therefore, characterized by the presence of several frequencies and periodic motions. In the analysis of the percussive drill vibrations, the periodic vibrations of the system can be described by waveforms containing a combination of sines and/or cosines having fundamental and other frequencies through the use of an FFT (Fast Fourier Transform). It is also a basic concept to analyze the responses of the system measured while drilling.

According to the results from field tests with an ITH drill [10], the main force causing the hammer casing to vibrate, assuming a linear response, can be simply expressed by

$$f(t) = A_c(A_v + k_{rb}t) \quad (6.3)$$

where

$A_c$  = Constant related to the cross sectional area of the casing and piston

$A_v$  = Constant related to the cross sectional area of bit and piston, density of material, velocity of sound, and final velocity of piston

$k_{rb}$  = Constant related to rock property and bit condition

$t$  = Time

Then by use of an FFT, the excitation force has the form

$$f(t) = \frac{a_0}{2} + \sum_{n=1}^{\infty} a_n \cos(n\omega t) + \sum_{n=1}^{\infty} b_n \sin(n\omega t) \quad (6.4)$$

where,

$$a_n = \frac{\omega}{\pi} \int_{-\frac{\tau}{2}}^{\frac{\tau}{2}} f(t) \cos(n\omega t) dt \quad n = 0, 1, 2, \dots \quad (6.5)$$

$$b_n = \frac{\omega}{\pi} \int_{-\frac{\tau}{2}}^{\frac{\tau}{2}} f(t) \sin(n\omega t) dt \quad n = 0, 1, 2, \dots \quad (6.6)$$

and,

$$\omega = 2\pi/\tau \quad \tau = 2l_p$$

where,

$\tau$  = period

$l_p$  = length of piston

Therefore, it becomes very convenient for the simulations of ITH drill string vibration with numerical input of the excitation force (periodic forces). Two 3-D plots in figure 6.8 and figure 6.9 are the results of the two continuous system simulations, for the simple boundary condition and the complex boundary conditions (see figure 5.1 and figure 5.2 respectively), derived from simulation computer programs written by the author on the commercial software MATLAB.

## 6.5 Discussion of Results of the Simulations

### 6.5.1 Multiple-Degree-of-Freedom Model

#### • Validation of the MDOF Model

The result of the simulation of the MDOF (Multiple-Degree-of-Freedom or Forced-Discrete-Lumped-Mass) model was represented by figure 6.1. The main purpose of

the simulation is to validate the MDOF model in describing the ITH drill system, especially for the short rod case. When the input of the drill system was assumed as impulse force and the system characteristics and responses, such as elastic elements, acceleration, velocity, and displacement were taken from the field tests, the damping ratio of the drill system can be found to be related to the system responses. For example, from figure 6.1, the minimum or maximum points for the acceleration and the displacement at the top end of the drill string is almost always at the same points where sharp changes in the damping ratio were found (about 0.2 peak-to-peak changes). It was then confirmed that the damping of the drill system due to the friction between the drill rod and hole wall, dynamic responses of the shock absorber and variation in the geology can isolate or absorb the vibration from being transferred up the drill string. What should be noted is that this simulation of the MDOF model is only for the short rod case and the field test data used in the simulation was measured when drilling with a short string length. With the short rod, there is less friction between the drill rod and hole wall, lower Coulomb friction, less reflection waves by the joints of the drill string and fewer additional disturbances to the drill system.

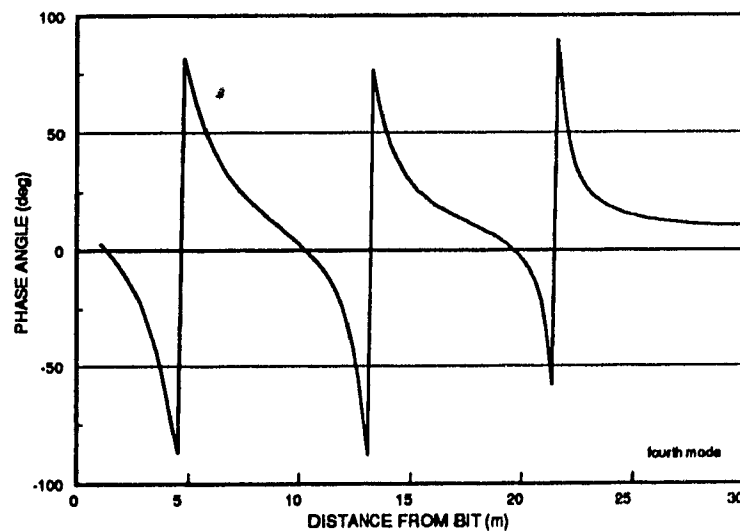


Figure 6.3: Phase Angle

### • Modal Analysis

The modal analysis is important in obtaining the forced-damped vibration responses of the drilling system by using the normal-mode function. The determination of the natural frequencies and normal-mode function depends on the boundary conditions of the system. For the percussive drill system investigated here, it is possible to have two choices for the boundary conditions of the system.

First, if the up-and-down and bouncing motion of the bit is considered to be smaller compared to the displacement of the string vibration, the bit end of the system can be assumed as fixed end. This means that the system is a fixed-fixed condition. The frequency equation then becomes,

$$\omega_n = n\pi c/l \quad n = 1, 2, 3, \dots \quad \text{rad/s}$$

where,  $l$  = the length of the drill string

A different normal-mode shape then results. From the above function, it is apparent that the system has a higher fundamental natural frequency.

A second case is when the bit end is fixed and top end of the string is free is assumed. Even though it has a complex structure at the top end of the string and thus more complex boundary conditions, there is little difference in the natural frequencies and opposite normal-mode shape. But the responses of any point in the system will be different, especially at each ends.

Figures 6.2 shows the normal-mode shapes of the drill string for the Fixed-Free boundary condition. Generally speaking, the modal analysis gives graphical results of the characteristics of the vibration at a certain boundary condition. For example, according to the fourth mode shape (normalized) in figure 6.2, the drill string obtains a maximum longitudinal stretch displacement amplitude at 17.8 m and at the bottom end, and maximum longitudinal compression amplitude at 8.9 m, and 26.7 m from

the bit on the Fixed-Free boundary condition. Figure 6.3 is a plot of the phase angle along the drill string while it vibrates. The instantaneous displacement and dynamic stresses for each point of the drill string can be calculated using the phase angle.

### 6.5.2 Continuous System

The simulation of the continuous system reveals the variant relationships of the vibration responses between the system frequencies, damping, and spring rate along the drill string and time under two boundary conditions. The amplitude variation of the longitudinal vibrations at different spring rates or damping ratios and vibration responses versus time or length of the drill string are represented by the 2-D or 3-D plots of the simulation results (figure 6.4-6.10).

Figures 6.3, 6.4 and 6.6 indicate how the shock absorber works in the drill system. The shock absorber plays an important role in reducing the vibration and stress of the drill string induced by the excitation force. Two curves in each of these plots indicate that the responses correspond to different damping or spring rates of the shock absorber under certain drilling conditions.

In figure 6.3 it can be found at one point of the drill string ( $x = 12.5$  m), with the maximum longitudinal vibration amplitude ratio versus the frequency and fixed spring rate of the shock absorber that the shock absorber can absorb large a amount of energy from the hammer casing vibration which otherwise would be transmitted to the string. Especially, the shock absorber has the maximum effect when the string is in a resonance situation. The solid line in this plot represents the case of small damping in either the drill string ( $r_1 = r_2 = 0.2$ ) or the shock absorber. The dashed line represents the case of the small damping along the drill string and large damping in shock absorber ( $r_1 = 0.8, r_2 = 0.2$ ). For most shocks used in mining industry, however, the damping of the drilling system comes mainly from friction between the drill string and hole wall rather than the spring elements in the shock absorber which are responsible in isolating or absorbing vibration.

Figure 6.4 shows more detailed results about how vibration is isolated by the action of the spring of the shock absorber. This mechanical spring is designed to act only in an axial direction. The solid line is with the stiffer spring (70,000,000 N/m), while the dashed line is for the softer spring ( $k = 49,000,000$  N/m). The responses of the drill string vibration were obtained for constant at damping ratios and at the point of the drill string for  $x = 12.5$  m. It is apparent that the softer spring is more effective in isolating vibrations to the string than the stiffer one. However, when the drilling system is in resonance, damage to the drill due to the vibration can not be avoided only by the spring elements of the shock absorber.

The effect of the natural string frequency on maximum amplitude of longitudinal displacement is also more conveniently displayed by figure 6.3 and figure 6.4. These plots indicate that the severe axial resonance of the string occurs at lower natural frequencies. By comparing the two plots, it can be shown that when the system is within resonant frequencies, the longitudinal vibration is mainly reduced by damping of the shock absorber rather than its spring elements. Figure 6.5 shows how the stress of the string is affected by the use of the shock absorber and how it changes along the string at certain drill conditions.

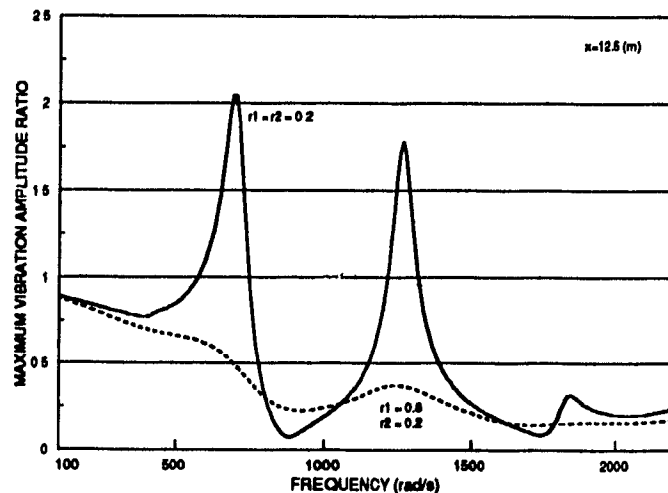


Figure 6.4: Maximum Vibration Amplitude Ratio with Different Damping Ratio

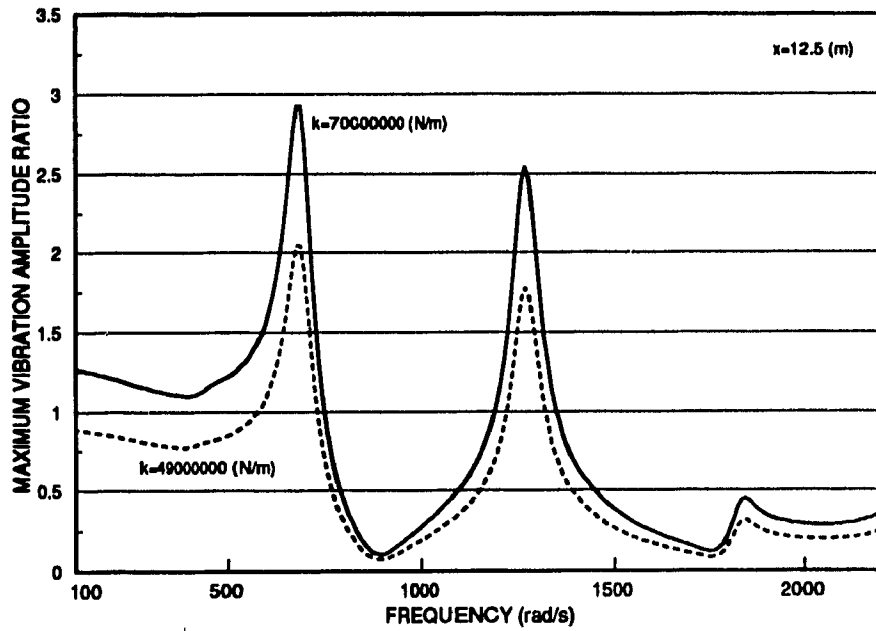


Figure 6.5: Maximum Vibration Amplitude Ratio with Different Spring Rates

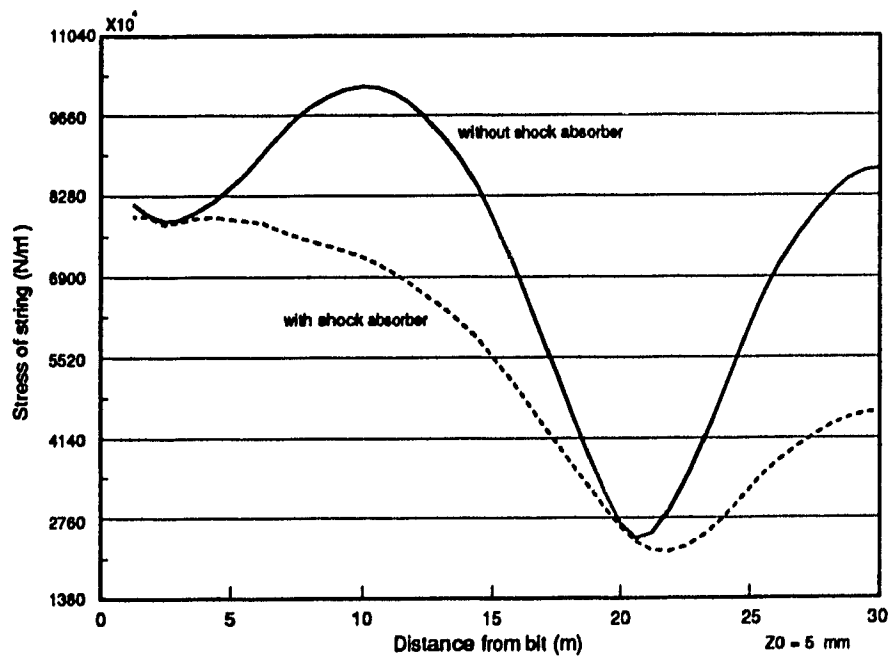


Figure 6.6: Stress Along the Drill String

The two curves in figures 6.6 and 6.7 are typical acceleration and velocity responses of a particular point ( $x = 12.7$  m) of the drill string at a certain frequency. By double or single differentiation of the equation, it is easy to derive the solution for acceleration and velocity for any point of the drill string at a particular frequency (see also figure 6.1.).

Figures 6.8 and figure 6.9 are 3-D plots of the results of the simulations for two different sets boundary conditions. The equations in chapter 5 indicated that the natural frequency of the system is related to the material and length of the drill string. Since the string is made of steel, its natural frequency is only a function of its length. With an increase in string length, as shown in the 3-D plots, the fundamental frequency will be lower. It also can be found from the plots, that since the length of the hammer casing is relatively short, its fundamental frequency tends to be higher. This means that the hammer casing can be treated as a lumped mass element rather than a discrete one. It should be noted that for figure 6.8, the fixed-free boundary condition has been used for the simulation so that the amplitude of vibration at the upper end of the string tends to be zero. While for figure 6.9, the amplitude of the longitudinal vibration either at the top or bottom end of the drill string will not be zero since the complex boundary condition was used in the simulation (see figure 6.2). The input of the vibrating system in the simulation are series impulse signals generated through the MATLAB program.

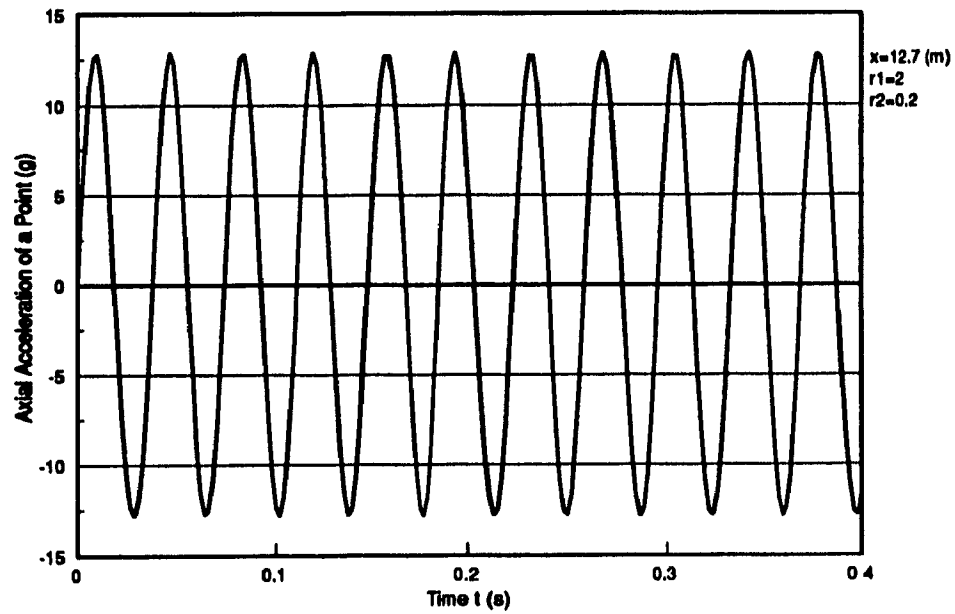


Figure 6.7: Axial Acceleration of a point of the String at a Certain Frequency (27 Hz)

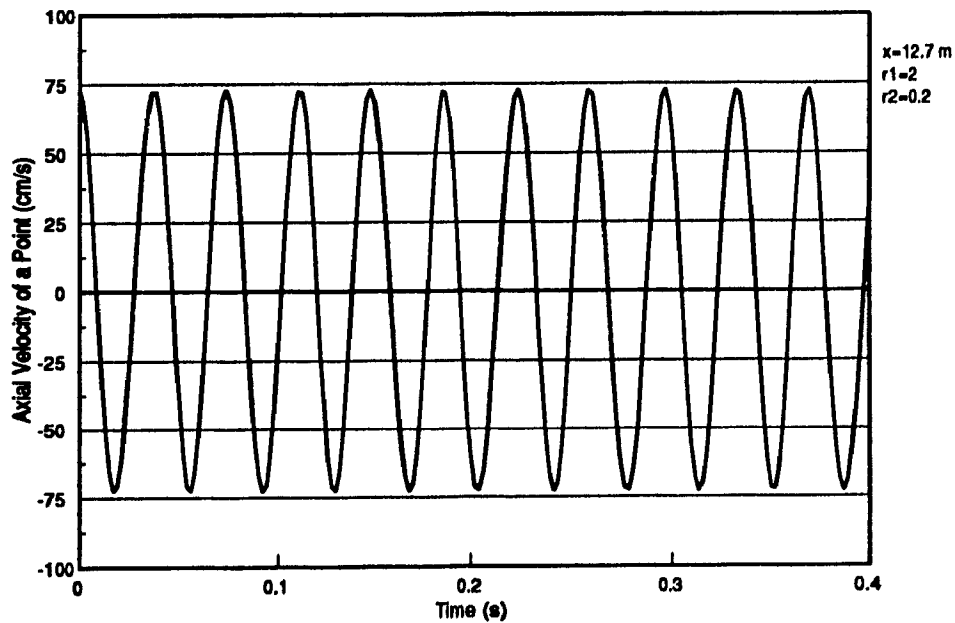


Figure 6.8: Axial Velocity of a point of the String at a Certain Frequency (27 Hz)

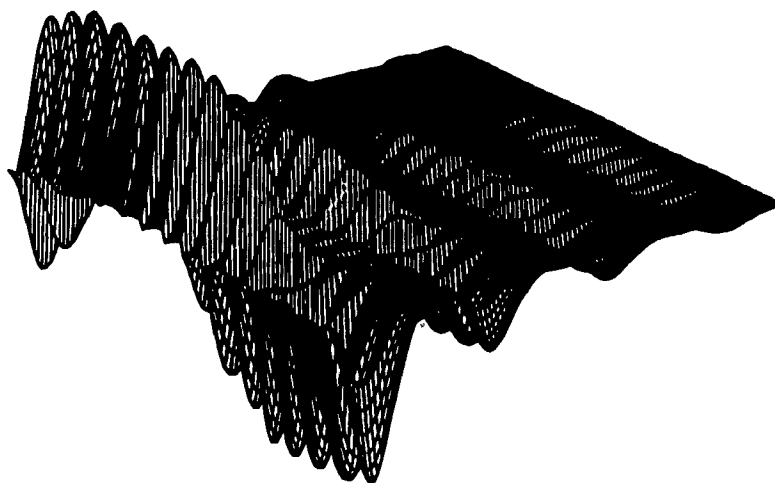


Figure 6.9: 3-D Plot for the Simulation Results

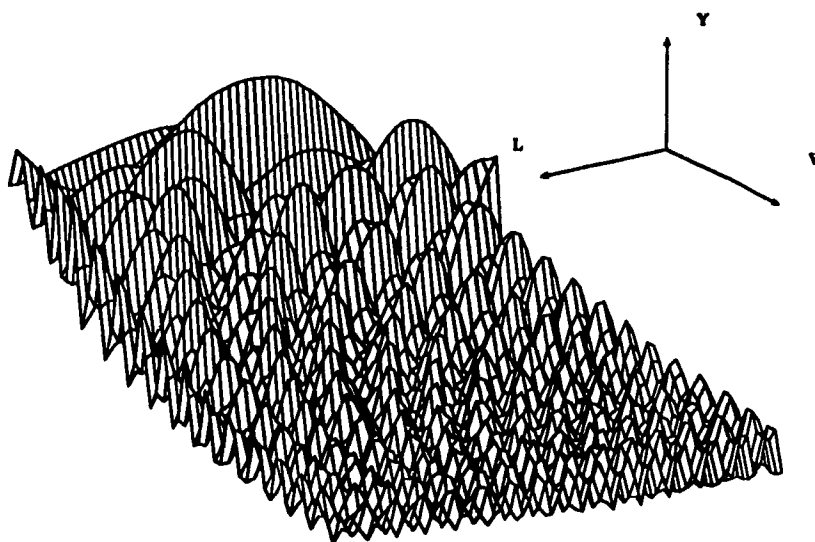


Figure 6.10: 3-D Plot for the Simulation Results for the Complex Boundary Condition

# Chapter 7

## System Identification and Spectral Analysis

Theoretical studies of longitudinal drill string vibration, including mass lumped, mass discrete and continuous system vibration, had been previously discussed in chapter 5 and 6. In this section, system identification and spectral analysis methods will be applied to the vibration data and other variables measured from a CD-90B ITH drill measured while drilling. It is also an objective of this chapter to determine the true relationship between the string vibration and other drilling variables such as feed force, torque and the damping of the drilling system. In addition, the efficiency of the shock absorber used during the drilling will be evaluated towards providing information to improve the performance of shock absorber.

### 7.1 The Drilling System

As discussed in chapter 3, to obtain the vibration responses of the ITH CD-90B drill, appropriate sensors and transducers were placed on the drill head and/or on the last drill rod (by use of the test rig and telemetry system). According to this measurement method and for the purpose of further research work, the drilling system can be divided into two sub-systems as shown in figure 7.1. System I includes the drill

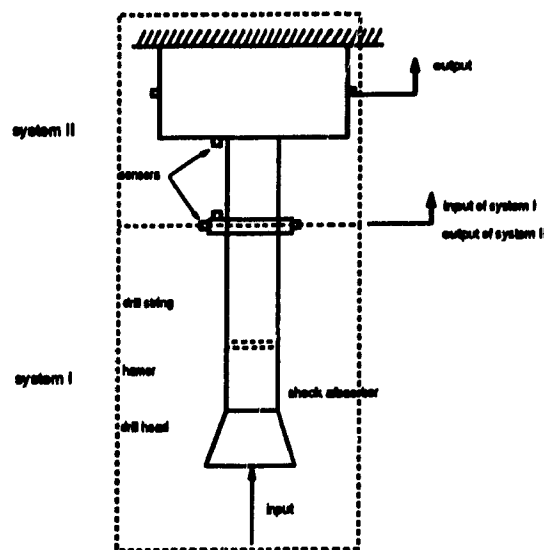


Figure 7.1: Input and Output Diagram of the Drilling System

bit to the midpoint of the last rod (at this point, the test rig was installed) while system II is from the midpoint to the drill head. The plant includes the drill string, the hammer, shock absorber, drill bit, the vibration sensor and the data acquisition hardware. The impact force acting on the hammer case is considered as the input to system I.

It was assumed that the input to system I are series impulse forces (the exact type of measured input signal is not known exactly but will be validated at a later time). Another assumption is that the drill rod is a uniform shaft without any joints. Actually, the numerous joints along a drill string will result in the generation of high frequency signals (reflected waves) and phase shifts on the drill rod. If the length of the rod is relatively short and the joints match well, the high frequency signal can be neglected or filtered out when the signal processing is undertaken. The results of the spectrum analysis will illustrate this aspect later on.

The data measured from underground field tests of a CD-90B ITH percussive drill consists of two sets of signals. One is from the sensors placed on the drill head and another comes from the sensors located on the midpoint of the last rod by using the telemetry system. These signals are considered to be outputs and/or

inputs to system I and/or system II. Each set of data is divided into two groups, one for system identification and another for the validation, to improve the accuracy of the identifications. All of the initial conditions of the system are assumed to be zero when A/D (Analog to Digital conversion) transformations are performed. The sampling interval is 0.001 second and the Nyquist frequency is 500 Hz when dealing with the vibration data.

## 7.2 Identification of the System

System identification deals with the problem of building or validating mathematical models of dynamic systems based on observed data from the system. For a linear and time-invariant system, the generalized model structure is

$$A(q)y(t) = \frac{B(q)}{F(q)}u(t) + \frac{C(q)}{D(q)}e(t) \quad (7.1)$$

where  $A(q)$ ,  $B(q)$ ,  $C(q)$ ,  $D(q)$  and  $F(q)$  are polynomials,  $y(t)$  is output of the system,  $u(t)$  is input of the system, and  $e(t)$  is the disturbance.

Which polynomials will be used depends on what type of model chosen as shown in Table 7.1. In this section, ARX (Autoregressive), ARMAX (Moving Average) and BJ (Box-Jenkins) models will be used for system identification of system II. The reasons for using ARX, ARMAX, and BJ models are (1) since it is not known exactly what is the kind of input to system I, finite impulse forces are assumed, (2) a comparison of several models is made to determine the effect of the disturbance of the system and (3) to obtain a best model to describe the identified system either at low or high frequency regions for the dynamic and spectrum analysis.

Table 7.1 Polynomials Used In the Models

<i>Models</i>	<i>Polynomials</i>
ARX	A,B
ARMAX	A,B,C
BJ	B,C,D,F

### 7.2.1 The ARX, ARMAX and BJ Models

In this section, the results of identifications obtained using several models such as the AR, ARX, ARMAX and BJ are discussed. Which model should be chosen depends on what signals will be processed and what system is to be identified. By comparing the simulated signal with the original output of the system and the Akaike's FPE (Final Prediction Error), the best fitting model will be more capable of describing the real system. Figure 7.2 (a) and (b) are original outputs and inputs of system I respectively. These signals were converted using an A/D transformation of 1 kHz and 1 ms sampling interval. Figure 7.2 (c) and (d) are spectrums of the input and output signal. It is noted that the input has very little relative energy above 127 rad while the output has considerable energy at some frequencies. Therefore, there must be some high frequency disturbances to the system. This also implies that the ARX model which ignores the disturbance to the system, will not be suitable to describe the real system. Because the impact between the piston and hammer is considered as the main source of the string vibration, these high frequency disturbances probably originate from the reflecting waves caused by both the impact between the drill bit and rock and the piston and the drill hammer. Figures 7.2 (c) and (d) also indicate that the original high frequency behaviour is uncertain.

Figure 7.3 is a plot comparing the original output signal with the simulation results. It can be noted that from this plot, there are difficulties when dealing with the high frequency components of the output. To get a true system, the data should be filtered to compress the data by a factor of four (i.e. Low-pass filter and pick

every fourth value). Figure 7.4 is a second plot of the ARX model using the filtered data where the results are much improved.

Figure 7.5 is another plot for the BJ model, and indicates that this model shows good agreement with agree with the real system. Figure 7.6 shows the results when the ARMAX model is also compared to the real system. Note the solid line for the simulated signal and dotted line for the original signal in this figure. The Loss Function and Akaike's FPE are shown as in Table 7.2.

<i>Models</i>	<i>Loss Function</i>	<i>Akaike's FPE</i>
ARX1	0.3559	0.3741
ARX2	0.0609	0.0634
ARMAX	0.0509	0.0534
BJ	0.0384	0.0407

In summary, due to considerable high frequency disturbances that result from reflected wave impacts of the drill bit and rock and the joints of the drill rod, the original signals have to be pre-compressed through filtering. It is then possible to build simple models that are capable of reproducing the validation set reasonably well. The BJ or ARMAX models can represent the real system better than the ARX model when dealing with the percussive drill string system due to the presence of such high frequency disturbances.

### 7.2.2 The Impulse Responses Models

As mentioned above, the input of system I was considered as a finite impulse force. In the identification of system I, a low-pass filter is used to filter the high frequency elements as a first step of the procedure. What the cut-off frequency is will depend on what low frequency region is to be examined. The third order model has been

estimated to derive two polynomials. Figure 7.7 is a discrete-time Bode Plot of the results of the identification of system I using the impulse forces as input. Comparing this plot with figure 7.2 (d), the model shows good agreement with the original system. According to the identified model, system I can be described as a third order discrete system (the sampling time is 0.001 sec). Its transfer function is:

$$G(z) = \frac{-0.292}{z^3 - 1.428z^2 + 0.187z + 0.271} \quad (7.2)$$

From the transfer function, the estimated damping ratio of system I can also be obtained, including the system damping and that of the shock absorber, and the natural frequency as:

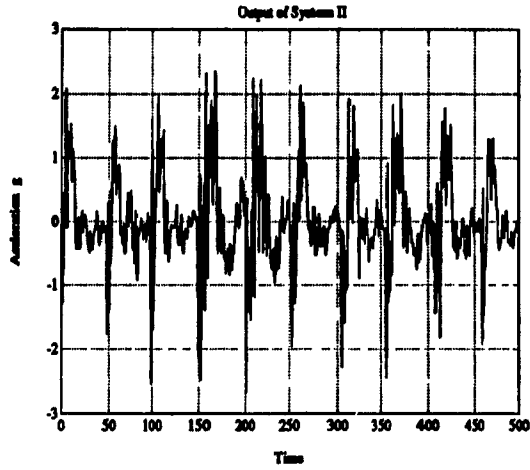
damping ratio:           0.65  
natural frequency:       158 rad/sec (25 Hz)

Figure 7.8 compares the two output signals of system I, where one is the original output and another is the simulation output using the simulated impulse signal as the input. This result also confirmed that the assumption regarding the finite impulse input of system I is correct.

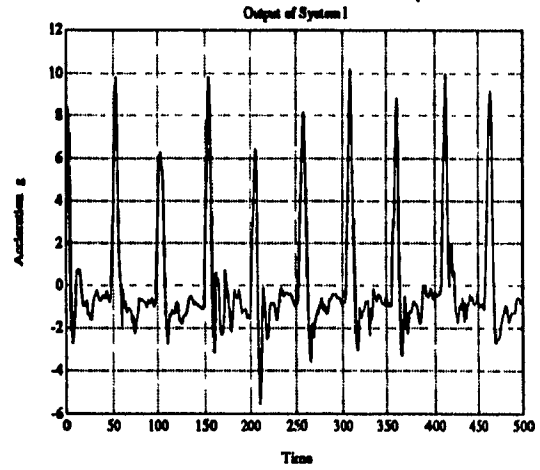
### 7.2.3 Comparison of the Simulated and Original Outputs

Figures 7.10 and 7.11 demonstrate some results from the model simulation. In these figures, which compare the outputs, one line indicates the filtered original signal and the other is the output of the simulation. The simulated model was that identified using the ARX or AR model with the original output data of the drilling system.

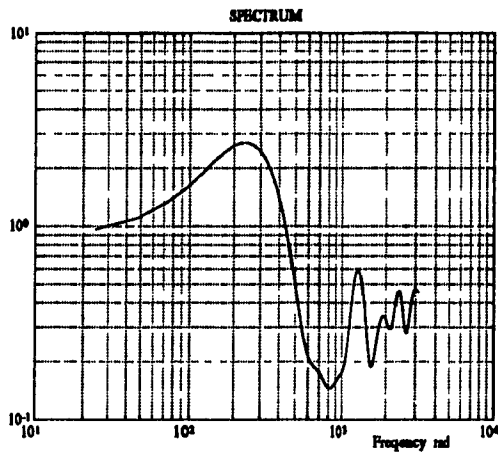
It is considered, therefore, by analyzing the results of the system identification applied to this drilling system, that it is possible to identify or diagnosis the changes in the damping of the drill system by using such methods under certain predefined conditions.



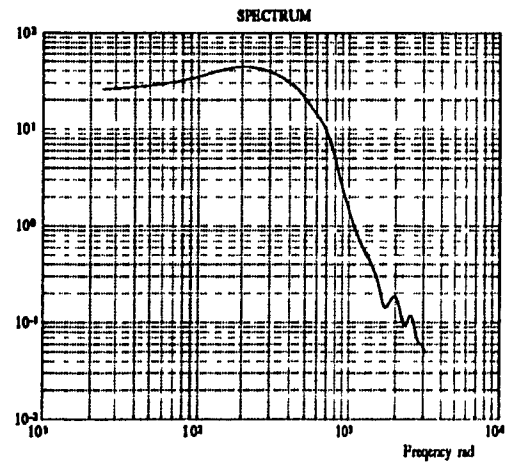
(a)



(b)



(c)



(d)

Figure 7.2: System Original Output and Spectrum: a) Original Output at the Drill Head; b) Original Output at the Drill Rod; c) Spectrum of Output at the Drill Head; d) Spectrum of Output at the Drill Rod

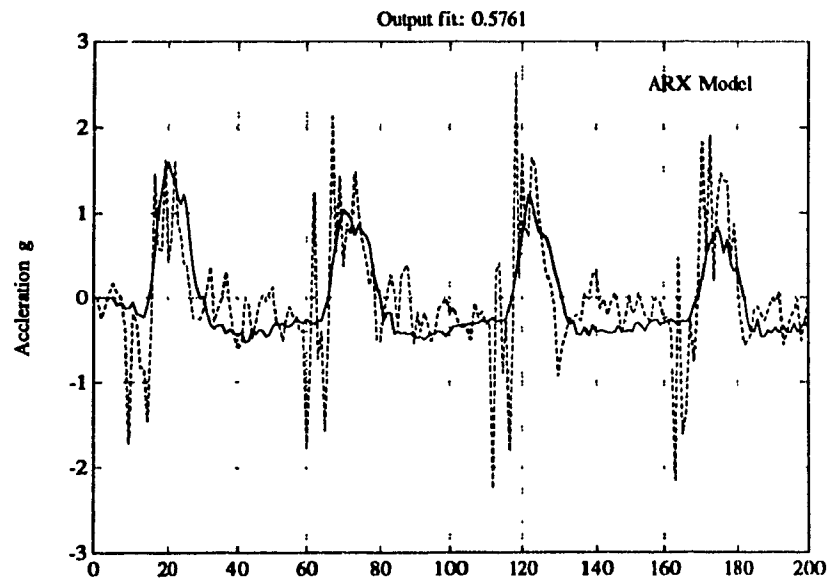


Figure 7.3: Comparison of Original the Output and Simulation Signal

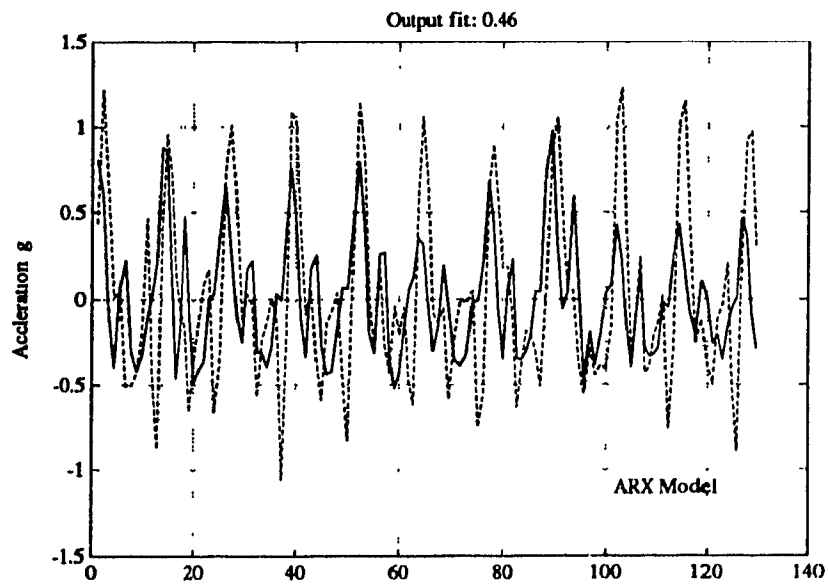


Figure 7.4: Comparison of the Filtered Output and Simulation Signal

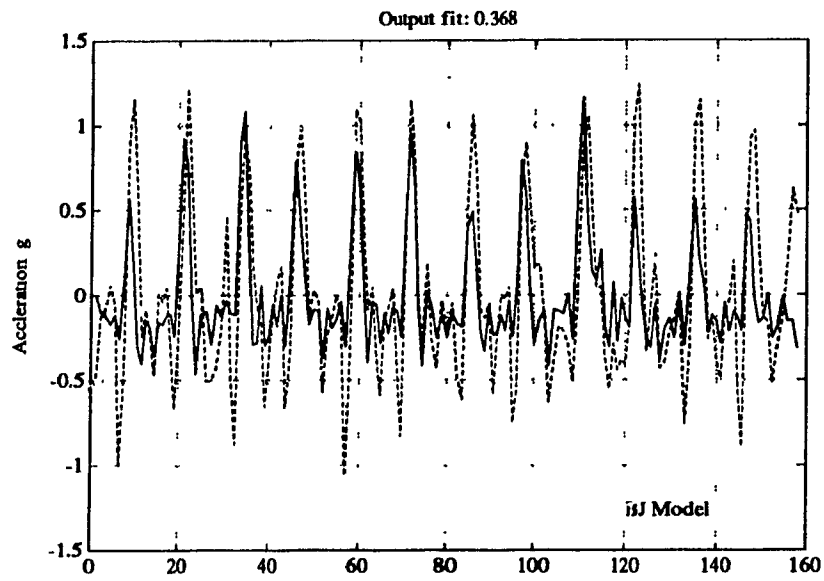


Figure 7.5: Comparison of the Output and Simulation Signal

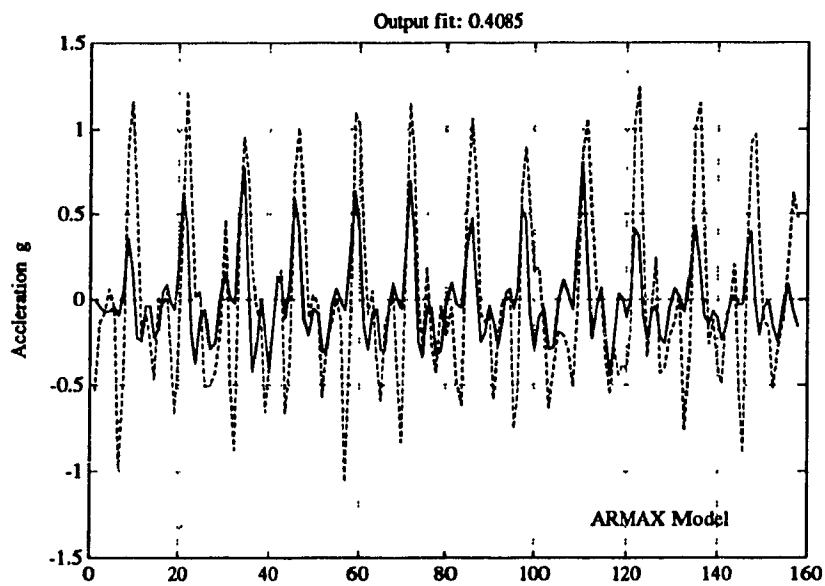


Figure 7.6: Comparison of the Output and Simulation Signal

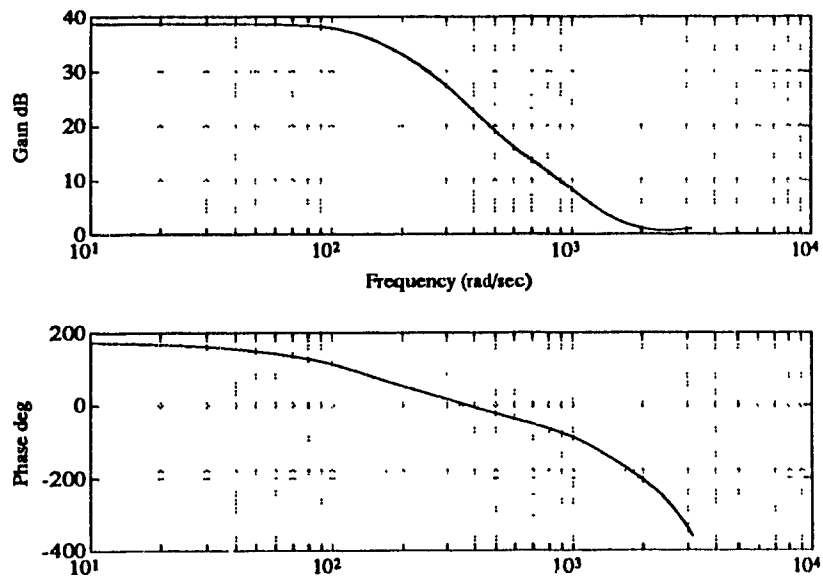


Figure 7.7: Bode Plot for the Identified System I

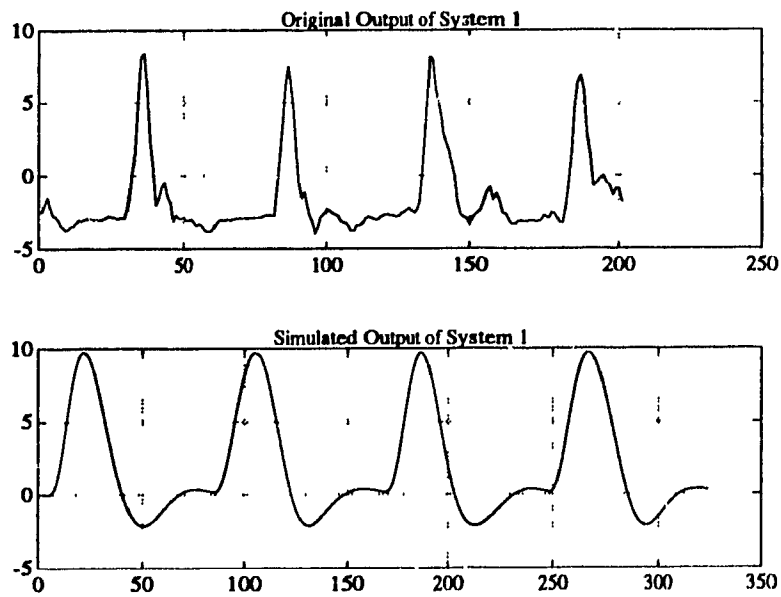


Figure 7.8: Comparison of the Original and Simulated Output of System I

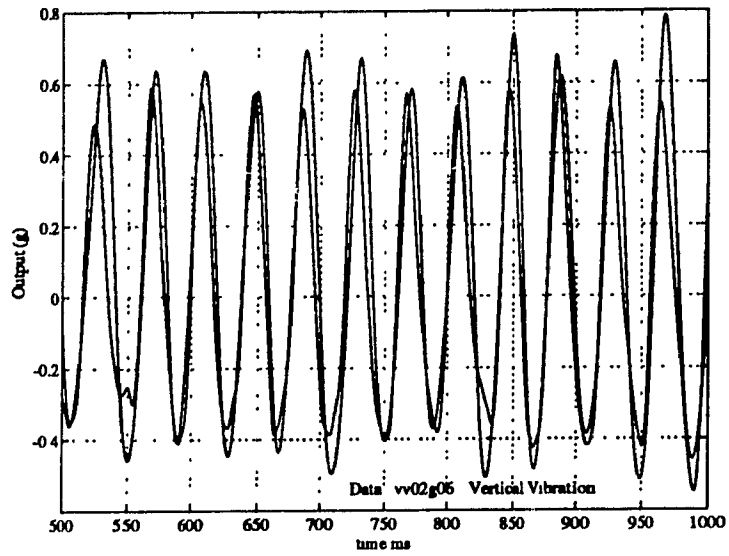


Figure 7.9: Comparison of the Output of Model and System

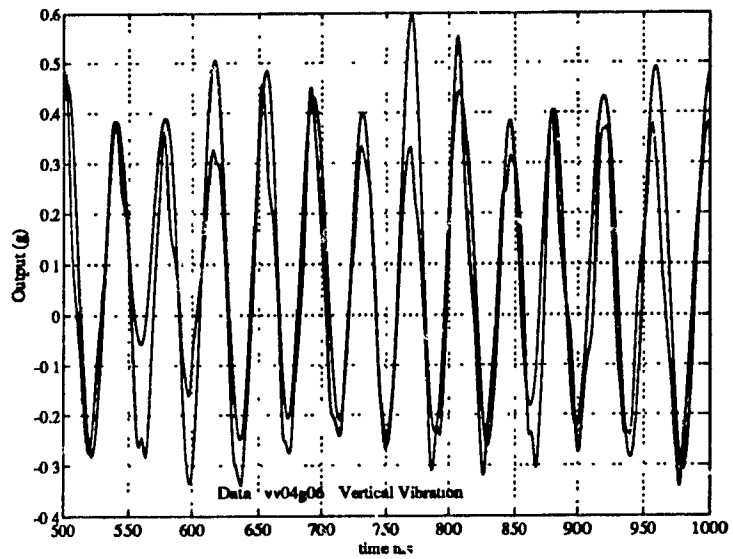


Figure 7.10: Comparison of the Output of Model and System

## 7.3 Vibration Analysis Using System Identification Methods

### 7.3.1 Spectral Analysis

In order to diagnose the drill condition or analyze the vibration, spectrum analysis is a principal tool. In this section, the focus will be the selection of a suitable method to perform a spectrum analysis of the vertical vibration of the drill string. The ETFE (Empirical Transfer Function Estimate) method will be tried first, using the data obtained from the underground experiments. Figure 7.12, is a spectrum of the output from system II where the dominant frequency components of 19, 40 and 59 Hz and their harmonics are clearly seen. The SPA (Standard Spectral Analysis) method gives another plot as shown in figure 7.13. This figure shows that when the SPA method is used, a very large Hamming window will be needed to identify any detail of the harmonic response. This situation indicates that the Standard Spectral Analysis method does not work well for the desired analysis. Figure 7.14 is a plot comparing several AR models of different order with the ETFE method. From this plot, it is seen that the parametric spectrum is not capable of picking up the harmonics because the AR models are strongly influenced by the higher frequencies, which are difficult to model. Therefore, the analysis will concentrate on the lower harmonics by prefiltering the data at a cut-off frequency 65 Hz which will encompass the 20, 40, and 60 Hz models. Figure 7.15 illustrates the results from using the filtered data. The three first peaks were clearly identified while the high frequency components were ignored. If the fourth or fifth harmonics ( around 80 and 125 Hz) were of interest, the cut-off frequency should be changed or another kind of filter used to prefilter the data. Figure 7.16 is a comparison of the spectrum of the original and simulation output of system I.

In summary, after prefiltering the data with low-pass filters, the parametric AR methods are capable of properly presenting the spectrum for the purpose of dominant

frequency analysis.

### 7.3.2 Data Analysis

In this section, the vibration analysis will focus on analyzing the changes in the vibration while drilling in an attempt to define the relationship between the damping ratio and the feed force and torque. This analysis will be undertaken for both the vertical and lateral vibrations using system identification methods. The data in this analysis was measured during the underground field tests in hole 02 and 04. Frequent changes made by the operator while drilling can introduce numerous difficulties to the system identification process. Therefore, the particular data set was selected due to the fact that the feed force and air pressure remained essentially constant while drilling the holes.

#### • Damping Ratio

It is believed that shock absorber can largely reduce the amplitude of the vibration of an ITH drill, a situation which was theoretically studied in a previous chapter. Figures 7.19 and 7.21 show the relationships between the system damping ratio and several drilling variables of the drilling conditions. Figures 7.11, 17 and 7.18 also indicate the changes to the drill system equivalent damping ratios with and without the use of a shock absorber for either the vertical and lateral vibration responses. Although the longitudinal vibrations of the drill system were not reduced by the damping elements but by the spring elements of the shock absorber, the equivalent damping ratio will still have a variation of about 0.3.<sup>1</sup> This is mainly due to the frictional force between the drill rods and the hole wall and that at the bit-rock interface. Changes in the rock properties, bending of the drill rod and the feed force will cause the variations in the damping ratio. The ability to attenuate the

---

<sup>1</sup>The shock absorber on the CD-90B ITH drill used in the underground field tests was one in which the main elements for isolating or absorbing the vertical vibration are springs. There is little friction force in these springs and thus relatively lower damping ratios

vibration through damping is different for the transmission of the vertical and lateral vibration and occurs in a different frequency range as shown in figures 7.19 to 7.24. On the other hand, the results indicate that the identified models can describe the system with enough sensitivity to account for any changes in the drilling conditions. Therefore, it is possible to identify any changes in the system damping by using system identification methods.

- **Feed Force**

In underground mines, drilling hole with high precision at high production rates is of utmost importance. To obtain the smallest deviation and the best penetration rate, an optimum feed force should be applied to the bit in order to maximize impact energy transference to the rock. It was observed from the field data that penetration rate was proportional to the feed force prior to the latter reaching an optimum point. When the feed force was excessive, i.e., higher than the optimum level, the bit will be forced against the rock at all times. The bit in an ITH hammer is designed to rebound after each impact, but if this is not possible the flushing clearance between it and the rock becomes restricted. As a result, cuttings are not being properly cleared and thus they build-up at the bit-rock interface to attenuate the impact energy. Less energy is delivered to the bit to break rock and, therefore, the penetration rate in such cases was reduced.

Vibration on the drill head and within the drill rods is considered as one of main factors to induce hole deviation. Vibration levels of the drill head were seen to be inversely proportional to the feed force as shown in figures 7.19 to 7.24. These figures show that the level of applied feed force directly affects the drilling vibration level. Comparing figure 7.19 with 7.20 (for Hole 02, vertical vibration), figure 7.21 with 7.22 (for Hole 04, vertical vibration) and figure 7.23 and 7.24 (for Hole 04, lateral vibration), it is seen that the higher the feed force, the vertical(longitudinal) vibration level usually decreases while the lateral vibrations are less affected. This

behaviour explained by the higher feed force resulting in better contact between the drill bit and the rock while also stiffening the drill string such that it has less acceleration when a stress wave passes through. This does not mean, however, that the strain forces generated in the rods are also less.

- **Torque**

There are many factors that affect the torque developed while drilling, for example feed force, air pressure, flow rate, hole depth, rock properties and even the flushing conditions at the bit-rock interface. The damping ratio always represents the torque level, since the torque is mainly generated by the force composed of the bit chipping action, the friction between the drill rods and hole wall and the friction from all rotating drill components. Figures 7.19 to 7.24 indicate that when the damping ratio increases, the torque increases sharply with the lower vibration responses, especially in the case of the vertical vibration responses.

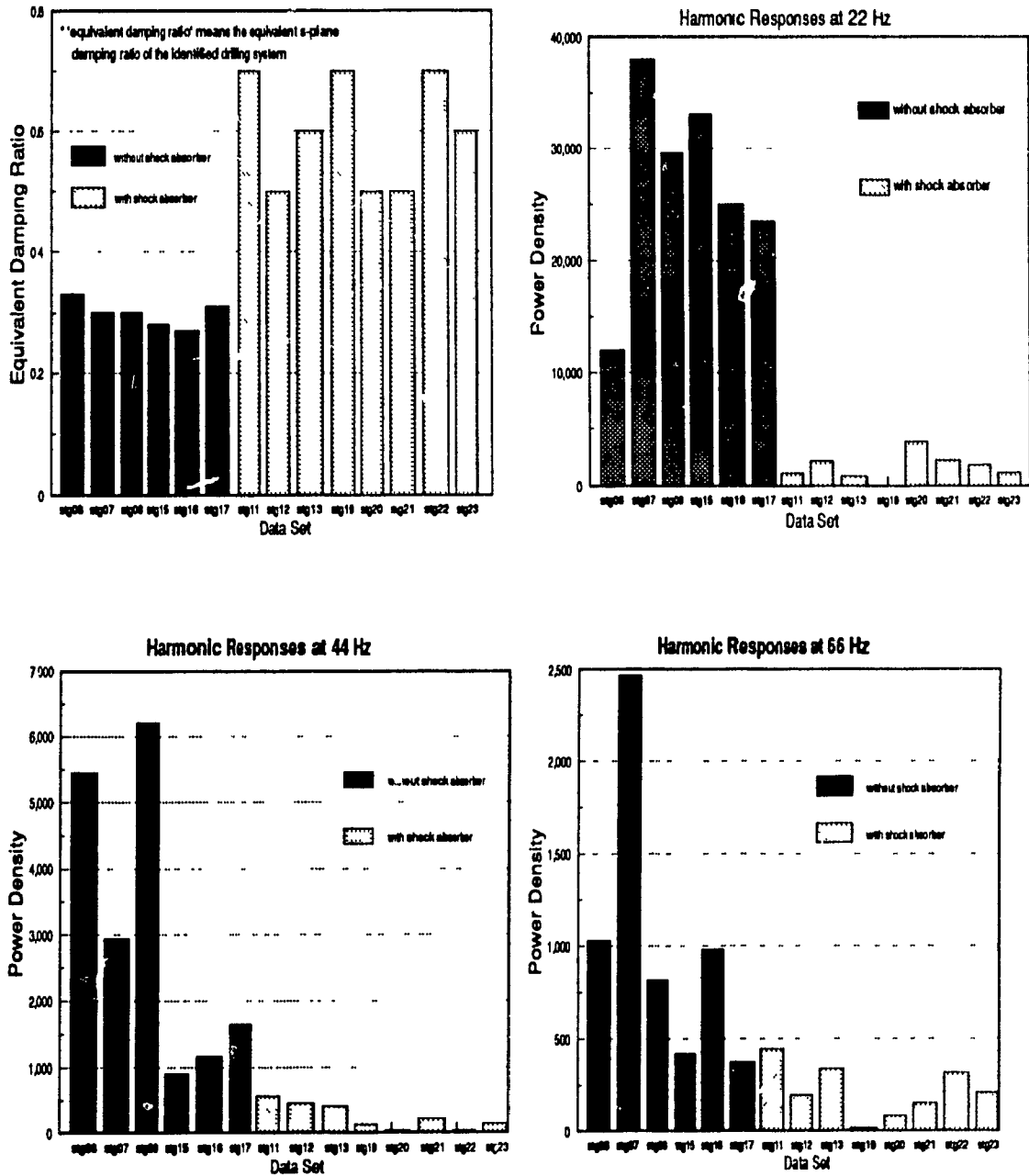


Figure 7.11: Equivalent Damping Ratio and Harmonic Responses of the Drilling System for Vertical Vibration

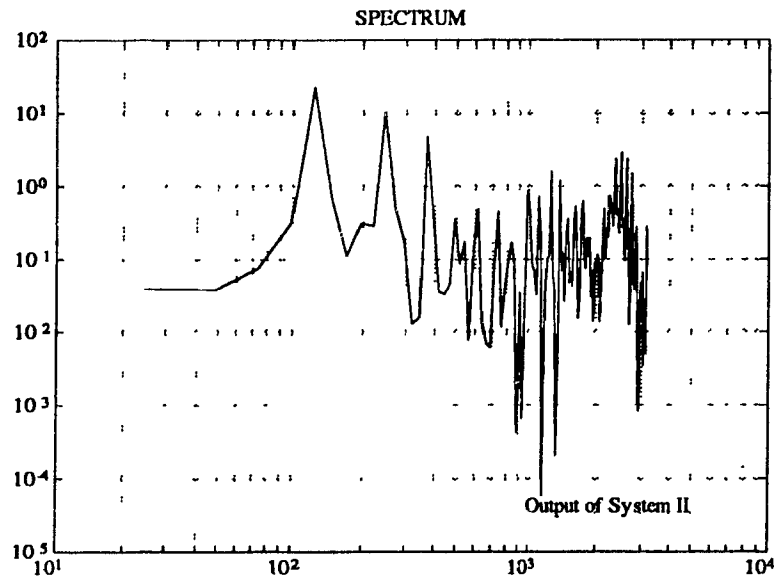


Figure 7.12: Spectrum of the Output of System II

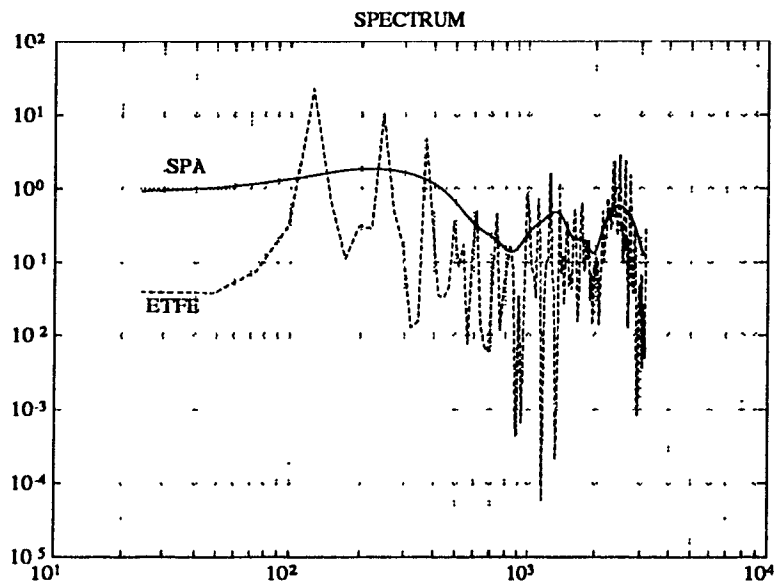


Figure 7.13: Spectrum of the Output of System II

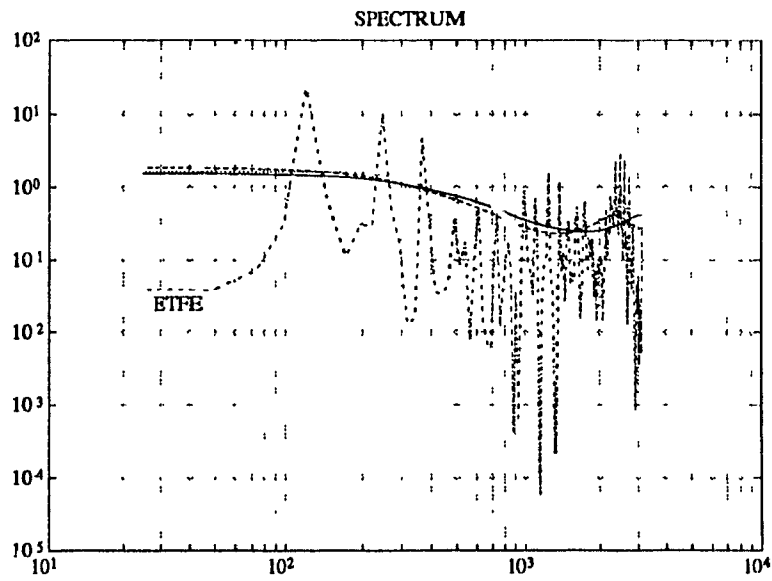


Figure 7.14: Spectrum of the Output of System II

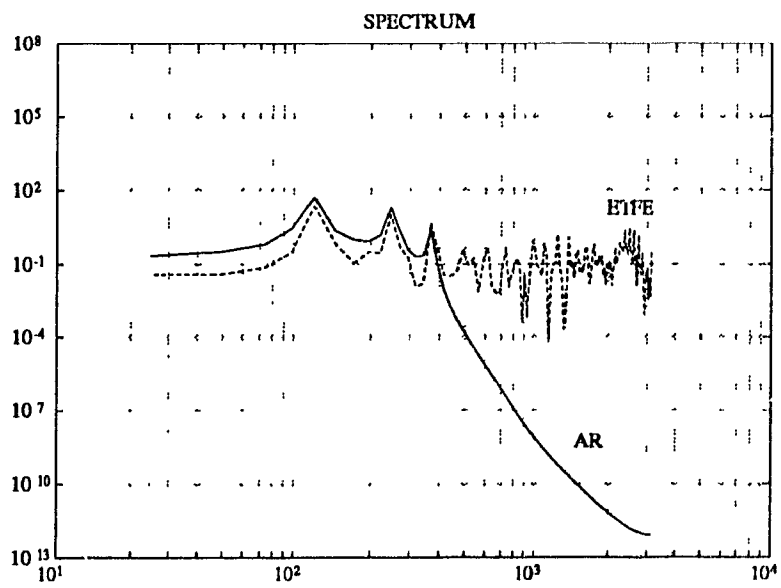


Figure 7.15: Spectrum of the Output of System II

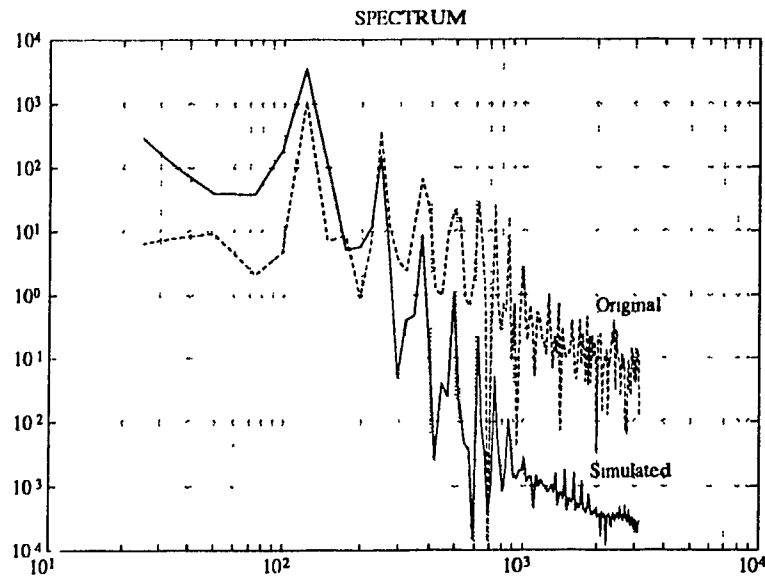


Figure 7.16: Spectrum of the Output of System I

### 7.3.3 Harmonic Responses

The shock absorber plays an important role in isolating the transmission of the vibration from drill bit to rod or head. At the measuring point on the drill head, the vertical vibration was effectively reduced through the use of the shock absorber, especially in the case of harmonic responses at lower frequencies (about 22 Hz and 44 Hz), see figure 7.9. Figures 7.17 and 7.18 are harmonic responses of Front-Back and Left-Right directions of vibration at the drill head with or without a shock absorber. These figures also indicate that the level of transmission of lateral vibrations can not be reduced effectively at both low and high frequencies. This response is due to the design of the shock absorber, which is composed of a series of vertical spring elements.

With an increase in the length of the drill string, the longitudinal vibration measured at the drill head, illustrated small harmonic responses at lower frequencies of 24 and 48 Hz and high level harmonic responses at 72 Hz. This behaviour is due to

the fact that as the length of the drill string increases, the damping of the drill system, as a result of friction between the drill hole and the drill string, will increase. The vibration at lower frequencies, therefore, will be damped by the increased damping. As the number of the joints increase with an increase in drill string length, the harmonic responses at the high frequencies will shift to high levels due to increased reflection.

For the lateral vibrations on the drill string and drill head, the situation is not the same as for the longitudinal vibration. When the drill string becomes longer, the possibility of bending the drill string increases. When the deviation or bending occurs, the friction between the drill hole and the drill string increases quickly, and, therefore, the high frequency vibration reflection which acts on the drill string will decrease. The harmonic responses at lower frequencies will be slightly changed in such situations. These results are shown in figures 7.19 to 7.24.

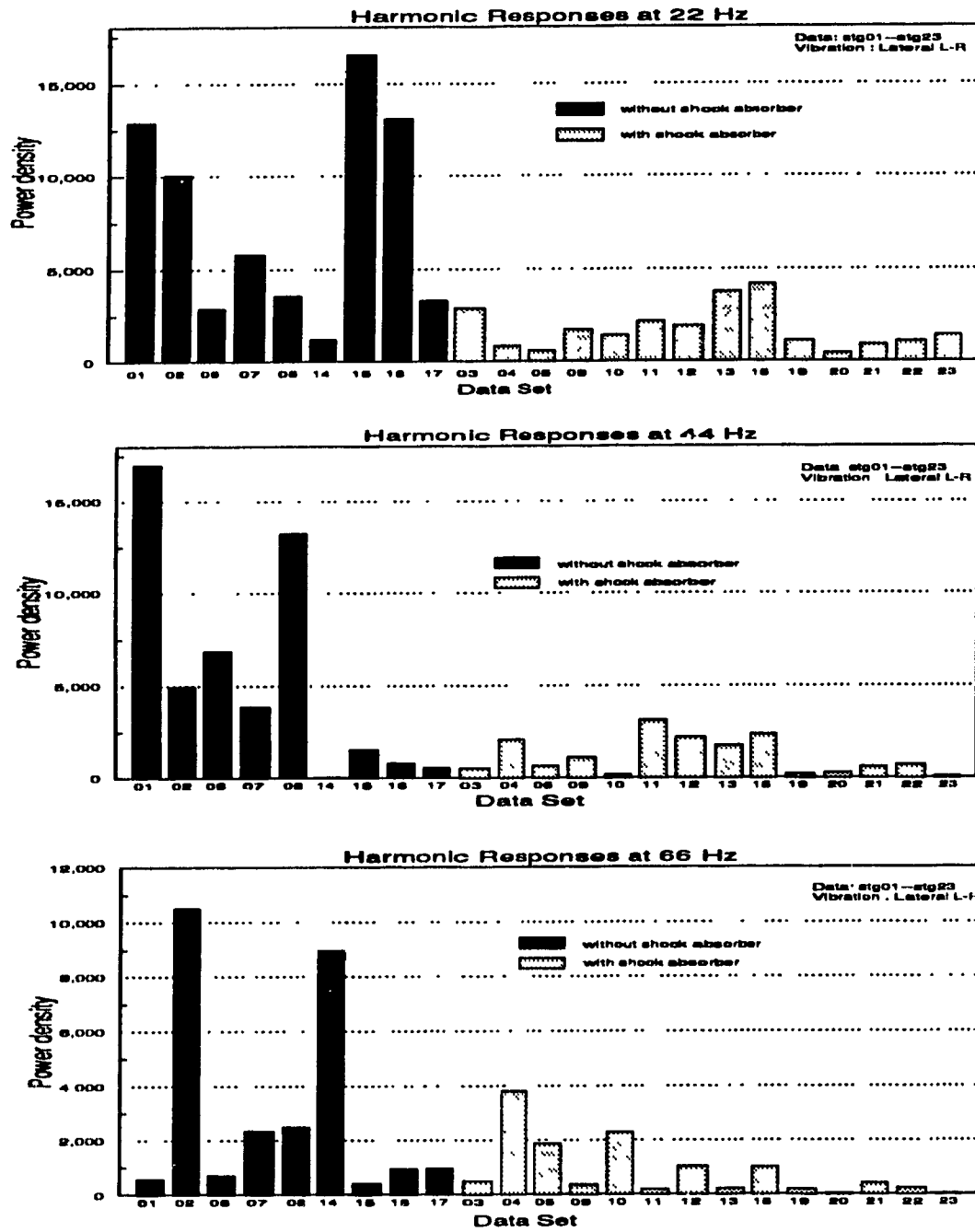


Figure 7.17: Harmonic Responses of Lateral Vibration (L-R)

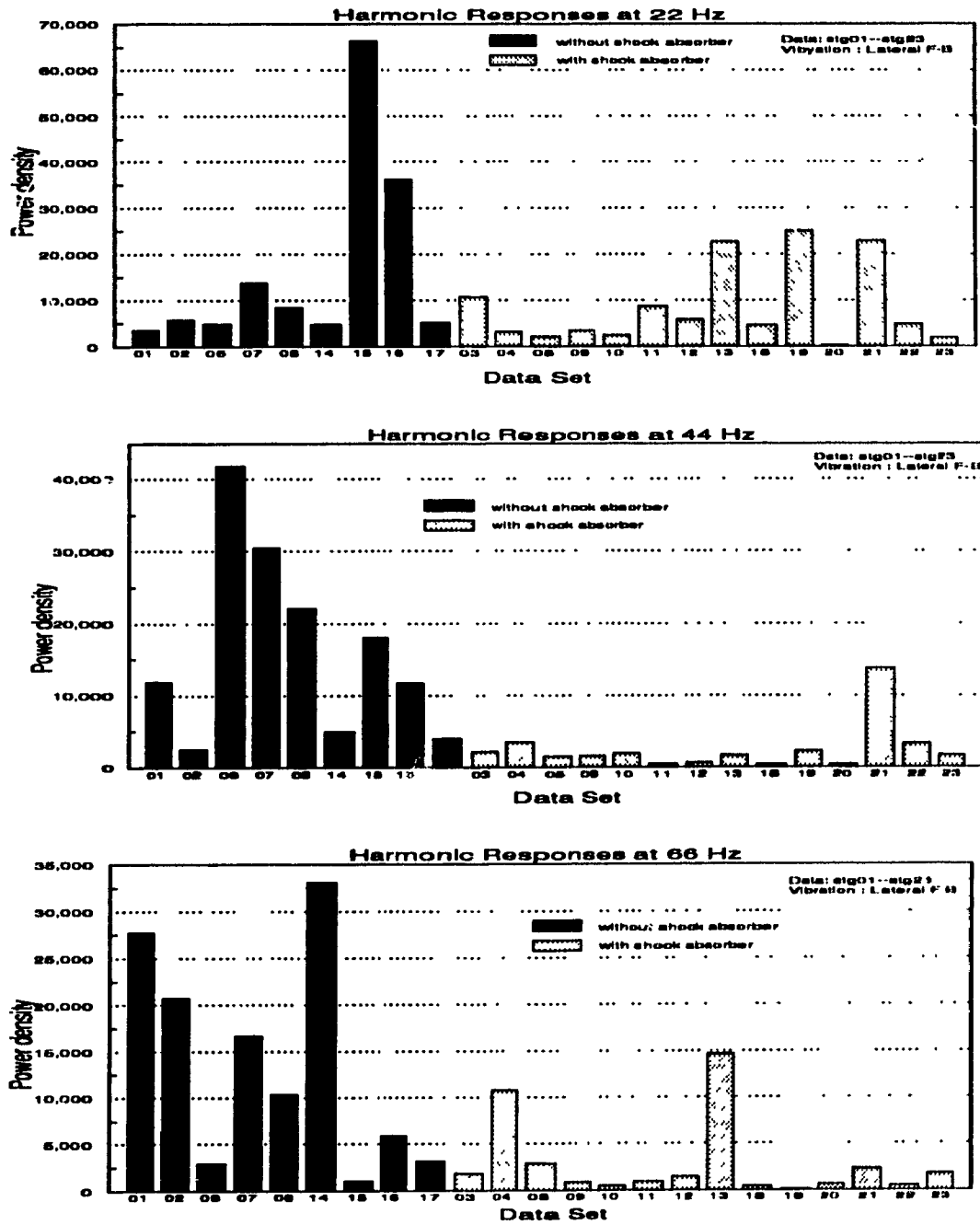


Figure 7.18: Harmonic Responses of Lateral Vibration (F-B)

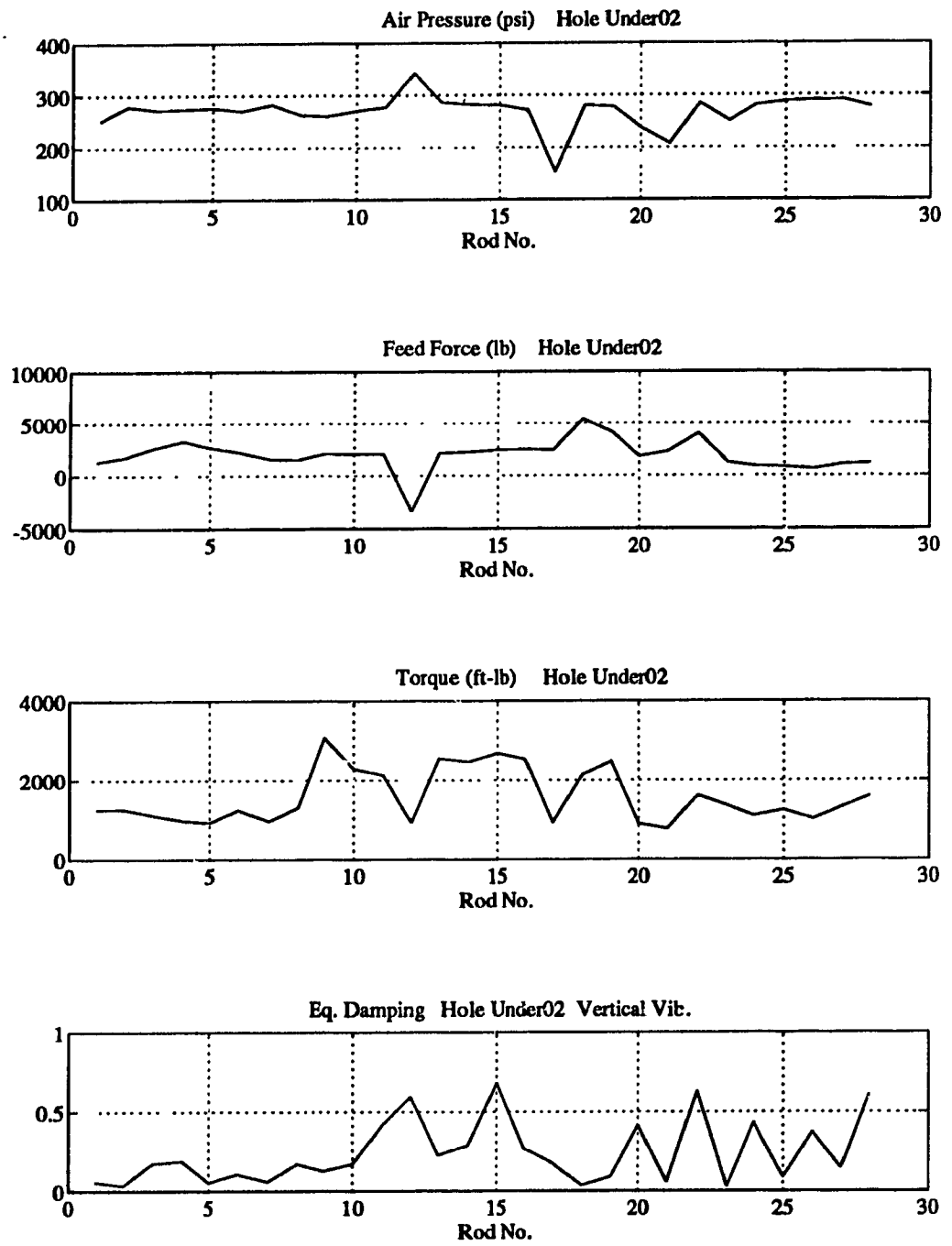
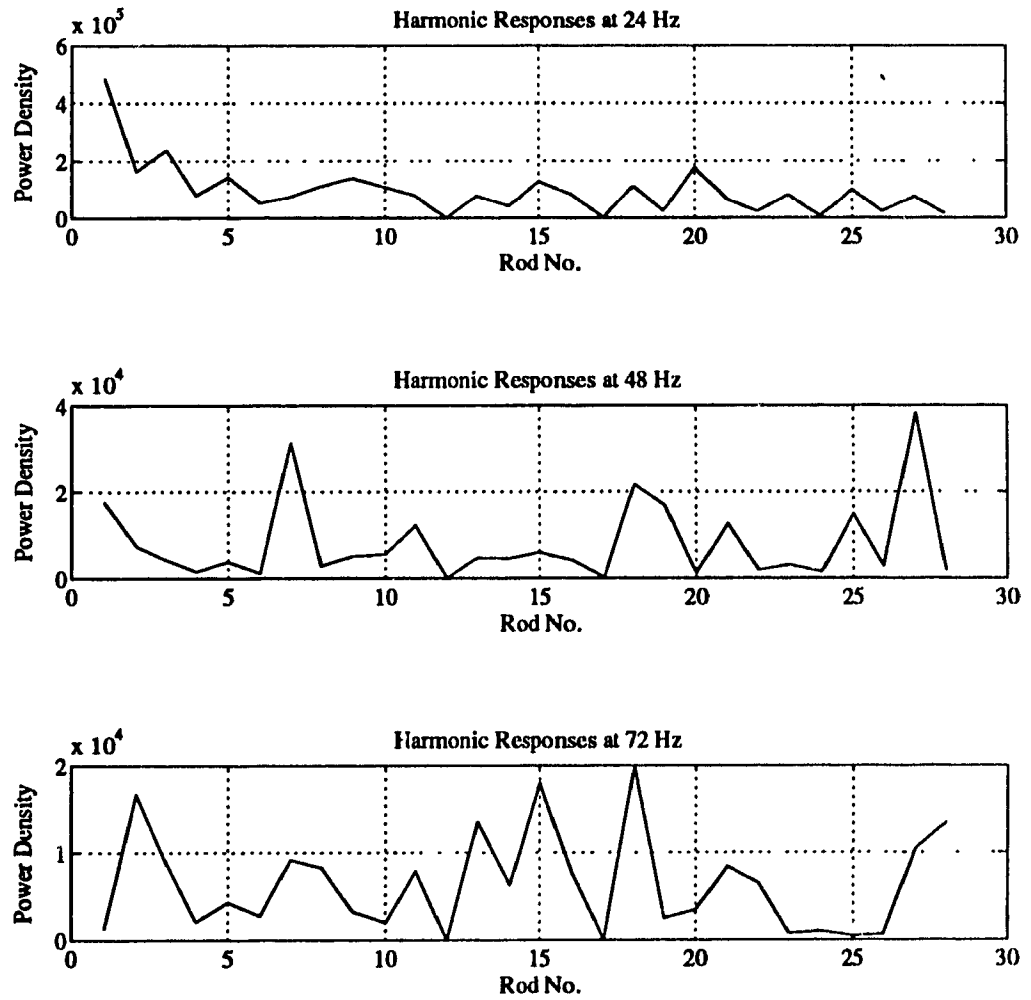


Figure 7.19: Variables and Damping for Hole Under02



Hole: Under02 Data: vv02g Vertical Vibration

Figure 7.20: Harmonic Responses of Vertical Vibration for Hole Under02

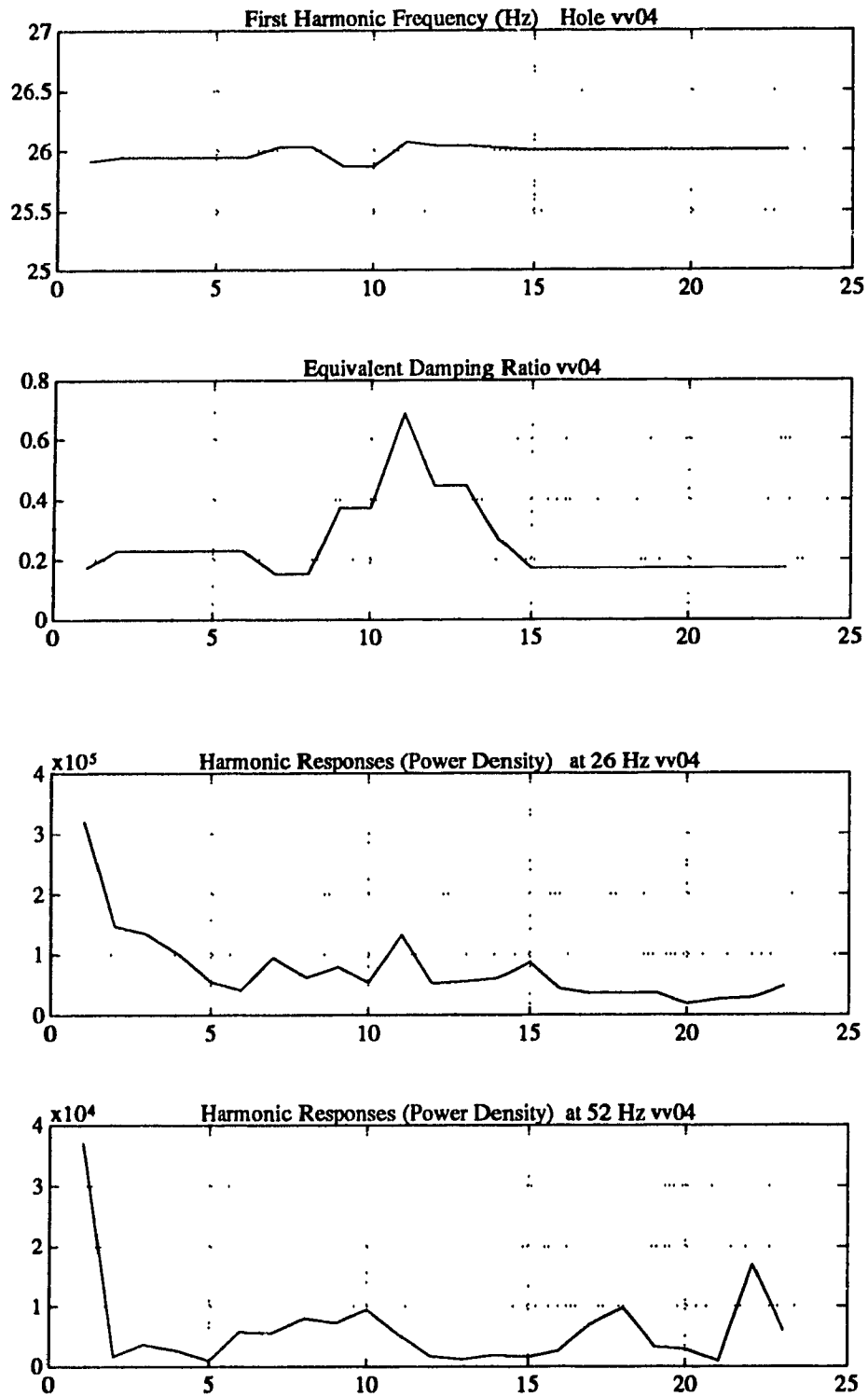


Figure 7.21: Harmonic Responses of Vertical Vibration and Equivalent Damping Ratio for Hole Under04

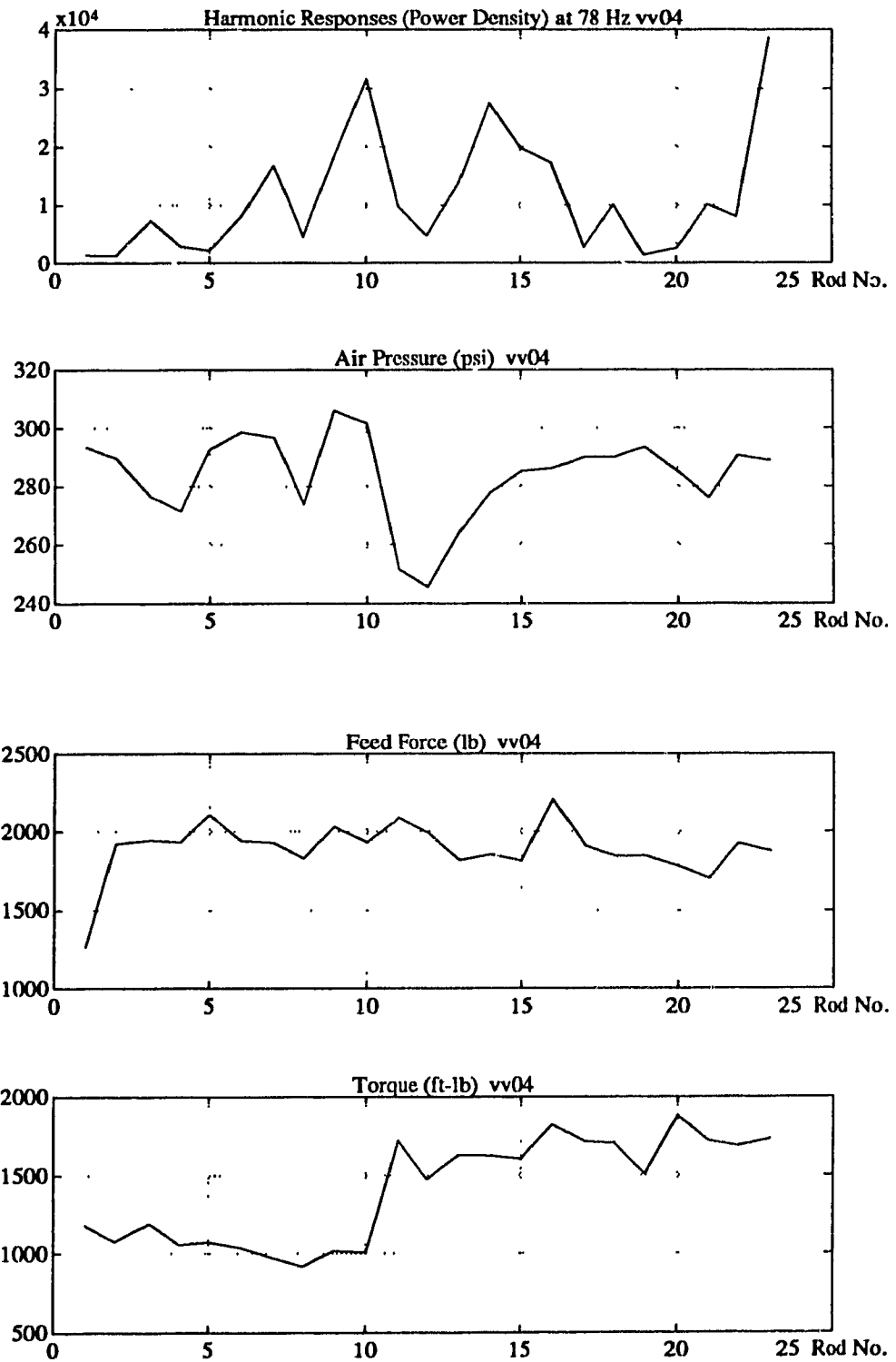
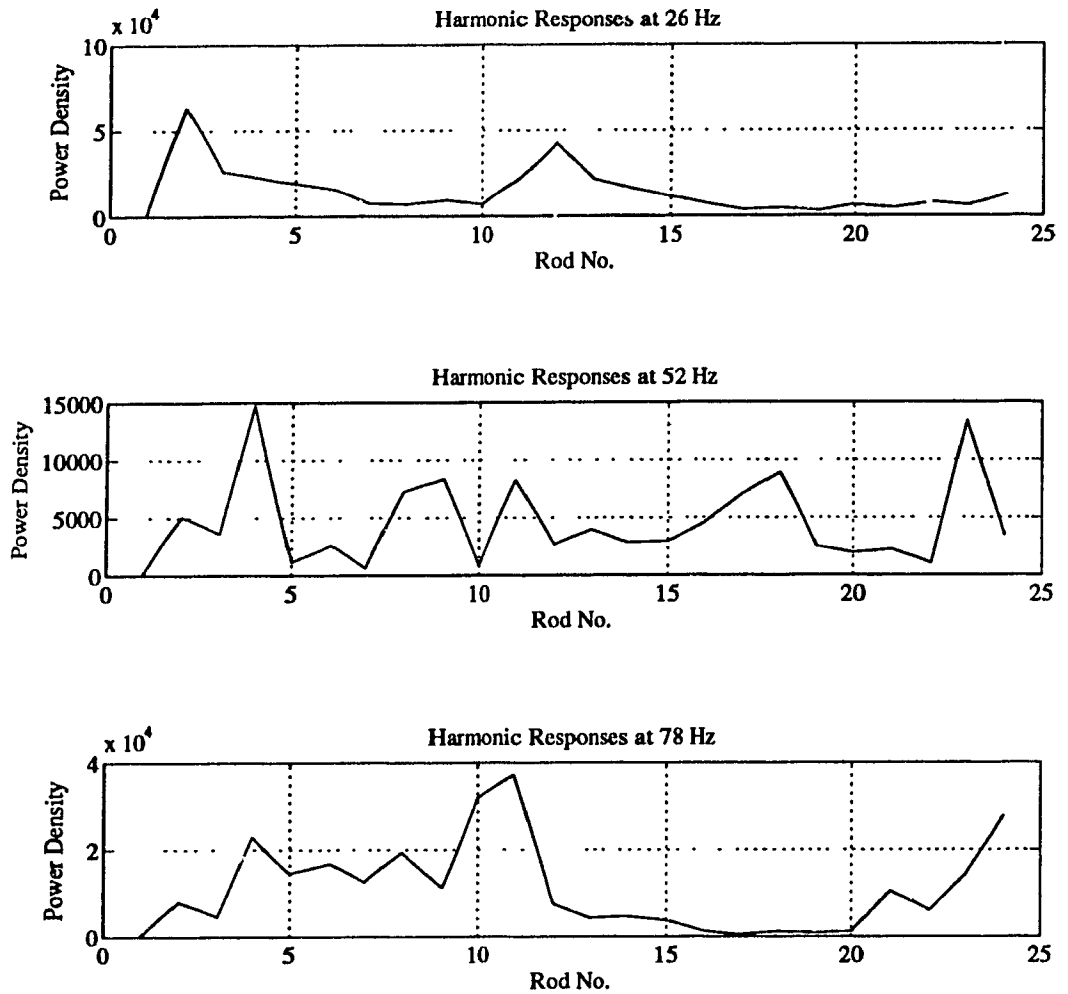
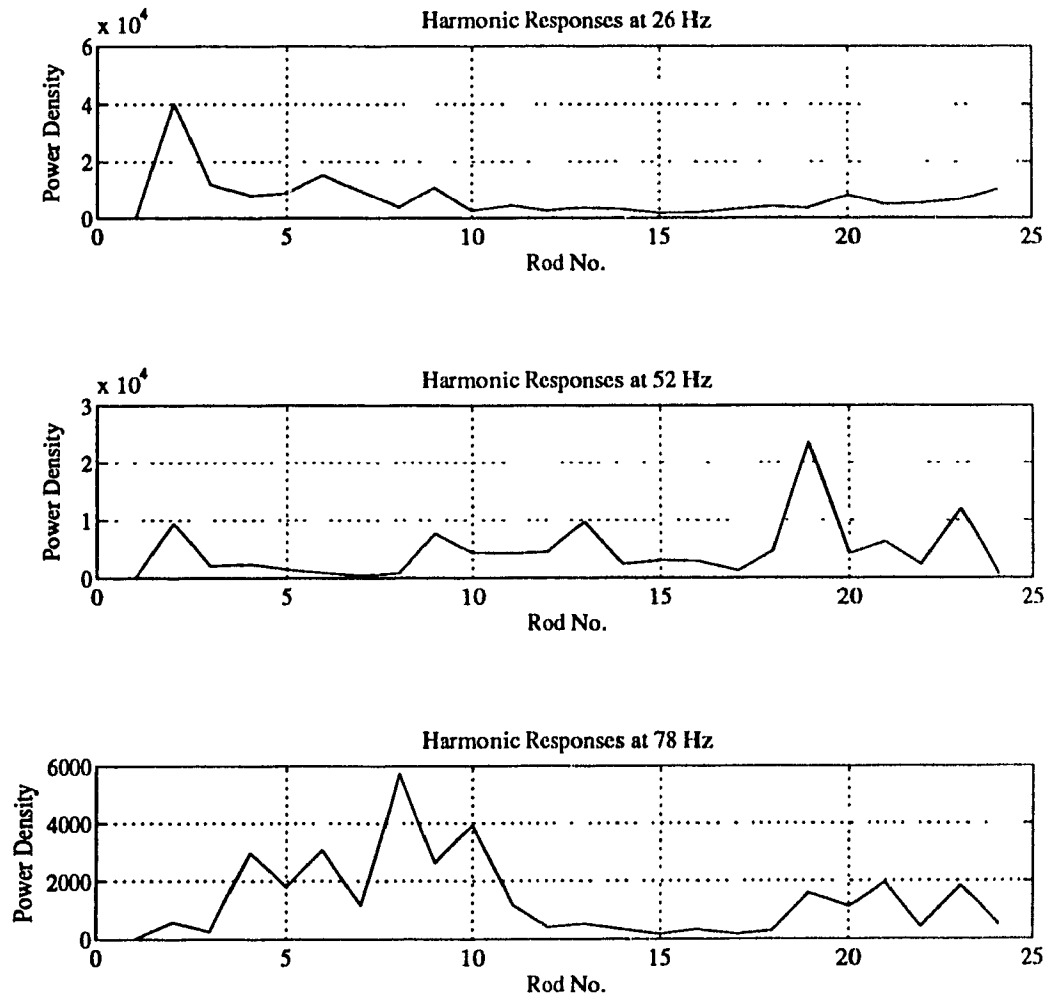


Figure 7.22: Harmonic Responses of Vertical Vibration and Variables for Hole Under04



Hole: Under04 Data: vv04g Lateral Vibration

Figure 7.23: Harmonic Responses of Lateral Vibration (F-B) for Hole Under04



Hole: Under04 Data: vv04g Lateral Vibration

Figure 7.24: Harmonic Responses of Lateral Vibration (L-R) for Hole Under04

## Chapter 8

# Conclusion and Further Work

### 8.1 Introduction

With decreasing prices for ore and dwindling reserves, it will be necessary for Canadian underground mines to improve current production practices and reduce operating costs to remain competitive. The advent and implementation of advanced monitoring and control systems on ITH drills will assist in achieving these goals. However, in order to properly design and develop these systems so that they meet the requirements of underground mining, additional research on drilling vibration and deviation mechanisms will be required. The more complex the system electronically, the more susceptible they will be to the vibration generated from both the ITH hammer percussions and when drilling difficult ground. Thus, suitable electronic systems can only be designed once the constraints of the environment in which these will be operating have been correctly determined and specified. The research in this thesis is a first attempt towards enabling the specification of design criteria for such electronic systems by providing a better understanding of the vibration regime surrounding ITH drills in hard rock, underground mines.

## 8.2 Conclusion

The research described in this thesis constitutes a primary component of work for projects initiated by Inco Mines Research involved in the development of advanced control systems for their ITH drills. The major conclusions of this research are outlined below:

### 8.2.1 Theoretical Studies

- The vibration responses of ITH percussive drills are completely different from those of tricone bit drills due to the fact that in the former, the main sources of drill string vibration are from the impact of the piston. This difference is especially prominent when the frequency responses of the vibration are examined and analyzed.
- For the static analysis of the drill string, the lateral forces at the bit are believed to be a major cause of initiating hole deviation while drilling. These forces are initially created, and increase substantially, as bending and buckling of the drill string occurs. The feed force should be never exceed a critical limit as the length of the drill string is increased to avoid further steel bending and buckling. After the drill string has been unstabilized under these conditions and with the lateral vibrations which act on it, hole deviations will develop.
- When the length of the drill string is very short, an MDOF model can be used to simulate the longitudinal vibration of the ITH drill. Under such conditions, the drill string tends to be a lumped mass transfer body, where there are small changes in the longitudinal vibration responses along the drill string while drilling.
- When the drill string is relatively short, the vibration generated at the drill bit will be isolated or absorbed by the spring elements in the shock absorber rather than be damped by either the damping of the shock absorber or due to friction between the

drill string and hole walls.

- From the simulation results, the complex boundary condition described in chapter 5 is considered to be more applicable to the continuous model of the drill string. Under the complex boundary condition, there are different vibration responses as compared to the other boundary conditions discussed, especially at low operating frequencies. In high frequency modes, the damping ratio, spring rate and weight of the drill head have less effect on the vibration responses as was shown in figure 6.16, which illustrated the 3-D plot of the results from simulation using the complex boundary condition.

### 8.2.2 Experimental Studies

- Shock absorbers can greatly reduce the amplitude of the longitudinal vibrations generated by ITH percussive drills. Softer springs are more efficient in absorbing these vibrations. The damping of the drill system also plays an important role in isolating the vibrations generated at the bit rock interface. When the drill system is in resonance, the vibrations were absorbed or isolated mainly by the damping of the drill system rather than by the spring elements of the shock absorber.

The particular shock absorber used in these studies was more efficient in isolating the longitudinal as opposed to the lateral vibration. This response is due to the fact that only vertical spring elements were used in the shock absorber.

The generated drilling vibration was mainly absorbed by the spring elements in the shock absorber rather than through damping. This is due to the shock absorber design in which there are only spring elements acting to isolating the vibration transmission. The damping of the drilling system is due to the friction between the drill rod and hole wall and also at the bit-rock interface. With an increase in the length of the drill string, the damping effects increase thus lowering the measured vibration amplitude.

- The shock absorber can absorb the vibration efficiently at the lower frequency range. The high frequency responses of the vibration transmitted from the drill bit to the head are mainly attenuated by damping due to the frictional effects surrounding the drill string.
- The feed force plays an important role in determining the amount of hole deviation and the penetration rate by its direct influence on the developed vibration level. When the feed force was kept in the optimum range, there were lower vibrations generated thus reduced possibilities for hole deviation and high production rates. These results show that when the proper levels of feed force are used, there is an efficient transfer of percussive energy from the hammer to the bit to break rock. As conditions at the bit-rock interface change, due to feed force or geological variations, the percussive energy transfer efficiency will also vary. For example, bit bouncing due to insufficient feed force will result in increased energy being reflected back through the drilling system, ie. high vibrations. Overthrusting will dampen the percussive energy preventing rock from being efficiently broken by the bit and thus prohibiting drill penetration. It was found that high feed force, if within the optimum working range, will decrease the vertical vibration level while the lateral vibrations are less affected.
- The torque was mainly induced by forces composed of the bit chipping action, the friction between the drill rods and hole wall and the friction from all rotating drill components. Thus, torque can be considered proportional to the damping ratio of the drill system.

### 8.3 Primary Contribution

- Although the main objective of the static analysis in chapter 3 was the derivation of the differential equations for ITH drill vibration, it also provided results describing the bending and buckling mechanisms of the drill string under the influence of the feed force. The critical feed force and/or length of the drill string were analyzed at different boundary conditions to examine their effect on hole deviation due to the bending and buckling of the drill string. Furthermore, the analysis of the lateral forces which result from the bending of the drill string has contributed to provide a better understanding of the factors responsible for hole deviation, a phenomenon of great concern in underground mines.
- The differential equations for Multiple-Degree-of-Freedom and Continuous System (mass lumped and distributed) describing ITH drill vibration have been derived and analyzed for several sets of boundary conditions. It is suggested that these differential equations form the basis for more comprehensive theoretical studies and modeling of the ITH drill vibration to be conducted. Solutions for the differential equations were also used in the modeling, calculation and simulation of the ITH drill forced-damped vibration for both the short drill rod (mass lumped) and long drill string (mass distributed) cases. The mathematical model derived for the continuous system also enabled the vibration to be investigated for two coordinates (time and length along the drill string) simultaneously.
- Simulations of the longitudinal vibration of ITH drills, based on the MDOF and Continuous System mathematical models and actual data for the CD-90B ITH drill, were undertaken. These efforts attempted to recover the vibration characteristics of the ITH drilling system and thus reveal the true responses of the longitudinal vibration along the drill string in real time and at different frequencies. A modal analysis and comparison of different damping ratios and/or spring rates of the ITH

drill for the vibration responses were also principal objectives of the simulations. Several comprehensive computer programs were developed to run these simulations.

- A series of vibration measurements from the underground field testing of a CD-90B ITH were selected for analysis. The lateral and longitudinal vibration responses of the drill string were measured using appropriate sensors and a telemetry system mounted on the drill rod – this effort had never before been attempted. The vibrations of the drill head were also monitored. Other sensors on the drill permitted the recording of penetration rate, air pressure, feed force and torque in parallel to the vibration data. The vibration responses on both the drill head and the drill string were monitored for conditions with and without a shock absorber installed behind the drill hammer. The data from these tests were the first attempt ever to be obtained while such a drill was actually drilling a hole. Thus, this data set is invaluable in providing insight into the dynamics of an ITH hammer and how these are affected by the introduction of a shock absorber under known geological conditions.

- Experimental studies of ITH drill vibration were completed through the use of signal processing, spectral analysis and system identification techniques using data from drilled production holes. Both the longitudinal and lateral vibrations of the ITH drill were examined using either their frequency or harmonic response. By comparing the amplitude of the vibration when drilling with or without a shock absorber, the efficiency of this device to isolate vibration was evaluated at different frequency ranges and for different types of vibration. Certain drilling variables and design criteria, such as damping ratio, feed force, air pressure and torque, were also investigated in an attempt to determine their relationship with vibration. The results of the vibration data analysis was aimed at providing results which could be used for new shock absorber or improvement of current designs while also forming the basis for further research work into drilling vibration.

## 8.4 Recommendation for Further Work

To meet the needs of the mining industry through the provision of higher production rates and lower cost drilling, the development of automated ITH drills becomes more and more important. The main problem with the development of suitable automation system is the control of ITH drill vibration. While the shock absorber is still considered as one of most efficient tools to attenuate the vibration.<sup>1</sup> As shown in this research, there has been limited research into both the improvement of current shock absorber designs or the development of new devices. Therefore, further research work is proposed based on the theoretical and the empirical studies in this thesis, to focus on the redesign and development of shock absorbers for ITH drills. For example;

- The data measured from field tests could be analyzed in greater depth to study the capability of a shock absorber to attenuate the changing vibration effects on drill penetration and drill deviation under variable downhole geological conditions.
- As indicated in the empirical studies in chapter 7, the lack of damping elements in a shock absorber results in poor damping of the vibration, especially when the drilling system is in the resonance frequency range. It would be, therefore, important to investigate the effect of introducing additional damping elements to the shock absorber and examine the results to drilling performance and energy dissipation.
- Since the lateral vibration on the drill rod is considered to have an obvious effect on hole deviation, it would be necessary to also investigate how to incorporate a lateral vibration damping capability into a new shock absorber design.

---

<sup>1</sup>actual control of feed force and possibly rotation speed would also reduce drilling vibration

## Reference

- [1] Erik Skaugen, Åge Kyllingstad, Thor Viiggo Aarrestad and Harald A. Tønnesen: *Experimental and Theoretical Studies of Vibrations in Drill Strings Incorporating Shock Absorbers*, SPE Paper 14760, February 1986.
- [2] Dareing, D.W.: *Guidelines for Controlling Drill String Vibrations*, Transactions of the ASME, Vol. 106, June, 1984, pp. 272-277.
- [3] Close, D.A., Owens, S.C. and MacPherson, J.D.: *Measurement of BHA Vibration Using MWD*, IADC/SPE Drilling Conference, Dallas, Texas, February 28 - March 2, 1988, pp. 659-664.
- [4] Bailey, J.J. and Finnie, I.: *An Analytical Study of Drill-String Vibration*, Journal of Engineering for Industry, May 1960, Vol. 82, pp. 122-128.
- [5] Dareing, D.W. and Livesay, B.J.: *Longitudinal and Angular Drill String Vibration*, Journal of Engineering for Industry, November 1968, Vol. 90, pp. 671-679.
- [6] Dareing, D.W.: *Drill Collar Length is a Major Factor in Vibration Control*, SPE Paper 11228, September 1982.
- [7] Deily, F.H., Dareing, D.W., Paff, G.H., Ortloff, J.E. and Lynn, R.D.: *Downhole Measurements of Drill String Force and Motions*, Journal of Engineering for Industry, May 1968, Vol. 90, pp. 217-225.

- [8] Cunningham, R.A.: *Analysis of Downhole Measurements of Drill String Forces and Motions*, Journal of Engineering for Industry, May 1968, Vol. 90, pp. 208-216.
- [9] Tseng H. and Dareing, D.W.: *Buckling and Lateral Vibration of Drill Pipe*, Journal of Engineering for Industry, November 1968, Vol. 90, pp. 613-619.
- [10] Jiao, D. and Edwards, J.B.: *A Simulation Model for ITH Percussive Drill with A Shock Absorber*, Inco Mines Research Progress Report No. 3, August 1990.
- [11] Jiao, D.: *Vibrations Involved in ITH Percussive Drilling*, CCARM Internal Research Report, 1992.
- [12] Mitchell, R. F.: *Lateral Vibration: The Key to BHA Failure Analysis*, World Oil, Vol. 200, No. 4, March 1985, pp. 101-106.
- [13] Ahid .D Nashif: *Vibration Damping*, John Wiley & Sons, New York, 1985.
- [14] James, M.L.: *Vibration of Mechanical and Structural System*, Harper & Row Publishers, New York, 1989.
- [15] Chander, R.: *An Identification Technique for Damped Distributed Structural System Using the Method of Collocation*, Proceedings on Damping '91, San Diego, California, pp GCA-1.
- [16] Agneni, A. and Balis Crema, L.: *Damping Ratio Estimates from Autocorrelation Functions*, Proceedings on Damping '91, San Diego, California, pp GCD-1.
- [17] Beasaisow, A.A and Payne, M.L.: *A Study of Excitation Mechanisms and Resonances Inducing BHA Vibrations*, SPE Paper 15560, 61st Annual Technical Conference and Exhibition of the Society of Petroleum Engineers, New Orleans, Oct. 1986.
- [18] Warren, T.: *The Effect of Hole Curvature on Drill Pipe While Drilling Inside*

*Casing or Open Hole*, SPE Paper 6780, 52nd Annual Fall Technical Conference and Exhibition of the Society of Petroleum Engineers of AIME, Denver, Colorado. Oct. 1977.

[19] Baird, J.A., Jordan, A., Caskey, B.C., Wormley, D.N. and Stone, C.M.: *A Bottomhole Assembly/Geological Formation Dynamic Interaction Computer Program*, SPE Paper 14329, 60th Annual Technical Conference and Exhibition of the Society of Petroleum Engineers, Las Vegas, Sept. 1985.

[20] Dunayevsky, V.A., Judzis, A. and Mills, W.H.: *Onset of Drillstring Precession in a Directional Borehole*, SPE Paper 13027, 59th Annual Technical Conference and Exhibition of the Society of Petroleum Engineers, Texas, Sept. 1984.

[21] Dunayevsky, V.A., Judzis, A. and Mills, W.H.: *Dynamic Stability of Drillstring Under Fluctuating Weights-on-Bit*, SPE Paper 14329, 60th Annual Technical Conference and Exhibition of the Society of Petroleum Engineers, Las Vegas, Sept. 1985.

[22] Millheim, K., Steven, J. and Ritter, C.J.: *Bottom-Hole Assembly Analysis Using the Finite-Element Method*, Journal of Petroleum Technology, Feb. 1978, Vol. 30, pp. 265-274.

[23] Dareing, D.W.: *Rotary Speed, Drill Collars Control Drillstring Bounce*, Oil & Gas Journal, June 6, 1983, Vol. 81, No. 23, pp. 63-68.

[24] Cooper, G.A., Lesage, M.L., Sheppard, M. and Wand, P.: *The Interpretation of Tricone drill Bit Vibration for Bit Wear and Rock Type*, RETC Proceedings, Volume 1, 1987, pp. 202-218.

[25] Jardine, S.I., Lesage, M.L. and McCann, D.P.: *Estimating Tooth Wear From Roller Cone Bit Vibration*, SPE/IADC 19966, Drilling Conference, Houston, February 1990, pp. 459-466.

- [26] Miller, C.E. and Rollins, H.M.: *Evaluation of a Vibration Damping Tool and of Drill Stem Torque Requirements From Data Recorded by an Instrumented Drill Stem Member*, Journal of Engineering for Industry, May 1968, Vol. 90, pp.226-230.
- [27] Paslay, P.R. and Bogy, D.B.: *Drill String Vibration Due To Intermittent Contact of Bit Teeth* , Journal of Engineering for Industry, May 1963, Vol. 85, pp. 187-194.
- [28] Angonna, F.A: *Drill String Vibration Attenuation and Its Effect on a Surface Oscillator Drilling System*, Journal of Engineering for Industry, May 1965, Vol. 87, pp. 110-114.
- [29] Frohrib, D.A. and Plunkett, R.: *The Free Vibration of Stiffened Drill String With Static Curvature*, Journal for Engineering for Industry, Feb. 1967, Vol. 89, pp. 23-30.
- [30] Cook, R.L., Nicholson, J.W., Sheppard, M.C. and Westlake, W.: *First Real Time Measurements of Downhole Vibrations, Forces, and Pressures Used to Monitor Directional Drilling Operations*, Paper of SPE/IADC Drilling Conference, New Orleans, Louisiana, February 1968.
- [31] DeVries, M.F., Saxena, U.K. and Wu, S.M.: *Temperature Distributions in Drilling*, Journal of Engineering for Industry, May 1968, Vol. 90, pp. 231-238.
- [32] Garrett, W.R.: *The Effect of a Down Hole Shock Absorber on Drill Bit and Drill Stem Performance*, Journal of Engineering for Industry, May 1968, Vol. 90, pp. 2-11.
- [33] Wijk, G.: *Rotary Drilling Prediction* , International Journal of Rock Mechanics and Mining Science & Geomech, 1991, Vol. 28, No. 1, pp. 35-42.
- [34] Brett, J.F. and Yoder, D.L.: *Use of the Engineering Simulator for Drilling for*

*Evaluating and Designing Drill Rings*, SPE/IADC 13480, Drilling Conference, New Orleans, Louisiana, March 1985.

[35] Burgess, T.M. and Lesso Jr, W.G: *Measuring the Wear of Milled Tooth Bit Using MWD Torque and Weight-On-Bit*, SPE/IADC 13475, Drilling Conference, New Orleans, Louisiana, March 1985.

[36] Karlsson, H., Brassfield, T. and Krueger, V.: *Performance Drilling Optimization*, SPE/IADC 13474, Drilling Conference, New Orleans, Louisiana, March 1985.

[37] Allen, M.B.: *BHA Lateral Vibration: Case Studies and Evaluation of Important Parameters*, SPE/IADC 16110, Drilling Conference, New Orleans, Louisiana, March 1987.

[38] Burgess, T.M., McDaniel, G.L. and Das, P.K.: *Improving BHA Tool Reliability With Drilling Vibration Models: Field Experience and Limitations*, SPE/IADC 16109, Drilling Conference, New Orleans, Louisiana, March 1987.

[39] Chen, W.C.: *Drilling Fatigue Performance*, SPE/IADC 16076, Drilling Conference, New Orleans, Louisiana, March 1987.

[40] Lesage, M.L.G., Falconer, I.G, Wand, P.A. and McCann, D.P.: *An Analysis of Bit Bearing Failures With Field and Laboratory Data*, SPE/IADC 17187, Drilling Conference, Dallas, Texas, February 1988.

[41] Boyadjieff, G.I.: *The Application of Robotics to the Drilling Process*, SPE/IADC 17232, Drilling Conference, Dallas, Texas, February 1988.

[42] Zamudio, C.A, Tlusty, J. and Dareing, D.W.: *Effect of Shock Absorber on Drag Bit Chatter*, SPE/IADC 17194, Drilling Conference, Dallas, Texas, February 1988.

[43] Thomas, L.M, Helmerich and Payne I.D.C.: *Case History: PC Analysis of Bit*

*Enhances Drilling Operations in Southern Alabama*, SPE/IADC 18632, Drilling Conference, New Orleans, Louisiana, February 1989.

[44] Vandiver, J.K., Nicholson, L.W. and Shyu, R-J.: *Case Studies of the Bending Vibration and Whirling Motion of Drill Collars*, SPE/IADC 18652, Drilling Conference, New Orleans, Louisiana, February 1989.

[45] TAMROCK *Surface Drilling and Blasting*, Handbook 1988.

[46] Jiao, D., Daneshmend, L., Jian, M., Muhamed, A. and Peck, J.: *CD-90B ITH Drill Monitoring and Controller Formulation Data*, Research Report to Mines Research, INCO, December 1992.

[47] Aboujaoude, C.D., *Modeling, Simulation and Control of Rotary Blasthole Drills*, Graduate Studies Thesis, December 1991.